HIGHER TECHNICAL INSTITUTE
NICOSIA 1968 CYPRUS

Review

No. 11 June 1982 Nicosia

Review

No. 11
June 1982
Nicosia

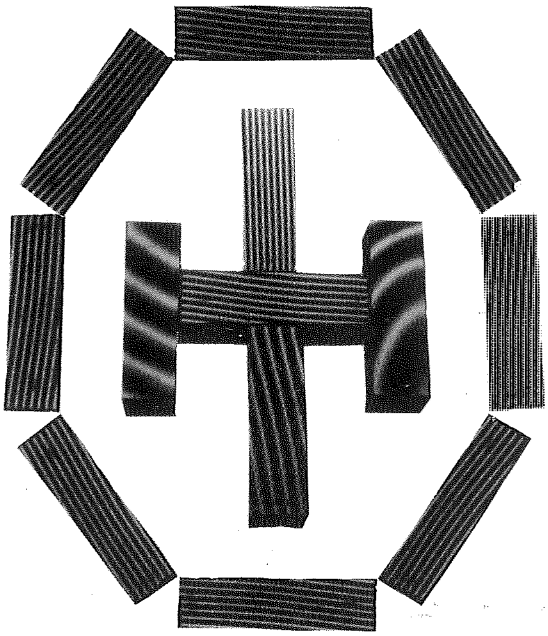

Cover photo by Ionas Angeli

An artistic view of the interference fringes formed by the flatness error of five block gauges under an Optical Flat.

H.T.I. Review is published by the Public Information Office In cooperation with the Higher Technical Institute, Nicosia. It accepts articles which promote and further new developments and knowledge in technology, especially with reference to Industries of Cyprus. Requests for further copies of the magazine and for information concerning the published articles should be made to Editor H.T.I. Review, Higher Technical Institute, P.O.box 3423—Nicosia.

Page CONTENTS

The Higher Technical Institute (H.T.I.) was established in 1968 as a Government of Cyprus project with assistance by the United Nations Development Fund (UNDP), the United Nations–Educational Scientific and Cultural Organisation (UNESCO), and the International Labour Office (ILO). Cyprus Government Executing Agency: The Ministry of Labour and Social Insurance.

HIGHER TECHNICAL INSTITUTE NICOSIA 1968 CYPRUS

Review

No. 11 June 1982 Nicosia

EDITORIAL

It is with great pleasure that we present this years H.T.I. review. Over the years, this magazine proved an effective Forum for the presentation of H.T.I.'s activities and the dissemination of technological knowledge. This tradition is continued with the present issue.

This years review includes articles of a professional nature, such as solar energy and applications, materials and processers, electrical installations, and others of more general nature and interest.

We hope that these articles will prove useful to those who read them, and will promote further discussions and exchange of opinion.

The Editorial Committee wishes to express its sincere thanks to all those who contributed, by whatever manner, to the development of this issue of the H.T.I. review.

The Editorial Committee

June 1982

Damage in the Cation Sublattice of α-Al_2O_3 Irradiated in the HVEM

by Dr A.Y. Stathopoulos, Lecturer at H.T.I., formerly at the Department of Metallurgy and Science of Materials, University of Oxford, Parks Road, OXFORD, ENGLAND.

Abstract

α-Al_2O_3 has been irradiated at high temperatures with 300 keV electrons at which energy only aluminium ions are displaced. Systematic examination in a 100 kV electron microscope revealed pure edge dislocations loops of interstitial character with **b**=1/3 [0001] *and* **b**=1/3 [10$\bar{1}$0] *lying on basal and prismatic* [10$\bar{1}$0] *planes respectively. The loops are stoichiometric but faulted on the aluminium sublattice. A model is proposed by which cation displacement at high temperatures results in aluminium interstitials precipitating between basal or* [10$\bar{1}$0] *prismatic planes with simultaneous diffusion of oxygen ions between the aluminium layers producing the faulted loops.*

1. Introduction

Ceramics are under consideration for a number of critical applications in fusion reactors as electrical insulators or as low-Z liners for the first wall. In these applications the structure of the materials will be exposed to radiation damage from fast neutrons of doses as high as $\backsim 10^{29}$ n/m^2 at temperatures between 800 and 1300K. In order to study these radiation damage effects it is necessary to use charged particle beams which will produce equivalent displacement doses but in a much shorter period of time, a technique which has been extensively employed in studying metals.

Damage processes in α–Al2O3, where an ionic and diatomic crystalline solid is involved, are expected to be more complicated than in metals. The number of aluminium and oxygen atoms displaced from their sites will be sensitively dependent on their respective threshold displacement energies (Ed), the mininium energy which must be imparted to an atom to displace it permanently from its lattice site, with large changes occurring if the thresholds of the two atomic species become significantly different from each another. Recently, Pells and Phillips (1979) have measured, using a high voltage electron microscope (HVEM) the minimum electron energy required to produce observable damage over a wide temperature range and found two distinct regions: A low temperature region with a value of $\backsim$ 390 KeV and a region at $\backsim$ 600K and above with a value as low as $\backsim$ 200 KeV. Additional absorption and luminescence measurements of the growth of F, F+ and V bands upon irradiation helped them to interpret these results. A consistent interpretation emerges if the oxygen and aluminium have widely different Ed of $\backsim$ 75eV and 18eV respectively, which then correspond to the high and low values of the threshold electron energy.

For the growth of dislocation loops upon irradiation of an ionic diatomic solid one would expect displacement of both atomic species, which then cluster in stoichiometric proportions. However, in the alkali halides it has been shown by Hobbs, Hughes and Pooley (1973) that displacement of only the anion species is sufficient to induce indirectly displacement of cation–anion pairs to produce such interstitial dislocation loops. It is not known whether an indirect mechanism is also operating in a–Al_2O_3 where the cation is thought to be the more easily displaced species. Recently, Howitt and Mitchell (1981) studied the defect structure produced in an HVEM by irradiating with 650 keV electrons at 1075K; this energy and temperature, however, are well within the range for displacement of both ionic species.

We have looked at the dislocation defect structure more closely in order to establish any differences in the form and nature below and above $\backsim$ 390 keV. In this paper we report the results of HVEM irradiations carried out at 300 keV at which temperature only aluminium might be directly displaced and at temperatures above 800K where dislocation loops form readily.

2. Experimental

Thin 3mm diameter, single crystal specimens with two different main crystal axis orientations were used: (a) With the basal plane parallel to the foil surface; these were grown from the vapour phase and supplied by Imperial College, London in the form of thin plates $\backsim$ 5 µm thick, (b) With the prism {01$\bar{1}$0} plane approximately parallel to the foil surface cut from single crystal boules supplied by Salford Electrical Instruments Ltd. The specimens were secured by hot pressing between two slotted gold grids and thinned from both sides using a 5 keV argon ion beam on an Iontech ion–beam thinning machine at an angle of 30° until red interference fringes could be seen at the centre corresponding to a thin area of 0.3 µm.

The specimens were electron–irradiated in the Harwell AEI–EM7 High Voltage Electron Microscope using a side–entry hot–stage with the specimen area differentially pumped to below 1x10–7 Torr by a turbomolecular pump and with liquid nitrogen cold fingers below and above the stage. The temperatures covered were in the range 300–1100 K and the electron beam had a flux density of $\backsim$ 8.10^{23} e/m^2/s as measured in the centre of a fully focussed beam. The damage created was observed and subsequently studied at 100 keV using a Siemens 102 high resolution transmission electron microscope equipped with a $\pm$ 45^0 double–tilt goniometer stage.

3. Loop Analysis Method

α–Al_2O_3 does not show significant deviations from elastic isotropy (Jones and Ed[illegible]ton 1972) and so the Burgers vector, **b**, of the loops can be determined from loop invisibility criteria using appropriate reflections via the application of the g.**b**=0 rule (Hirsch et al 1965). To avoid ambiguity ensuing from a possible confusion of residual contrast from loops with g.**b**.=0 (arising from the g.**bxu** term) and the weak contrast which sometimes arises from loops with g.**b**.=0, images were always recorded in both +g and—g, keeping the deviation parameter w constant. True residual contrast will be invariant in the +9 and —g images, whereas no invariance is observed for false g.**b**=0 invisibility. Due to the large number of b vectors possible for the defects in an h.c.p. lattice, large angle tilting work in the electron microscope was essential and electron micrographs under several independent, two–beam conditions were obtained in order to determine the **b** vectors of the loops.

The interstitial or vacancy nature of the loops was investigated using the well–known "inside–outside" technique (Hirsch et al 1965); for this it is necessary to know the sense of inclination of the loops in the foil which was determined by tilting the specimen through a large angle in a known sense and noting the resulting change in shape of the image. The loop habit planes were also determined by specimen tilting through the direction that made the loops appear edge–on on the screen.

4. Results

Irradiations at 300 keV and T=1055K

The point defects were found to cluster readily and form dislocation loop networks within seconds from the start of the irradiation. In order to analyse the loops in detail we observed the gradual development of the damage by analysing areas exposed to diffrent doses in the HVEM.

(a) Loop analysis on prismatic [01$\bar{1}$0] foils

Fig. 1 shows two such areas irradiated for differenttimes. A high concentration of edge-on loops is seen to have nucleated rapidly but more importantly their clustering does not occur randomly but along the [01$\bar{1}$0] direction giving considerable loop image overlap in bright field images when recorded at the prism orientations.

Analysis of the individual loops without the complications from their subsequent growth was carried out by studying areas exposed to a current density of 2.5x10^{23} e/m2/s for 2 secs. The loops lie edge-on in the foil, on (0001) planes and were identified as being edge loops with b=1/3 [0001]. This was done by using micrographs obtained at orientations and in reflections summarized in Table I with their | **g.b** | product values. In Fig. 2 we give examples of these micrographs together with one taken under weak-beam conditions. Even in cases where the loops are sufficiently far apart from each other for no apparent image overlap in bright field, the interaction can still be observed to have began taking place under the weak beam imaging conditions. Also when the foil is tilted away from [10$\bar{1}$0], as shown in Fig. 2(e), the linear alignment of the loops is destroyed showing that the loops align invariably in bands on (0001) planes.

The coalescing small basal loops give rise to very large irregularly shaped compound loops with b=1/3 [0001] containing the compound stacking fault of the constituent loops. This is illustrated in Fig. 3, where an area of damage is shown imaged in bright field at [10$\bar{1}$0] with the loops edge-on and also in weak beam with the foil tilted away along the 1216—band. The weak beam micrograph shows clearly the stacking fault fringes and also regions around the extended loops where unfaulting has occurred. However no completely unfaulted loops were observed.

Edge loops with b=1/3 <01$\bar{1}$0>, although not so copiously present in numbers as the basal loops, were also identifiable in these foils and a more complete search for them was carried out using basal foils, where their contrast behaviour will be illustrated.

(b) Loop analysis on basal foils

The Burgers vector analysis of loops formed in irradiated basal-type foils was carried out mainly in order to look for loops with other than a c-component of **b**. At the [0001]-orientation the planes of types (hki0) lie perpendicularly to the basal plane and only loops with some a-component are visible at this orientation, a and c are the characteristic distances in the hexagonal unit cell as defined by Kronberg (1957). Fig. 4 shows examples of loop images obtained at the [0001] - orientation in the three [3300] type of reflections. Only the three possible $\{0110\}$ planes were found to be habit planes for loops and the loops marked A, B and C on the figure are illustrative examples of the contrast behaviour of edge loops with **b**=1/3 [$\bar{1}$100] **b**=1/3 [10$\bar{1}$0], **b**=1/3 [01$\bar{1}$0] respectively. The basal loops with **b**=1/3 [0001] were also present in these foils but are out of contrast in Fig. 4 as they have no **b**-vector component in the image plane; their presence was established by tilting to other orientations.

5. Nature of the dislocation loops

In each experiment the foil was tilted mainly about a single axis, not all the possible sets of loops being analysed in each case. The results are illustrated in Fig. 5 for the case of b=1/3 [0001] loops: (a) and (b) were taken in $\pm$g =[10$\bar{1}$1] under diffraction conditions satisfying positive s, where s is the excitation error of the operating reflection. The inclination of the loop, also indicated, was determined by tilting the specimen. A large number of loops with diameters ranging between 5nm and 200nm from all the different irradiation conditions were examined yielding the same result for both 1/3 [0001] and 1/3 [01$\bar{1}$0] loops, that is they all are of the interstitial type.

6. Discussion

Analysis of loops after electron irradiation at 300 keV and at T=1055 K has shown them to be of extrinsic nature with Burgers vectors either 1/3 [0001] or 1/3 <01$\bar{1}$0>. A tendency for loops to form in bands was observed and demonstrated on (0001) planes which then grow into each other to form extended defects with the same b-vector and possibly unfault as they grow in size. In this discussion we are principally interested in the structure and formation of the loops and consideration of the alignment and unfaulting effects will be given in a second paper where more complete observations under a wider range of conditions of energy and temperature will be available.

The structure of the α-Al2O3 lattice is that of interleaving h.c.p. layers of oxygen anions with the aluminium cations occupying only 2/3 of the octahedral positions and displaced towards one apex (Kronberg 1957). If we represent oxygen layers with capital and aluminium layers with small letters, in the usual notation, the stacking sequence of layers (above one another) with be of the form

AaBbAcBaAbBc.........

along the c-axis. The same sequence as given above can still represent the stacking interchange (next to each other) along a prismatic <01$\bar{1}$0> direction (although strictly A,B and a,b and c are now inherently different planes with different chemical bond lengths, ionic densities and interplanar distances) as is clear from looking at a ball and spoke model of corundum. The envisaged loop structure, therefore, for both types of loop can be equivalently represented by the diagram of Fig. 6 and although the two **b**-vectors have of course diffrent lengths, they both involve only faults on the cation sublattice and for extrinsic faults two extra cation and two anion layers must be incorporated as shown in the figure. As far as this identification is concerned, the present results are in agreement with those of the recent independent publication of Howitt and Mitchell (1981) on loops produced by electron irradiation at 650 keV.

We will, however, also proceed to consider a model to explain the structure and formation of these loops.

7. Loop formation mechanism

In establishing a mechanism for loop formation we need to examine all the structural possibilities which are consistent with the electron microscope evidence, i.e. all the possibilities that can eventually lead to the creation of faulted interstitial loops with b=1/3 [0001] and b=1/3 <01$\bar{1}$0>.

(a) Simple loop model

One interpretation of the loop structure would be if the loops formed by the condensation of stoichiometric numbers of cation and anion interstitials both displaced entirely in the primary damage process. This, otherwise obvious model, may not however be correct because of the requirement for displacement of the ionic species in both the cation and anion sublattices.

Spectroscopic evidence from studying the growth of various optical absorption bands in the spectrum of α-Al2O3 has established firmly that the V-bands at 3eV are due to the aluminium ion vacancy (e.g. Gamble et al 1964, Cox 1971, Turner and Crawford 1975, Lee et al 1976), whereas the F-centre has been associated in more recent work (Evans et al 1976, Lee and Crawford 1977) with the 6.0 eV band. Pells and Phillips in their HVEM threshold energy work also studied the growth of these bands as a function of electron beam energy and found that the 3eV band did not grow until the electron energy was >175 keV, whereas an energy > 410 keV was needed to make the 6eV band grow. These energies corresponded to displacement energies of 18eV and 75eV for aluminium and oxygen displacement respectively. If these values of Ed are independent of temperature the present irradiation conditions using 300 keV electrons displace only aluminium ions. Consideration therefore, of this aspect of the radiation damage behaviour and the fact that the oxygen sublattice in the faulted loop remains perfect makes it improbable that this loop formation model is correct.

(c) Displaced-cation diffusing-anion loop model

We now outline the mechanism which we consider leads to a faulted loop shown in the configuration of Fig. 6 by circumventing the problems inherent in the simple loop model just described. We envisage that radiation-induced cation displacement results in the insertion of charged aluminium interstitial layers in the channels between (0001) or $\{01\bar{1}0\}$ closest-packed planes. These aluminium rich zones may be considered to contain a high concerntration of anion vacancies such that the juxtaposition of positive charge is relieved by very rapid diffusion and interpositioning of oxygen ions into two layers between the aluminium ions. Consequently two faulted aluminium layers alternating with two unfaulted oxygen layers collapse to form a faulted loop with **b**=1/3 [0001].

We now suggest how this may come about by considering the formation of loops in three conceptual stages.

StageI: Creation of aluminium Frenkel defects

An electron colliding directly with an atom in the α-Al_2O_3 lattice imparts an amount of energy which is different for each of the two component species depending on their respective masses of 27 and 16. If the displacement threshold energy of aluminium is 18eV (Pells and Phillips 1979) then a direct collision requires a primary electron energy of 0.175 MeV. A minimum of 76eV is required to displace oxygen, corresponding to an electron energy of 390 keV Therefore, at 300 keV the predominant primary defects are Frenkel pairs on the aluminium sublattice.

The first stage, therefore, is the displacement of aluminium ions which may then aggregate in the space between the close-packed planes in the lattice; on the basis of the experiemental evidence the aggregation occurs between the basal (0001) planes or the prismatic $(01\bar{1}0)$ planes. The simplest case is illustrated in Fig. 7(a) where an extra plane of aluminium atoms introduced onto the basal plane of the lattice adjacent to an aluminium lattice plane in which the normally vacant one-third of "aluminium" lattice sites may also now contain aluminium atoms.

Stage II: Electrostatic equilibrium rearrangement

The arrangement of aluminium ions in Fig. 7(a) is electrostatically unfavourable, and we envisage that the extra aluminium layer may separate into two regular a and b layers in addition to layer c as in Fig. 7(b) If the initial interstitial aluminium layer was close packed in a similar arrangement to that of the adjacent aluminium lattice plane then on separation the resulting three planes would have the defect structure of the aluminium sublattice in α-Al_2O_3 (one-third of the available lattice sites unoccupied) whilst the gaps between the three aluminium layers may be considered to contain oxygen vacancies.

Stage III: Oxygen diffusion between the Aluminium layers

As Stage II takes place, oxygen ions may diffuse into the vacancies so as to separate the aluminium layers, i.e. between the a–b and c–d layers in Fig. 7(c). The two extra A and B layers are necessary to make the final structure electrically neutral.

Supporting evidence which is presented in the following section suggests that oxygen diffusion would be sufficiently rapid at the temperature of irradiation to allow this restructuring to take place.

Stage IV: Electrostatic equilibrium restored, the configuration collapses to produce a stable extrinsic structural fault in the aluminium sublattice surrounded by a dislocation loop line with **b**=1/3 [0001] or **b** 1/3 $<10\bar{1}0>$ for basal or prismatic collapse respectively. The oxygen sublattice stacking remains unchanged.

Thus, loops enclosing stacking faults, are formed by precipitation of aluminium interstitial atoms and the concomitant diffusion of oxygen into the precipitate.

Correlation between oxygen mobility and loop growth

Loop growth becomes appreciable at temperatures above 800K. Consideration of the available self-diffusion data (see Mohapatra and Kroger 1978) indicates that aluminium is more mobile than oxygen with measured activation energies for diffusion of $\backsim$ 2.5 eV although there is a wide variation in experimental data. These high activation energies for motion are completely at variance with the calculations of James (1979) and the experimental observations by Pells of the annealing of radiation damage induced colour centres. The calculation by James gave an activation energy for isotropic vacancy diffusion of aluminium which was slightly higher than that of oxygen, 1.81 eV and 1.77 eV respectively. Pells has shown that isochronal annealing of neutron irradiated sapphire produces growth of the oxygen divacancy (F_2 centre) opitical absorption band which starts at 520K and reaches a peak at 690K. Over this temperature range the number of oxygen monovacancy centres (F-centres) falls. All of the F type centres have annealed out by 1020K. The reduction of F centre concentration could result from either vacancy migration to interstitials or equally migration of interstitials to be captured at oxygen vacancies. However, the growth of the F2 centre does not suffer from such an ambiguity and must follow from the migration of oxygen vacancies. The value for the activation energy for F_2 centre growth was 0.6 ± 0.2 eV. It should be pointed out that several optical absorption bands in sapphire grow in a similar manner and temperature range to that of the F_2 centre. Some of these bands are thought to be higher aggregates of oxygen vacancies so that it is unlikely that the F_2 band growth follows from oxygen vacancies boiling off larger anion aggregates or the trapping of interstitials by aggregates.

Such low activation energy may correspond to localised oxygen diffusion in the small anion triangle within the oxygen plane normal to the c axis for which James calculated an activation energy of 1.12eV. This would lend support to James value of 1.77 eV for isotropic diffusion. Using James values of 1.81 and 1.77 eV for aluminium and oxygen respectively gives a time interval per jump of 0.04 s at 723K and 0.002 s at 873K which is in agreement with the temperature regime where the loop growth becomes rapid in our experiments.

Summary of results and conclusions

HVEM irradiation of α-Al_2O_3 at energies below 390 keV and at temperatures >800K results in the formation of pure edge dislocation loops with **b**=1/3 [0001] and **b**=1/3 $[10\bar{1}0]$ of interstitial character and lying on basal and prismatic $\{10\bar{1}0\}$ planes respectively. These loops are stoichiometric and contain a 4-layer fault of alternate aluminium and oxygen layers but the faulting occurs only in the cation sublattice, while the hcp oxygen sublattice remains perfect. Unfaulting of some pairs of loops in evident.

A model has been proposed by which cation displacement at high temperatures results in aluminium-ion interstitials precipitating between basal and $\{01\bar{1}0\}$ prismatic planes with simultaneous diffusion of oxygen ions between the aluminium layers producing the faulted loop.

Acknowledgements

The author wishes to thank Mr G.P. Pells and Drs. C.A. English, A.E. Hughes and M.L. Jenkins for helpful discussions and the United Kingdom Atomic Energy Authority for provision of laboratory facilities and financial support at A.E.R.E. Harwell.

References

1. Cox, R.T., 1971, Solid State Commun., **9**, 1979.
2. Evans, B.D., Hendricks, H.D., Bazzarre, F.D. and Bunch, J.M., 1976, "Jon Implantation in Semiconductors", 265.
3. Gamble, F.T., Bartram, R.H., Young, C.G., Gilliam, O.R. and Levy P.W., 1964, Phys. Rev., **134**, A589.

4. Hobbs, L.W., Hughes, A.E. and Pooley, D., 1973, Proc. Roy. Soc. Lond., A**332**, 167.

5. Howitt, D.G. and Mitchell, T.E., 1981, Phil. Mag. A., **44**, 229.

6. James, R., 1979, Harwell AERE T.P. 814.

7. Kronberg, M.L., 1957, Acta Met., **5**, 507.

8. Lee, K.H. and Crawford Jr. J.H., 1977, Phys. Rev. **B**, **15**, 4065.

9. Lee, K.H., Holmberg, G.E. and Crawford Jr, J.H., 1976 Solid State Commun., **20**, 183.

10. Mohapatra, S.K. and Kroger, F.A., 1978, J. Amer Ceram. Soc., **61**, 106.

11. Pells, G.P. Unpublished work.

12. Pells, G.P. and Phillips, D.C., 1079, J. Nucl. Mat, **80**, 207.

13. Turner, T.J. and Crawford Jr, J.H., 1975, Solid State Commun., **17**, 107.

TABLE 1

Orientation Z	$10\bar{1}0$					$2\bar{1}\bar{1}3$		
g	$1\bar{2}16$	$\bar{1}2\bar{1}3$	$1\bar{2}1\bar{3}$	0006	$1\bar{2}10$	$1\bar{2}1\bar{1}$	$0\bar{3}30$	$\bar{1}011$
| **gb** |	2	1	1	2	0	1/3	0	

Conditions used in imaging b=1/3 [0001] loops

Figure Captions

1) Damage in prismatic foils irradiated with 300 kV electrons at 1055K with a flux density of 8 x 10^{23} e/m^2/s for:

(a) 60 s, (b) 180 s. The figures show loop alignment and coalescence in bands parallel to $\langle 10\bar{1}0 \rangle$ direction,

2) Analysis of loops before coalescence. The loops were produced by 300 kV electron irradiation at 1055K to a fluence of 5x10^{23} e/m^2. The same area is imaged with six different g vectors, a–d were taken at **z**=$10\bar{1}0$ and c–f at z=$2\bar{1}\bar{1}3$. (a) g=0006, (b) **g**=$1\bar{2}10$, (c)=$1\bar{2}1\bar{3}$, (d)=$1\bar{2}16$, weak beam g (2.8g), (e) g=$\bar{1}011$, (f) g=$1\bar{2}1\bar{1}$. All except (d) are kinematical bright field micrographs.

3) Faulted basal loops **b**=1/3 [0001] in a prismatic foil irradiated at 300kV with T=1055K to a fluence of 2.9x10^{25} e/m^2 and imaged in : (a) g=0006, bright field at $\langle 10\bar{1}0 \rangle$, (b) g=$1\bar{2}16$ weak beam, dark field, tilted by ∽ 25^0 from $\langle 1010 \rangle$ showing stacking fault fringes and regions where loop unfaulting has occurred.

4) Prismatic dislocation loops in basal foils imaged in (a) g=$\bar{3}300$, (b) g=$\bar{3}030$, (c) g=$0\bar{3}30$ at the [0001] pole.

5) Loop nature determination in prismatic foil irradiated at 1055 K with 300 kV electrons to a fluence of 2.75x10^{25} e/m^2.

(a) g=$10\bar{1}1$, outside contrast, $\vec{g}.\vec{b}.\vec{s} > 0$,

(b) g=$\bar{1}0\bar{1}\bar{1}$, inside contrast, $\vec{g}.\vec{b}.\vec{s} < 0$.

The image behaviour is consistent with an interstitial loop inclined with respect to the electron beam as shown in the diagram between (a) and (b).

6) Faulted dislocation loop schematic showing the layer sequence for oxygen and aluminium, **b**=1/3 [0001] or b=1/3 $\langle 0\bar{1}\bar{1}0 \rangle$ depending on whether the axes are $000\bar{1}$ $\uparrow\rightarrow 01\bar{1}0$ or $0\bar{1}10$ $\uparrow\rightarrow 0001$ respectively.

7) Schematic of the loop formation model.

(a) Cation interstitials precipitate between an oxygen B and an aluminium c layer

(b) The interstitial sheet splits into two.

(c) Oxygen diffusion from both sides of the loop restores the electrostatic balance and creates a four-layer loop faulted on the cation lattice only.

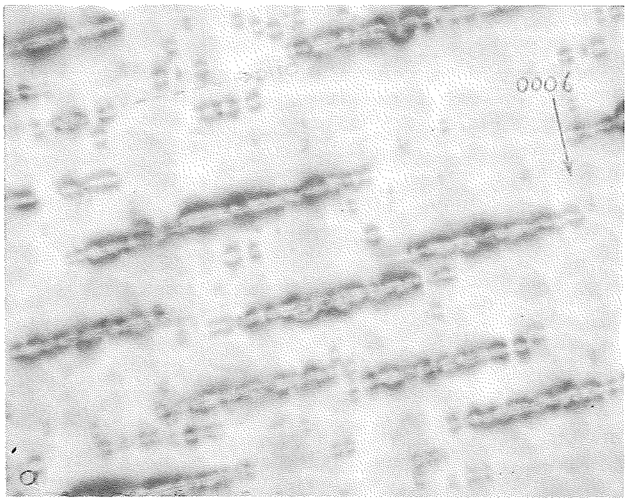

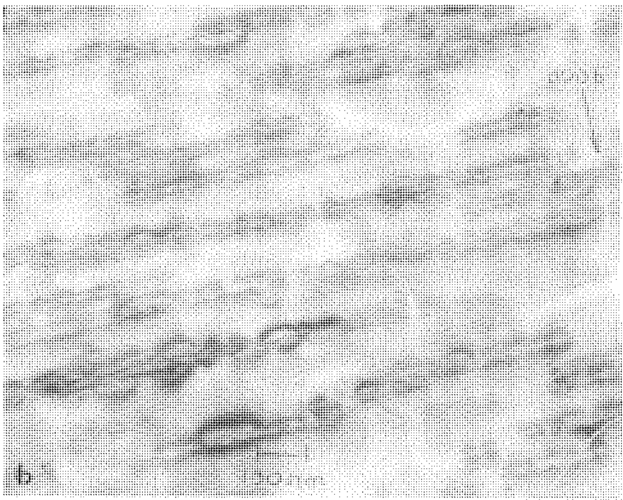

Fig. 1

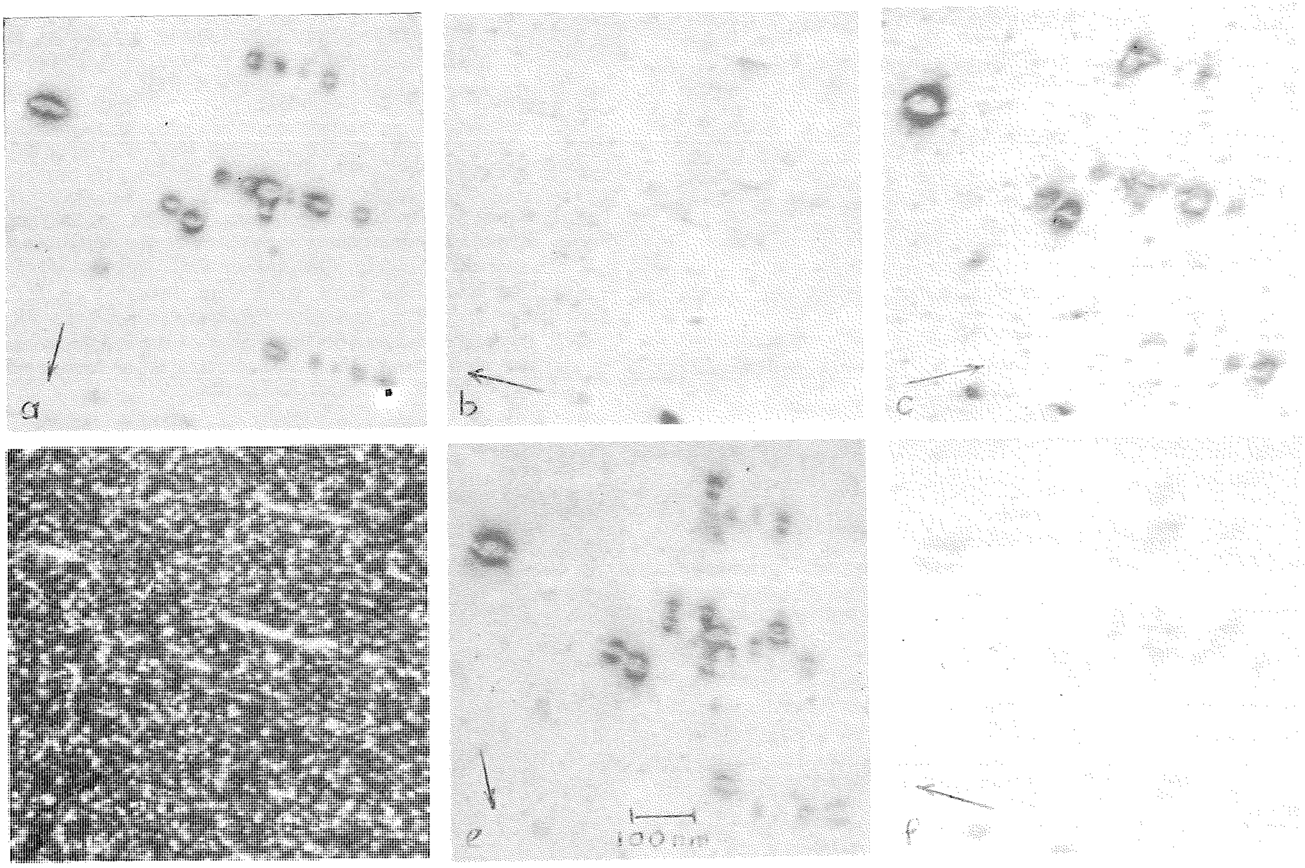

Fig. 2

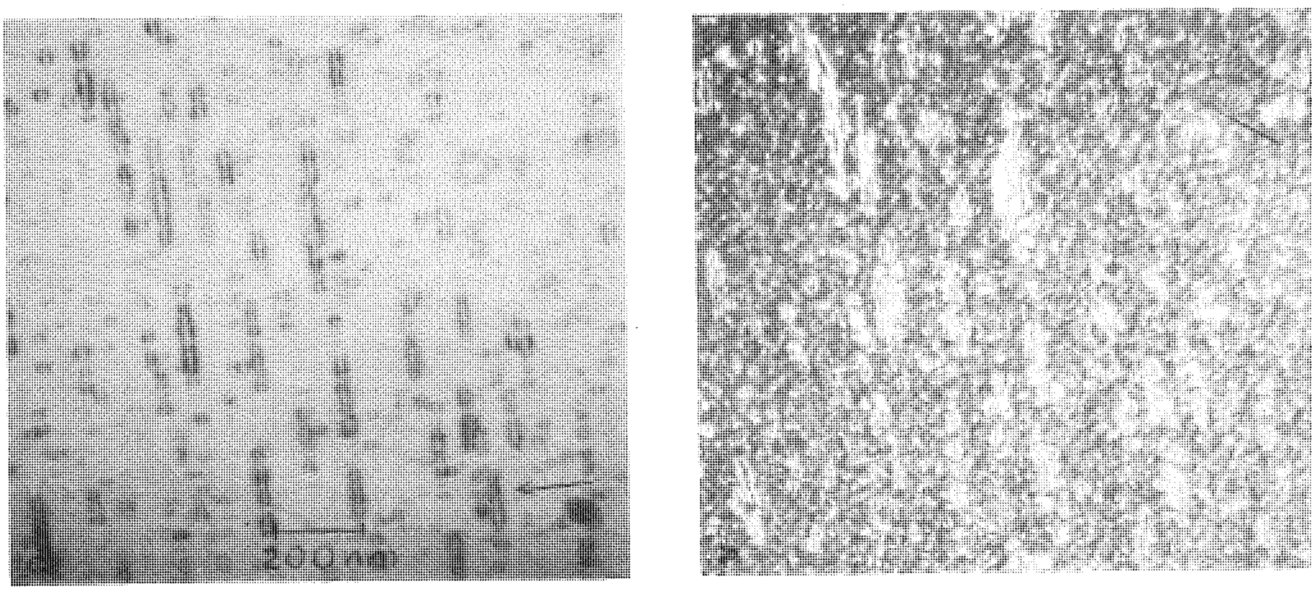

Fig. 3

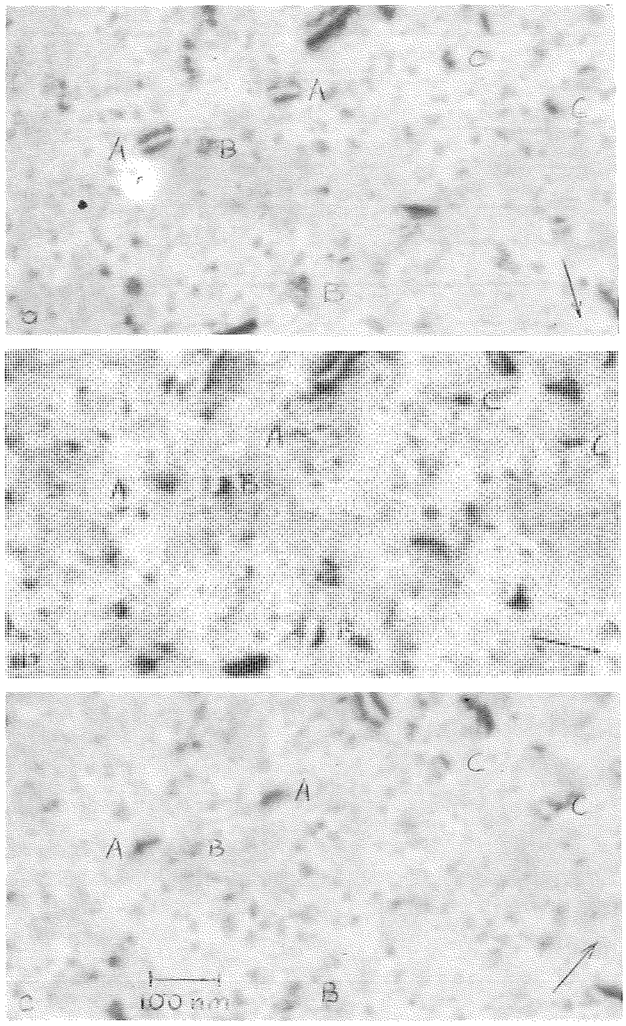

Fig. 4

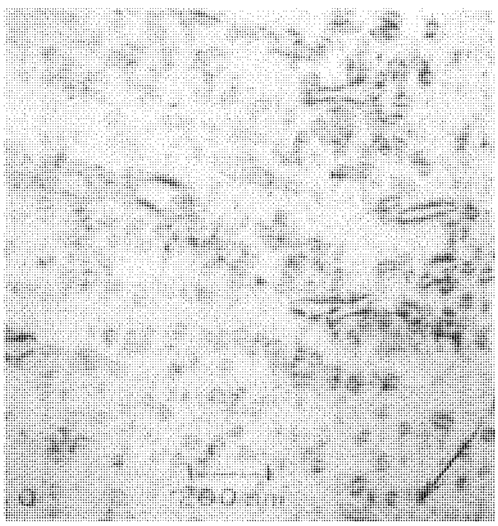

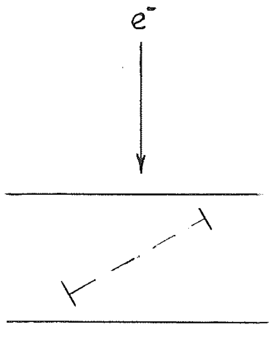

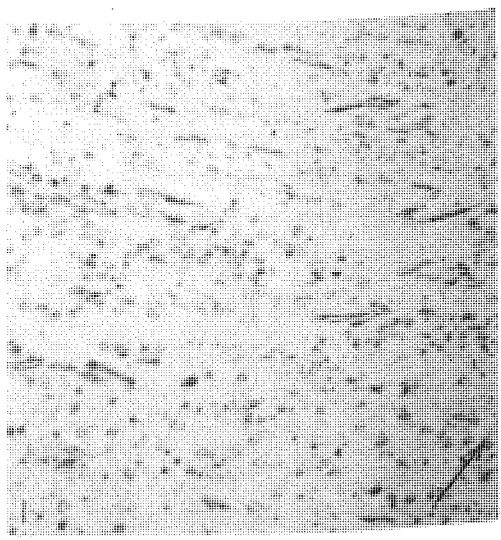

Fig. 5

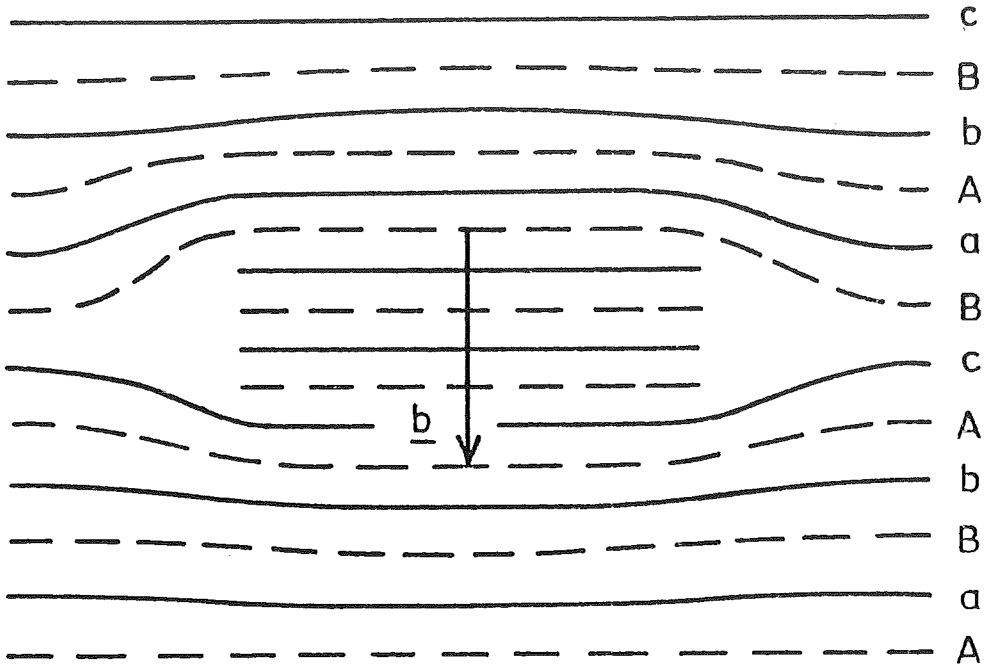

Fig. 6

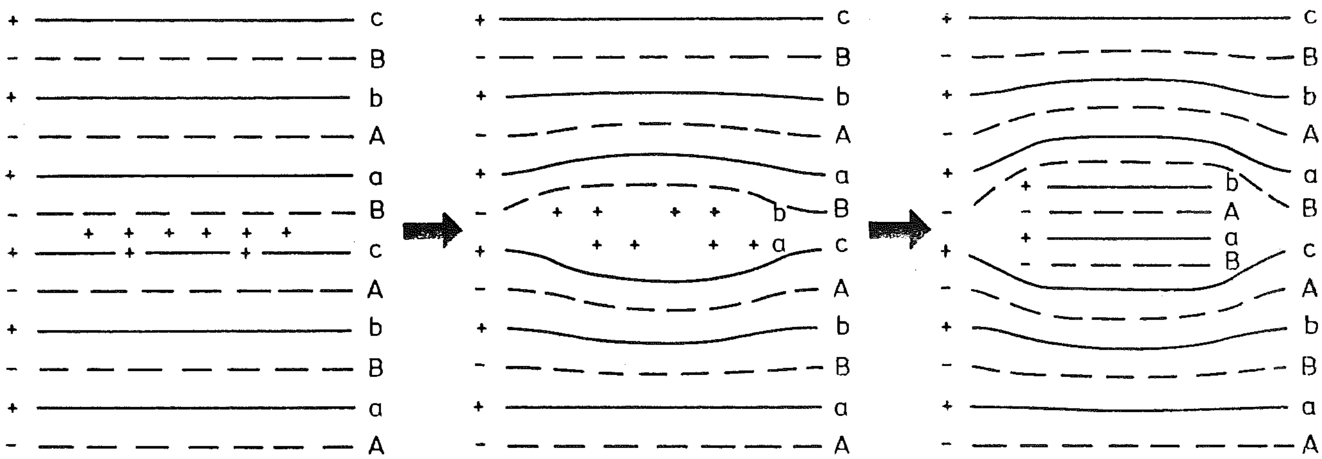

(a) (b) (c)

Fig. 7

Modelling of a tunnel furnace in the ceramic industry

by Dr M. Kassinopoulos, Lecturer H.T.I.

Abstract.

A theoretical study was developed in order to optimise the operation of a 50m long tunnel furnace producing 30 tons of horticultural pots per day. The first step in this study consisted of modelling the thermal behaviour of the furnace by taking into account the geometrical parameters of the tunnel and of the products to be burnt and the physico-chemical properties of the different elements constituting the plant.

A mathematical model was first established for a continuous advance of the charge and then modified to account for periodic displacements in the real situation. A set of non linear hyperbolic equations was obtained and solved using the Carlson method. Thus the temperature profiles could be obtained, knowing the control distribution, which consisted of about twenty gas burners.

The model was linearised to simplify the optimisation study. A parameter identification and a numerical simulation were required. Numerical results and graphs are given.

Introduction

When energy was cheap, only an empirical knowledge of the operation of tunnel furnaces in the ceramic industry (bricks, tiles, horticultural pots, etc) was sufficient. Today the optimal profitability of such furnaces must be determined. Two main criteria have to be taken into account.

(a) minimising the quantity of broken products by optimising thermal gradients throughout the furnace.

(b) minimising energy consumption by determining an optimal control law, according to the number and position of burners and thermocouples.

Such a study requires a phenomenological model of heat and mass transfer in the furnace. Some of the parameters had to be identified, using experimental data from the operating furnace.

To adapt the model for an easier optimal control study, a set of partial differential equations had to be linearised.

The work was performed in a tunnel furnace producing horticultural pots. It should be noted that one of the main problems resulted from the heterogeneity of the charge in the furnace.

Physical Description of the Tunnel Furnace

The ceramic industry furnace under study is a 50 meters long tunnel furnace (fig. 1). Its effective cross section is 1.64 m wide and 0.92 m high. The walls are made of refractory bricks covered by an insulating cement, and building bricks placed only on the sides. This furnace consists of four zones:

- a 6m long feeding zone (closed by a sash-door)
- a 15m long preheating zone
- a 10m long burning zone
- a 19m long cooling zone

The burning zone is equiped with three independent groups of gas burners: the burners are distributed along the two side walls (about twenty burners).

The pots are loaded onto special carriages 2.5m long and 1.58m wide (fig. 2) and pushed through the tunnel by a hydraulic pusher (0.50 m every 30 minutes). Each carriage consists of two layers of refractory bricks separated by a space located at the level of the burners. The carriages are cooled in the cooling zone by a blow of 'secondary air' flowing in the opposite direction. This air is mixed with combustion gases in the burning zone. All these gases are drawn out at the end of the feeding zone.

The butane gas flowrates are regulated by P.I.D. controllers, from temperature measurements made with three thermocouples located in the burning zone.

The ratio of 'primary air' to butane gas for a group fo burners is maintained at a constant value by means of a pressure control system.

The gas temperature profile is reconstituted by means of twelve thermocouples distributed under the ceiling of the tunnel.

A test carriage, equipped with three thermocouples, allowed us the thermal profile in the charge along the furnance to be approximately estimated.

For an optimisation study, the following parameter measurements are needed:

a) gas temperature (chiefly in the critical zones where temperature is about 830^{0}K)

b) butane gas and primary air flowrates

c) secondary air flowrate.

Temperature Model

A mathematical model was formulated with the following assumptions:

a) the charge is homogeneous

b) the gas flow is one-dimensional

c) the secondary air is transparent to radiation

d) the conduction resistance is negligible with respect to the convection and radiation phenomena

e) the temperatures are defined in a section of the tunnel by their average

f) the wall surface temperature dynamics is such that its derivative with respect to the time variable is formally equal to zero.

Thermodynamic balances can be established on three levels, considering heat transfer by convection and radiation and mass transfers (pots, gas, air).

a) Temperature T(x,t) of the charge

$$S_T \left[\frac{\partial}{\partial t} (\rho_T c_T T + U_T \frac{\partial}{\partial x} (\rho_T c_T T) \right] = \alpha_{GT} (G-T) + \beta_{GT}(G^4-T^4)$$

$$+ \beta_{PT} (P^4-T^4) \triangleq \mathcal{G}_T (T,G,P) \qquad \text{------} (1)$$

b) Temperature $G(x,t)$ of the gas

$$S_G\left[\frac{\partial}{\partial t}(\rho_G c_G G - \frac{\partial}{\partial x}(U_G \rho_G c_G G)\right] = \alpha_{GT}(T-G) + \alpha_{GP}(P-G)$$

$$+\beta_{GT}(T^4-G^4) + \beta_{GP}(P^4-G^4) + \alpha_a(T_a-G) + \sum_{i=1}^{N} Q_i\,\delta(X-X_i) \quad --(2)$$

c) Temperature $P(x,t)$ of the wall surface

$$\alpha_{GP}(G-P) + \alpha_{PTO}(T_o-P) + \beta_{GP}(G^4-P^4) + \beta_{PT}(T^4-P^4) \triangleq$$

$$C_P(T,P,G) = 0 \quad ------------- (3)$$

d) Mass balance

$$S_G \frac{\partial}{\partial x}(U_G \rho_G) = -\sum_{i=1}^{N} (16.5 + \gamma 15.5)\, m_i\, \delta(x-x_i) \quad --- (4)$$

with $x \in \,]\, 0, L\, [$ (L=44 m)

Notation:

ρ_T : density of charge

ρ_G : density of gas

C_T : specific heat of charge

C_G : specific heat of gas

U_T : charge velocity

U_G : gas velocity

S_T : vertical section of charge

S_G : vertical section of gas flow

T_a : air temperature under carriages

T_o : ambient temperature (T0=300°K)

Q_i : Q_i = 10955 x m_i with

m_i : butane flowrate per burner (i=1,2,.....N) γ: excess of air

α_{GT} and a_{GP} are unit length conductances to the convective heat transfer between gas and charge, and between gas and wall.

α_α : thermal conductance between charge and air which is under carriages

α_{To} : thermal conductance between the internal wall surface and the surroundings

β_{GT} β_{PT} β_{GP}: radiation coefficients depending on the emissivities and the configuration of the radiative systems.

Equivalent Model

Considering equality (4), the differential equation (2) can be written in the following form:

$$S_G\left[\frac{\partial}{\partial t}(\rho_G c_G G) - U_G \rho_G \frac{\partial}{\partial x}(c_G G)\right] = \alpha_{GT}(T-G) + \alpha_{GP}(P-G)$$

$$+\beta_{GT}(T^4-G^4) + \beta_{GP}(P^4-G^4) + \alpha_a(T_a-G)$$

$$+\sum_{i=1}^{N} (10955 - c_G\, G\,(16.6 + 15.5\gamma))\, m_i\, \delta(x-x_i) \triangleq$$

$$c_G(T,G,P) + D_G(G) \quad ----------- (5)$$

Moreover, analytically developping the different coefficients of the model (2), we get a differential system of the type:

$$A_T \frac{\partial T}{\partial t} + B_T \frac{\partial T}{\partial x} = C_T(T,G,P) \qquad (6)$$

$$A_G(G)\frac{\partial G}{\partial t} + B_G(G)\frac{\partial G}{\partial x} = C_G(T,G,P) + D_G(G) \qquad (7)$$

$$0 = C_P(T,P,G) \qquad (8)$$

$$A_G = 114{,}4\; S_G(0{,}051\; G^{-0{,}78} + 0{,}28\; 10^{-4} G^{0{,}22})$$

$$B_G = -M_G(0{,}232 + 0{,}48\; 10^{-4}\; G)$$

$$A_T = S_T \rho_T c_T$$

$$B_T = U_T S_T \rho_T c_T$$

These coefficients were obtained after calculation.

Resolution by Carlson's method

Carlson's discretisation method is very useful because it is unconditionally stable (at least for linear systems) and fits perfectly into the case of counterflow processes (Richtmyer, 1967).

This method consists of writing the differential system

$$\left[\frac{1}{v}\frac{\partial}{\partial t} + M\frac{\partial}{\partial x}\right] u(x,t) = S\, u(x,t)$$

(M: diagonal matrix) in the form

$$\left[\frac{1}{v}\frac{\partial}{\partial t} + \hat{M}\frac{\partial}{\partial x}\right]\hat{u}(x,t) = \hat{S}\,\hat{u}(x,t)$$

with $\hat{M}$ split into four parts:

$$\hat{M} \triangleq M_1 + M_2 + M_3 + M_4$$

where

M_1 contains those positive diagonal elements of M which are $> \Delta x / v\Delta t$

M_2 contains those positive diagonal elements of M which are $< \Delta x/v \;\; \Delta t$

M_3 contains those negative diagonal elements of M which are $> -\Delta x/v \;\; \Delta t$

M_4 contains those negative diagonal elements of M which are $> -\Delta x/v \;\; \Delta t$

Δx and Δt being the space and time discretisation step

The difference equations are:

$$\frac{\hat{u}_j^{n+1} - \hat{u}_j^{n}}{V \Delta t} + M_1 \frac{\hat{u}_{j+1}^{n+1} - \hat{u}_j^{n+1}}{\Delta x} + M_2 \frac{\hat{u}_j^{n} - \hat{u}_{j-1}^{n}}{\Delta x} + M_3 \frac{\hat{u}_{j+1}^{n} - \hat{u}_j^{n}}{\Delta x}$$

$$+ M_4 \frac{\hat{u}_j^{n+1} - \hat{u}_{j-1}^{n+1}}{\Delta x} = \hat{S} \hat{u}_j^{n}$$

n : time index

j : space index

Although Carlson's scheme is implicit, the numerical solution can be easily performed. Boundary conditions are defined at point x=0 or at point x=L, according to the sign of coefficients of M (respectively positive or negative).

In the case of the tunnel furnace, equations (6) and (7) are:

$$\frac{\partial T}{\partial t} + \frac{B_T}{A_T} \cdot \frac{\partial T}{\partial x} = \frac{C_T}{A_T} \qquad (9)$$

$$\frac{\partial G}{\partial t} + \frac{B_G}{A_G} \cdot \frac{\partial G}{\partial x} = \frac{C_G + D_G}{A_G}$$

OR

$$\left[\frac{\partial}{\partial t} + \begin{bmatrix} \frac{B_T}{A_T} & 0 \\ 0 & \frac{B_G}{A_G} \end{bmatrix} \frac{\partial}{\partial x} \right] \begin{bmatrix} T(x,t) \\ G(x,t) \end{bmatrix} = \begin{bmatrix} \frac{C_T}{A_T} \\ \frac{C_G + D_G}{A_G} \end{bmatrix}$$

Therefore

$$\hat{M} \triangleq M_1 + M_2 + M_3 + M_4 = [0] + \begin{bmatrix} \frac{B_T}{A_T} & 0 \\ 0 & 0 \end{bmatrix} + [0] + \begin{bmatrix} 0 & 0 \\ 0 & \frac{B_G}{A_G} \end{bmatrix}$$

decomposition linked to the choice of the numerical values of Δx and Δt.

The global discretisation of the system leads to the following equations:

$$T_j^{n+1} = T_j^n - \left(\frac{B_T}{A_T}\right)(T_j^n - T_{j-1}^n)\frac{\Delta t}{\Delta x} + \left(\frac{C_T}{A_T}\right)\Delta t$$

$j = 1, \ldots N_L \qquad n = 1, \ldots$

$$G_{j-1}^{n+1} = G_j^{n+1} + \left(\frac{A_G}{B_G}\right)(G_j^{n+1} - G_j^n)\frac{\Delta x}{\Delta t} + \left(\frac{C_G + D_G}{B_G}\right)\Delta x$$

$j = 1, \ldots N_L \qquad n = 1, \ldots$

The algebric equation (8) which can be solved analytically, gives the temperature P(x, t), knowing temperatures T(x,t) and G(x, t), solutions of system (10) (11).

The boundary conditions are

$T(o, t) = T_o =$ constant

$G(L, t) = C_L =$ ambiant temperature

We chose a space discretisation step equal to the distance between the burners (ΔX=0.5m), the time step being equal to a few seconds.

Parameter Sensitivity Study

The complexity of the mathematical model lies in the fact that a number of geometrical or physical parameters exist, for which the numerical value is not always well known. A preliminary study of parameter sensitivity allowed us, in fact, to retain only four of them for identification, the other parameters being determined by their mean value. These four parameters are given in decreasing order of sensitivity:

- the product $M_c \cdot c_T$
- the secondary air flowrate
- the surface of pots per meter
- the loss coefficient under carriages

The product $M_c \cdot c_T$ is imperfectly known since the charge consists of many different materials.

The secondary air flowrate was at first considered as a system parameter but will be chosen later as another control variable.

The measurement of the pots' surface was not easy because of the piling configuration and heterogenity of the charge throughout the furnace.

The loss coefficient under the carriages was not easily calculable for the type of carriage under consideration.

Parameter Identification

Parameter identification was made on the basis of a measurement set obtained during several carriage pushes, and by considering the mathematical model (6) to (8), in which carriage velocity is assumed constant (1m/h).

The "method model" was used, which consists of minimising the difference between the temperature measurements and the model output with respect to the unknown parameters. The minimisation algorithm was based on a discretised gradient method (Powell, 1964).

In order to solve the boundary value problem leading to the steady state solution, the differential system was discretised by the Euler method and the unknown boundary conditions were determined using a classical iterative numerical method.

The numerical results of this identification are:

(a) A =1270 kcal/0K

(b) Secondary air flowrate ...1450 kg/h

(c) Mean surface of pots =28.7 m2/m

(d) Loss coefficient =9.34 kcal/0k

Model Linearisation

The proposal of the optimisation study was the determination of a closed loop control, connected to the thermal regulation around a desired temperature profile in the charge (fig. 3).

The cóntinous operation of the furnace throughout the year and small temperature variations, justified a linearisation of the obtained model.

A numerical study allowed the determination of the nominal control $m_d(x)$ corresponding to the obtaining of the desired profile $T_d(x)$ in steady state, the simulation giving the desired profiles $G_d(x)$ in the gas and $P_d(x)$ on the wall.

The temperature variations of charge, gas and wall, around the desired regime, and:

$$T(x,t) = T_d(x) + \alpha(x,t)$$

$$G(x,t) = G_d(x) + \beta(x,t) \qquad (12)$$

$$P(x,t) = P_d(x) + \gamma(x,t)$$

$$m_b(x,t) = m_d(x) + \mu_b(x,t) \qquad (13)$$

the variation of mass flowrates of butane at the burners.

According to (12) and (13), we expand the non linear terme of the model (6) to (8), retaining only terms of order less than 2. For example:

$$T^4(x,t) = (T_d + \alpha(x,t))^4 \simeq T_d^4(x) + 4\,\alpha(x,t)\,T_d^3(x)$$

After calculation, we got a linear model in which the algebric equation allowed us to express $\gamma(x,t)$ as a function of $\alpha(x,t)$ and $\beta(x,t)$. So, we obtained a linear differential system with two variables $\alpha(x,\lambda)$ and $\beta(x,t)$ of the form:

$$\begin{bmatrix} \dot\alpha(x,t) \\ \dot\beta(x,t) \end{bmatrix} = \begin{bmatrix} K_{11}(x) + K_{12}\frac{\partial}{\partial x} & K_{13}(x) \\ K_{21}(x) & K_{22}(x) + K_{23}(x)\frac{\partial}{\partial x} \end{bmatrix} \begin{bmatrix} \alpha(x,t) \\ \beta(x,t) \end{bmatrix} + \begin{bmatrix} u_1(x,t) \\ u_2(x,t) \end{bmatrix} \qquad (14)$$

with the following boundary conditions:

$\alpha(o,t)=o$ $\qquad$ $\beta(L,t)=o$

In fact, model (14) is valid only if we consider a continous displacement of carriages. In the real case for which carriage velocity is zero between two pushes, the former calculations lead to a model having an additional term, due to the fact that the nominal control $m_d(x)$ no longer corresponds to the steady state. This model is of the form:

$$\begin{bmatrix} \dot\alpha(x,t) \\ \dot\beta(x,t) \end{bmatrix} = \begin{bmatrix} K_{11}(x) & K_{13}(x) \\ K_{21}(x) & K_{22}(x) + K_{23}(x)\frac{\partial}{\partial x} \end{bmatrix} \begin{bmatrix} \alpha(x,t) \\ \beta(x,t) \end{bmatrix} + \begin{bmatrix} C_T(x) \\ 0 \end{bmatrix} + \begin{bmatrix} u_1 \\ u_2 \end{bmatrix} \qquad (15)$$

Simulation results

Figure 3 represents the temperature profiles in the gas and the charge compared with the desired profile in the charge for the case where the simulation is carried out for the nominal control and the carriages are moving in a continuous way We verify that the furnace works as a heat exchanger by considering the respective position of the profiles in the left and right parts of the furnace. The distance between the desired profile and the obtained profile in the charge is relatively small. But if we wish to make this distance smaller it will be necessary to modify the number and positions of the actuator configuration.

In order to show that the linearisation of the model is valid we have represented in figure 4 the response of both the linear and non linear models at three characteristic points (one in the preheating zone, one in the burning zone and the other in the cooling zone).

The simulation results of the linear system between two consecutive advances are shown in figure 5, where the model in which the carriage velocity is zero is used. The more important variations seen on the right hand side are due to the physical differences in the wall materials. For the same type of simulation when the carriage velocity is non zero we note that the dynamic response of the model is much slower (about 3^0 in 1/2 hour).

We conclude that both models (zero and non zero velocity of carriages) can be used, but for different optimisation problems:

—the zero velocity model for short term optimisation (between two consecutive advances).

—the non-zero velocity model for long term optimisation (time horizon of several hours).

We are now in the process of studying an optimisation problem which takes into account the short and long term optimisation and which leads to two feedback controls.

References

Kassinopoulos M., Modelisation et commande sous-optimale d'un four d'industrie ceramic, These de 3eme Cycle Universite Paul-Sabatier, Toulouse (30 juin 1980).

Powell, an efficient method of finding the minimum of a function of several variables without calculating derivatives. Comp. J. Volume 7, 1964.

Richtmyer R.D., Morton K.W. Difference methods for initial value problems, John-Wiley and Sons, 1967.

Acknowledgements

This work is supported by BERNAT SAULIERES COMPAGNIE (Castres, France).

* Presented at the I.F.A.C. conference on System, Approch for development "Modeling of a tunnel furnace in the ceramic, Industry"

Morocco-November 1980 By Barreteau D., Laguerie C., Babary J.P., and Kassinopoulos M, L.A.A.S-C.N.R.S. Toulouse-France

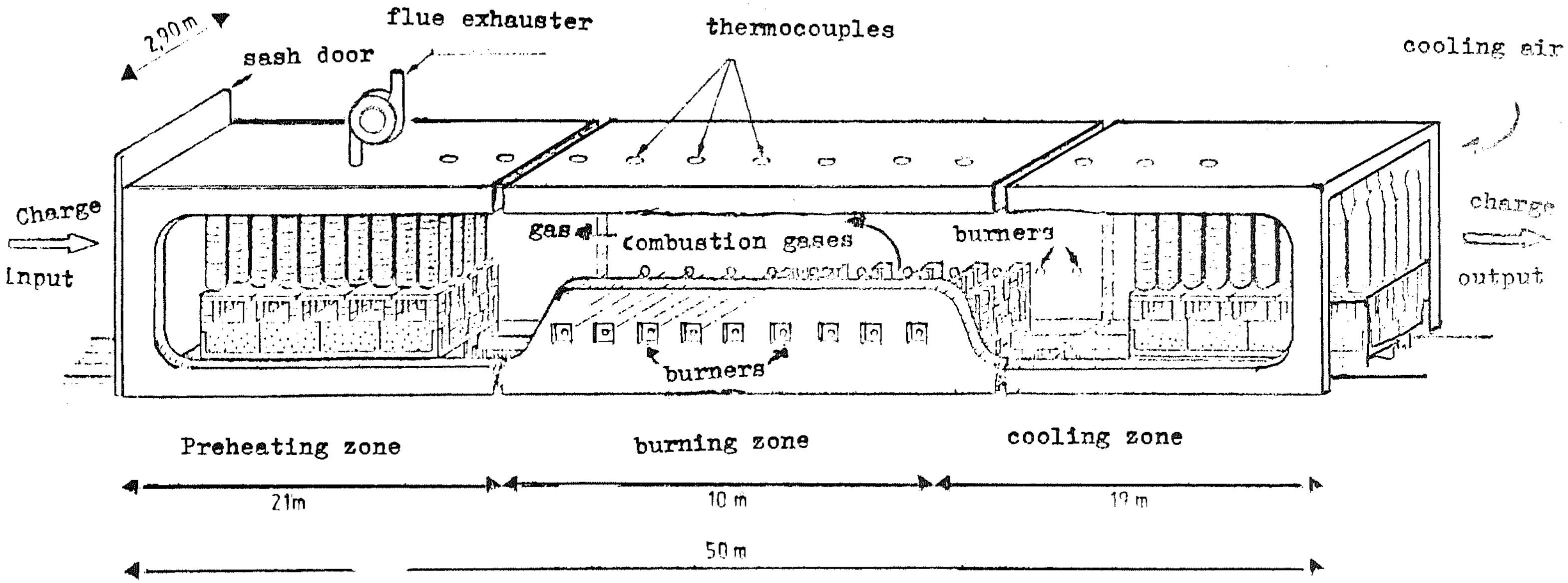

Fig. 1 Tunnel furnace for ceramic Industry

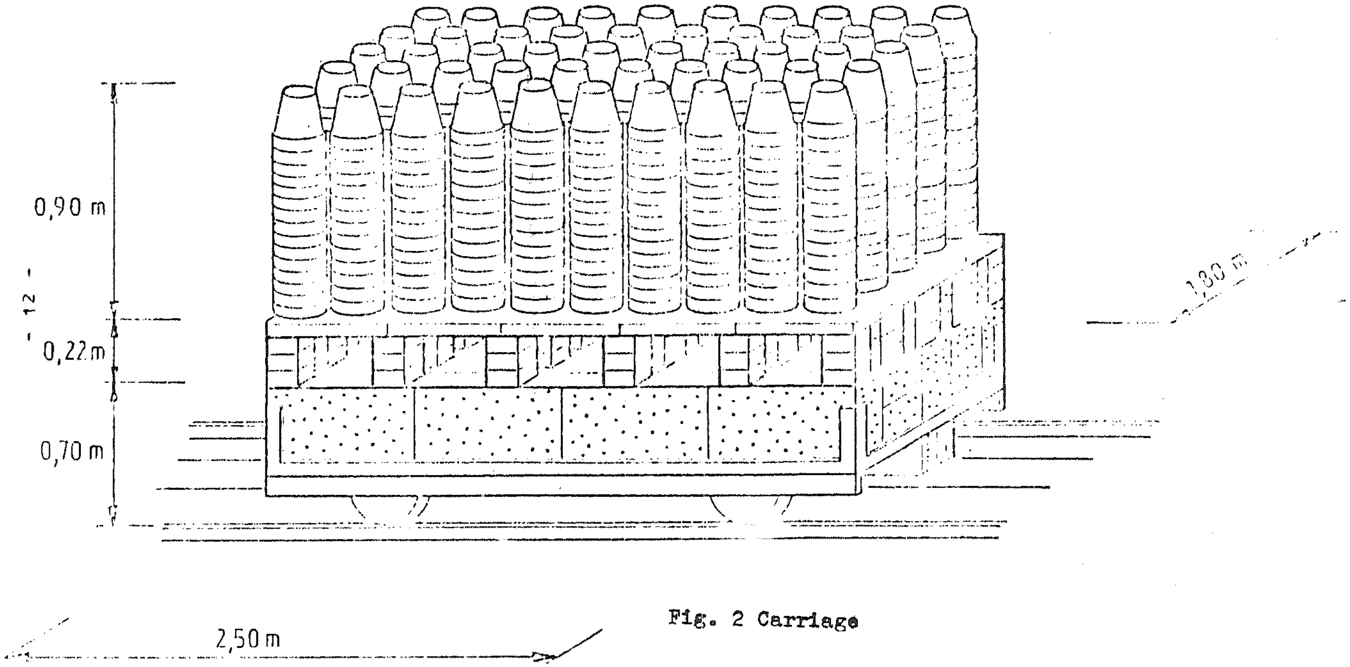

Fig. 2 Carriage

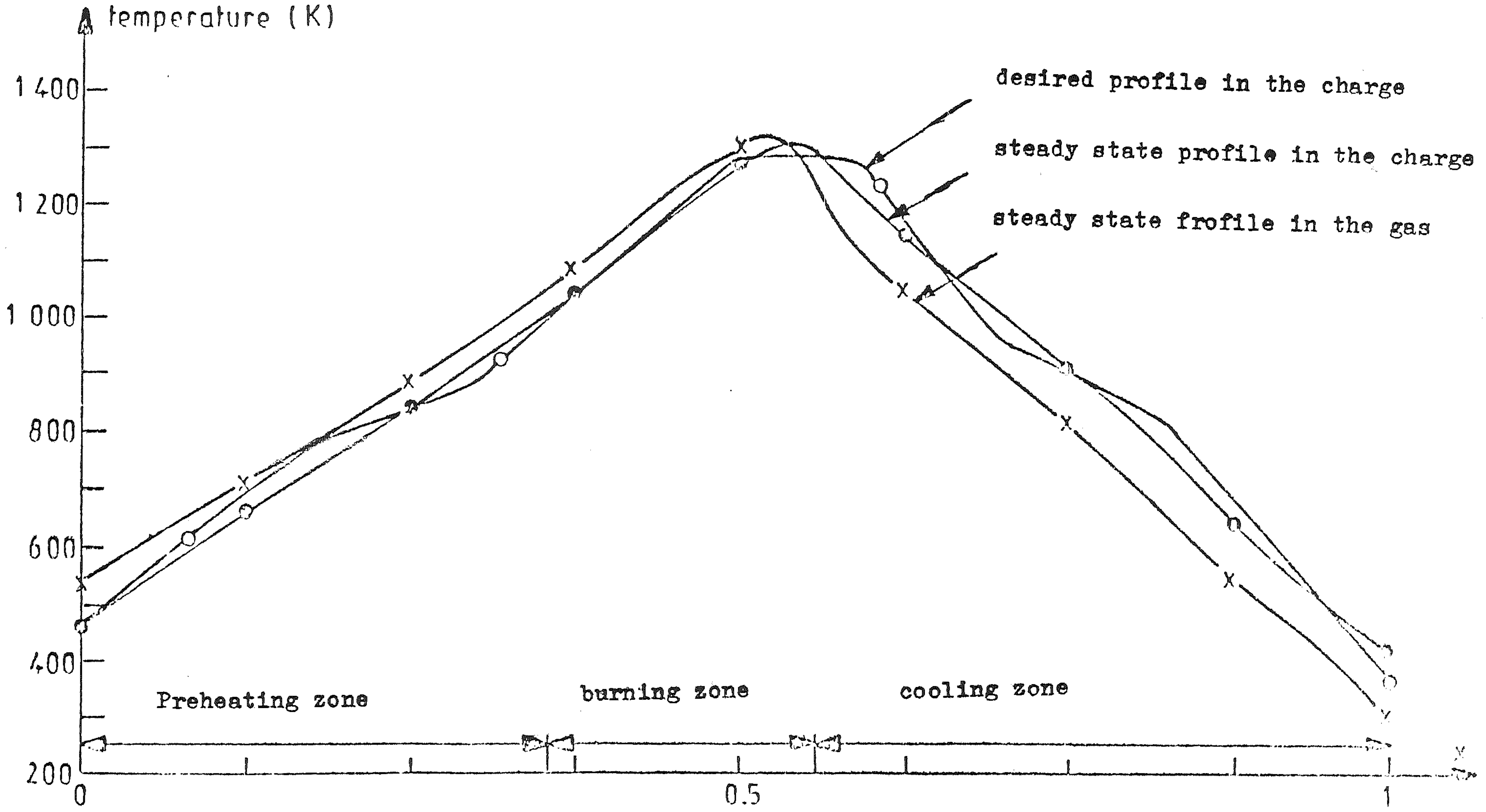

Fig. 3 Temperature profiles in steady state

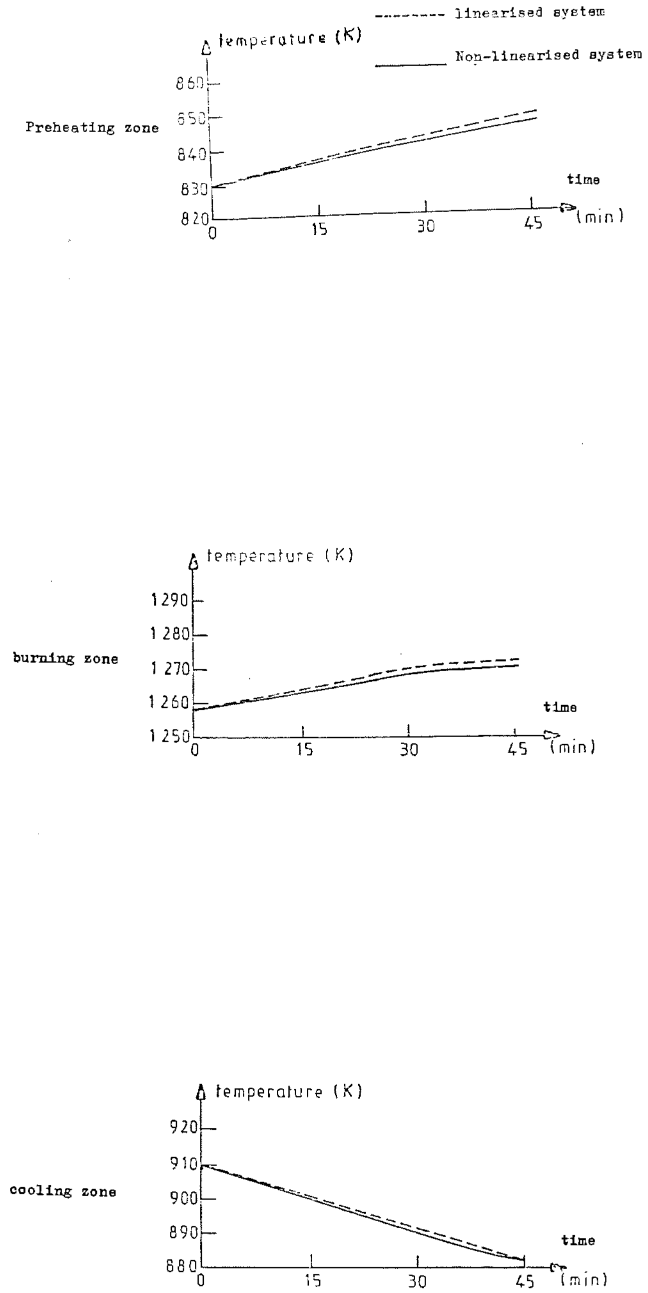

Fig. 4 Comparison of non linear and linear solutions

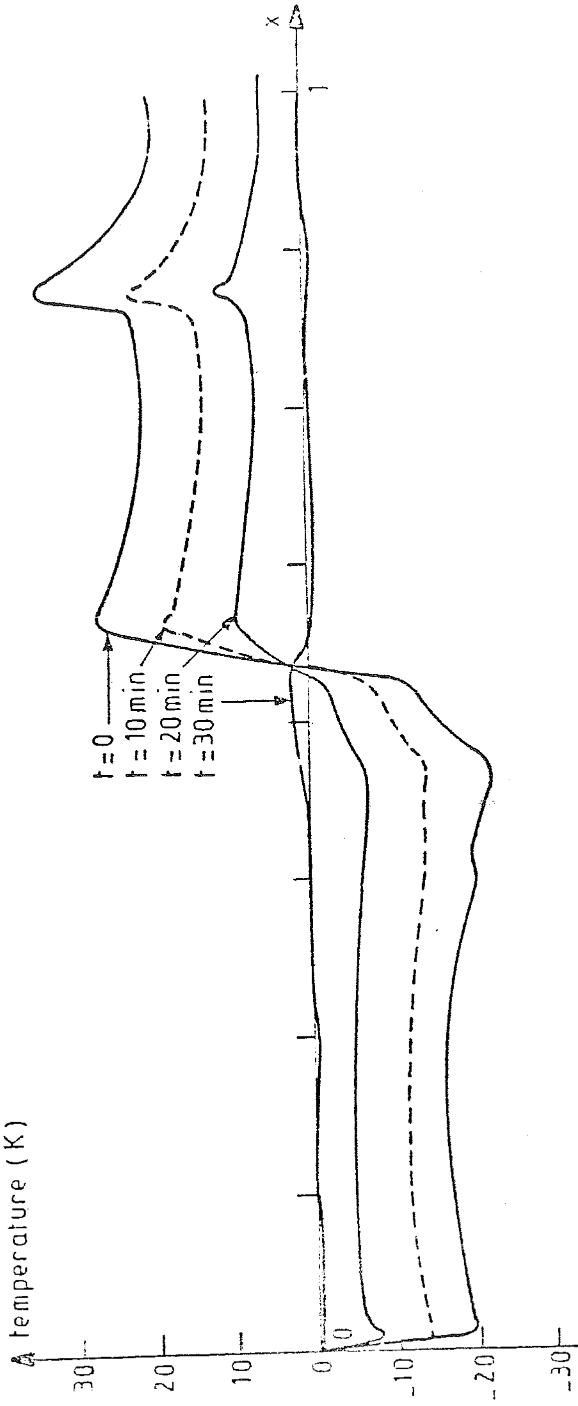

Fig. 5. Temperature variation in the charge

Electricity from the wind

by Marios Pattichis, M.Sc., D.I.C., A.C.G.I., O.C.B.S. Lecturer, HTI

This article aims to outline the basic principles and design considerations of small, electricity producing aerogenerator systems. Experimental work is currently conducted at H.T.I. on three different types of aerogenerator with the general aim of evaluating the reliability, costs and technical problems of such systems for domestic applications.

Power coefficient and tip-speed ratio

Consider an aerogenerator, fig. 1, of radius R which rotates with angular velocity ω in a wind of velocity V, density ρ and viscocity μ.

The mechanical power, P, extracted from the wind depends on the above parameters

$$P = \text{function } (\rho, V, \omega, \mu, R) \qquad (1)$$

and through the method of dimensional analysis it can be shown that

$$\frac{P}{\frac{1}{2}\rho AV^3} = \text{function}\left(\frac{\omega R}{V}; \frac{\rho VR}{\mu}\right) \qquad (2)$$

where $P/1/2\ \rho\ AV^3$ is the power coefficient Cp (note that this is the aerodynamic efficiency as it is the ratio of power extracted P, to power available in the wind $1/2\ \rho\ AV^3$) and A is the swept area of the aerogenerator; the term $\omega R/V$ is the tip-speed ratio, X, (this is the ratio of tip velocity ω R to wind velocity V); finally, the term $\rho VR/\mu$ is the Reynold's number for the flow, Re

$$Cp = f\ (X; R_e) \qquad (3)$$

Now it turns out that Cp, varies extremely slowly with Re when the latter is greater than 10^5 (and here we are talking about aerogenerators about 20 cm in diameter or more). In practice than

$$C_p = f\ (X) \qquad (4)$$

where the function f depends on type of aerogenerator. It can be shown mathematically that Cp cannot have a value greater than 0.593, but most well designed aerogenerators achieve maximum Cp values of about 0.4 and then the maximum power that can be extracted from the wind is

$$P = 0.4 \times \tfrac{1}{2}\rho\ AV^3$$

In fig. 2 below are shown the Cp Vs X characteristic curves for different types of aerogenerators, e.g. Savonius, vertical axis, horizontal axis etc. In figs 3a, 3b, 3c are shown some actual constructions of small aerogenerators.

Note

1. For the same conditions i.e. same R, same V, the Savonius and the Multiblade types rotate much slower (about 5 times less) than the other types and hence require a correspondingly higher transmission step-up.
2. For a given aerogenerator type the bigger the size R then the slower the rotation at a given velocity V.
3. The effect of Reynold's number on the Cp Vs X curves is small for Reynold's numbers greater than 10^5.

Example

Consider a Giromill aerogenerator of radius 2m and height of blades 2m in a wind of velocity 8 m/s. If the aerogenerator operates at tip speed ratio 5 with a maximum Cp value of 0.4 then the angular velocity, ω, is

$$\omega = \frac{X_o V}{R} = 20 \text{ rad/s}$$

where Xo signifies the tip speed for maximum Cp. The power extracted is

$$P = 0.4 \times \tfrac{1}{2}\ \rho\ AV^3 = 0.4 \times \tfrac{1}{2} \times 8 \times 8^3 = 1000 \text{ w}$$

Transmission and generator Efficiencies

If the aerogenerator is to generate electricity then the mechanical power has to be converted to electrical through a step up system and an electrical generator system. The common car alternators reach full power at around 1500 rpm so the generator shaft has to rotate at around 160 rad/sec. This means that for the above example the step up ratio must be 8.

The electrical power produced is less than the mechanical power extracted from the wind as the transmission and generator efficiencies have to be taken into account. In fig. 4 are shown the various losses along the path of wind power to power supplied to an electrical load.

In aerogenerator design practice the electrical power Pe supplied by the generator is estimated by

$$Pe = c\ AV^3 \qquad (5)$$

where c varies between 0.05 and 0.1 and includes the 1/2 $\rho c_p \eta_t \eta_g$ terms. Now an alternator has the Power v r.p.m. curve as shownin fig. 5.

The generator speed N_R is the speed at which full rated power is reached, whereas speed Nc is that at which power is just produced (cut–in–speed).

The expression (5) therefore should be applied to the point at which the wind velocity V is such that the generater has reached N_R r.p.m. An appropriate value of V must be found therefore at which the aerogenerator operates at maximum Cp and the generator through the step–up system is close to the rated speed N_R.

Matching of Aerogenerator to Generator

For a given site the wind velocity distribution is shown in fig. 6a. However, the energy depends on V^3, and therefore the Energy vs Velocity curve peaks at a higher velocity, fig. 6b, at about 2V′, where V′ is the mean velocity at the site. Since the energy available at a site is highest at a velocity (known as rated speed V_R) around 2V then we must ensure that the aerogenerator operates near the maximum Cp point and the generator is operating at rated power when the wind velocity is V_R. This means that if we denote "Xo" the tip–speed for maximum Cp and "i" the step up ratio then,

$$Xo = \frac{\omega R}{V_R} \qquad (6)$$

$$2\Pi \frac{N_R}{60} = i\ \frac{X_o\ V_R}{R} \qquad (7)$$

Example

In the above example if the rated speed is 8 m/s and the rated power of the generator is reached at 1500 rpm then the calculated step up of i=8 is correct.

Expression (7) illustrate several important points:

(a) Sites with high V_R require less step–up,

(b) Large aerogenerators require high step–up and

(c) Generators with low N_R are desirable for low step up.

Now the generator will start producing electricity at a speed Nc r.p.m. This means that since the step up is fixed the wind velocity at which Nc is reached is N_R/N_C times smaller than the V_R velocity and is known as the cut–in–speed Vc.

For most generators N_R/N_C is about 2.5 which makes the Vc about 40% of V_R and about 70% of V′.

Furling Speed

For structural reasons the aerogenerator system hus to be shut down for wind velocities higher than the furling speed V_F. One can design an aerogenerator to withstand stresses up to all wind speeds but this makes it unnecessarily heavy and expensive. In practice the furling speed is about 4V′ because the energy available for greater velocities is neglibigle. due to the relative scarcity of such high wind velocities.

Savonius Aerogenerator

This type of aerogenerator, fig. 7, has a lot of advantages: it is easily constructed, it is self starting, does not require alignment into wind; however it suffers from rather poor Cp and has low angular velocities. From extensive research done abroad on Savonius performance, for different configurations, the best geometry is that shown in fig. 8a. The various parameters that define this shape have been developed and can be used to obtain the shape for any value of R. The Cp Vs X curve for this best geometry is shown in fig. 8b.

A Savonius aerogenerator system is currently under construction at H.T.I. Unfortunately in Nicosia the mean annual velocity is 2 m/s whereas for the seaside areas around 5 m/s. The design is based on the latter areas, thus the rated velocities can be fixed at 10 m/s. The aim is to match the Savonius to an ordinary car alternator, a Lucas 12V, 30A alternator, with a cut in speed at 600 rpm and rated speed at 1500 rpm. (maximum allowable speed 11000 rpm). Using equation (5) the required area is calculated

$$A = \frac{Pe}{0.05\ V_{R3}} = \frac{360}{0.05 \times 10^3} = 7m^2$$

where a realistic value for c=0.05 is used. The step up ratio can be calculated by using equation (7).

$$i = \frac{2\Pi N_R/60}{(Xo\ V_R/R)} = 20$$

where the radius is taken as 1m (the height will be 3.5m)

Giromill Aerogenerator

This type is not self starting, but this can be overcome with the aid of a small Savonius acting as a starter, fig. 9. The Giromill constructed at H.T.I. will use a Lucas 12V, 30A alternator and from (5) the area is

$$A = \frac{P_e}{0.1\ V_R{}^3} = \frac{360}{0.1 \times 10^3} = 3.6 m^2$$

The blades will be located at a radius 1.5m from the axis and have a height 1.2m. From (7) the step–up ratio required is

$$i = \frac{2\pi N_R/60}{X_o\ V_R/R} = 6$$

where a value of Xo=4 is used here.

Solidity:

From theoretical work (and practicalexperience) aerogenerators which use airfoil shaped blades must have a certain "solidity" for optimum operation. Solidity is defined as Area of blades/Area A, and in fig. 10 is shown the solidity as a function of tip–speed ratio. In our case the solidity must be around 0.125 which means that the total blade area is 0.4 m^2. Hence if the blades are 1.2m high the chord length must be 12.5cm for optimum operation. The shape of the blade is that of NASA 0012 (Ref. 1).

Horizontal axis Aerogenerator

This requires rather higher technological know-how than the above two types. However, it has a high cp value and requires less step–up. From (5) the area A is

$$A = \frac{360}{0.1\ V_R{}^3} = \frac{360}{0.1 \times 10^3} = 3.6\ m^2 \rightarrow R = \sqrt{\frac{3.6}{\pi}} = 1m$$

Note that for Nicosia the radius R would be 4m since the rated wind speed is around 4 m/s. The horizontal axis aerogenerator operates at a tip speed ratio of about 6. The step up is thus

$$i = \frac{2\pi N_R/60}{X_o\ V_R/R} = 3$$

As the proposed design is for 2 blades and the solidity is 0.05 then each blade must have an area of 0.09 m^2 or a chord of 10 cm approximately. The main parts are shown in fig. 11.

Discussion

The above show the determination of area A and step–up ratio for optimum performance of the three different designs in areas where the annual mean velocity is around 5 m/s (coastal areas). The aim of constructing three different designs is to evaluate the costs and technical problems arising in each and come to a conclusion as to the best design. A major constraint in this exercise is to use locally available materials and technical knowhow.

The construction of the blades presents a major problem. The various possibilities are shown in fig. 12 while at H.T.I. a construction similar to the rib–tube spar and sheet metal skin is investigated as well as a fiber glass construction. The applications are illustrated in fig. 13.

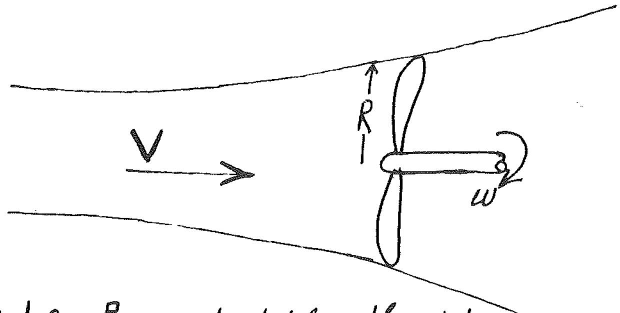

Fig 1 : Power extracted from the wind

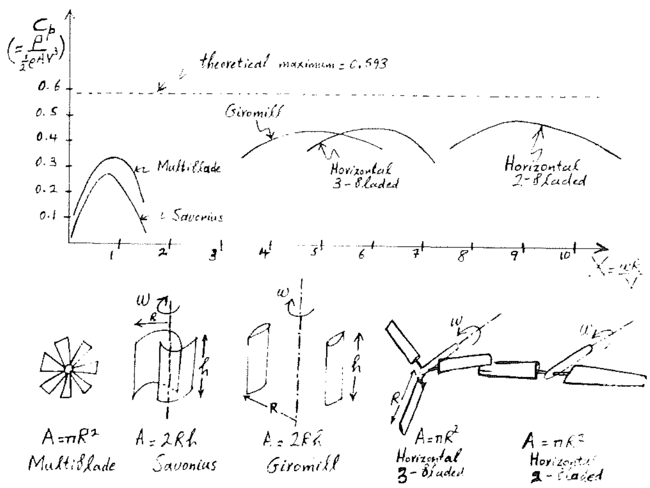

Fig 2 : Common types of Aerogenerators

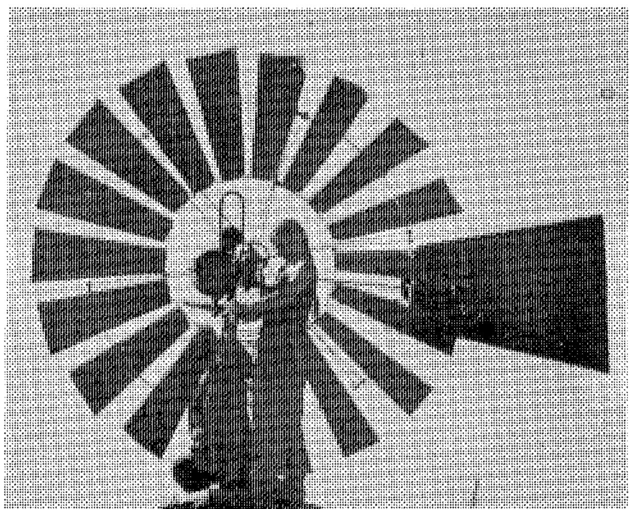

With a diameter of 6 feet, this wind machine can lift about 500 gallons of water per hour in a 15 mph wind.

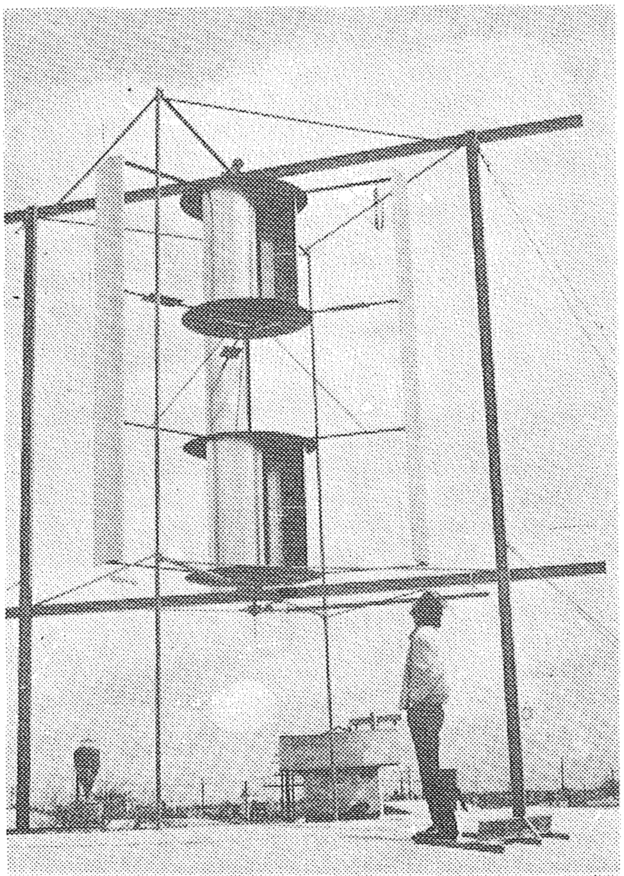

Small Savonius rotors along the axis help accelerate this straight-bladed Darrieus rotor through the stall region.

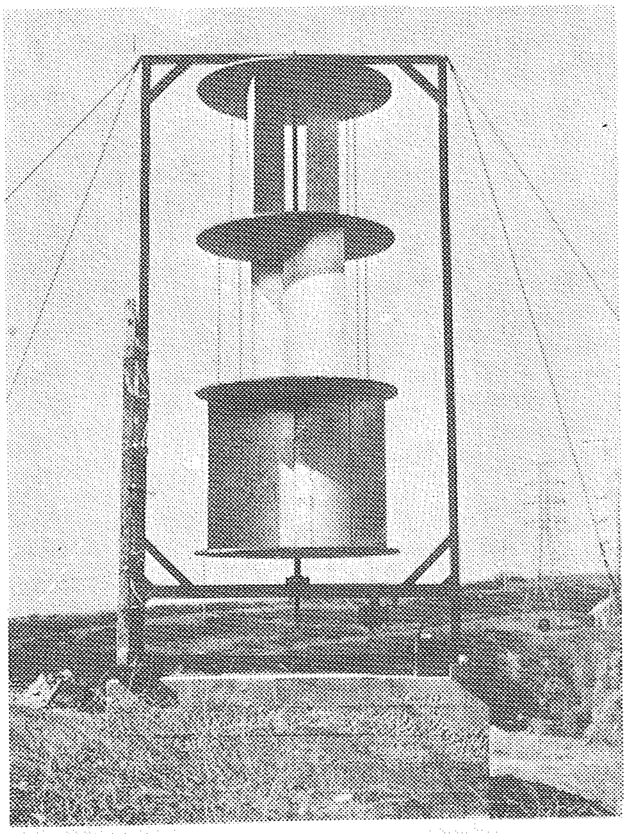

A three-tiered Savonius rotor designed to generate electricity.

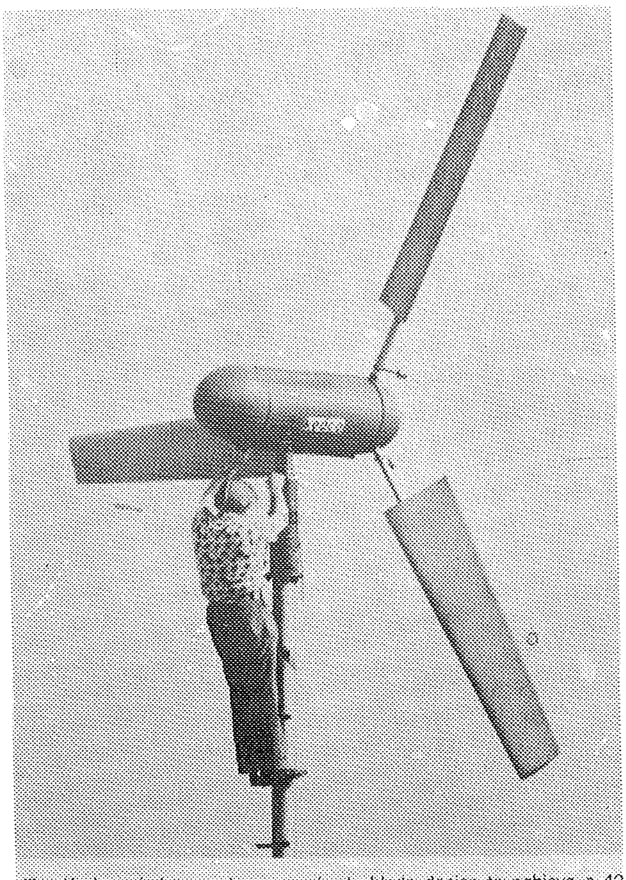

The Kedco wind generator uses simple blade design to achieve a 42 percent peak rotor efficiency.

Fig. 3

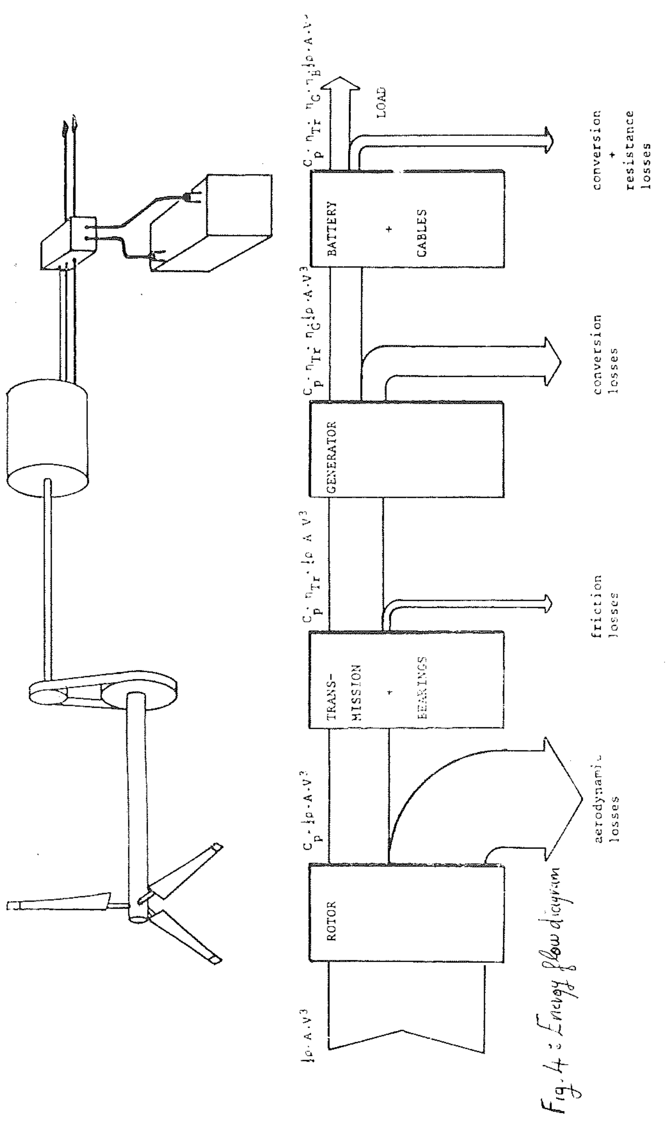

Fig. 4: Energy flow diagram

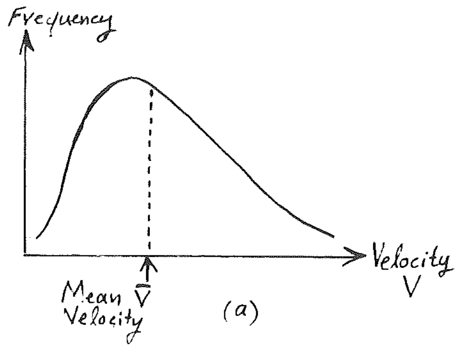

(a) Velocity frequency curve;

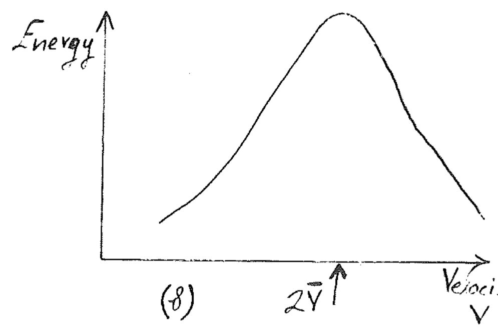

(b) Energy distribution curve

Fig 6

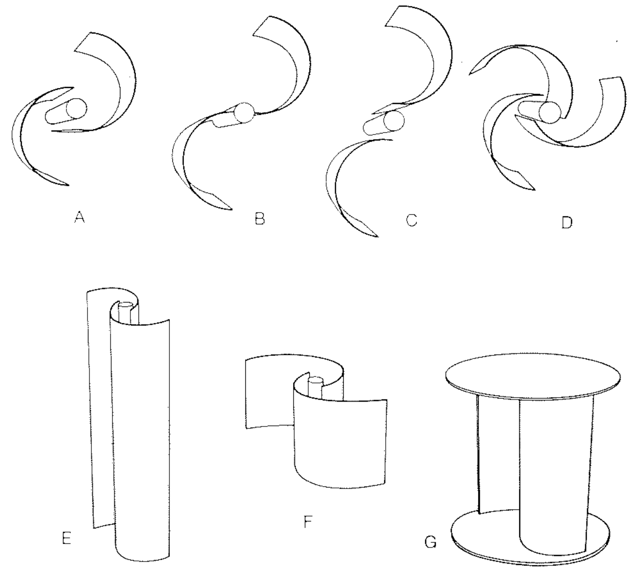

Savonius rotor design options include the intervane gap, number of vanes, aspect ratio, and tip plates. Option E has a much higher aspect ratio than F, and the tip plates in option G improve the rotor performance at low rpm.

Fig. 7

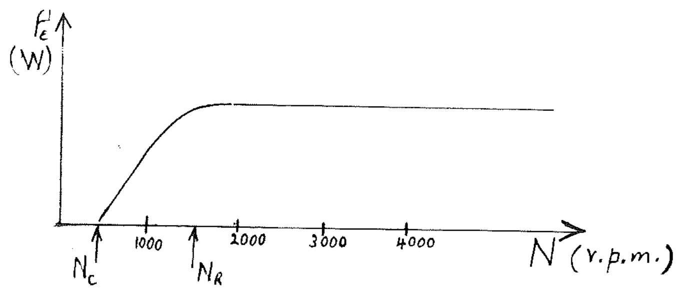

Fig 5 : Electrical power output of a typical car alternator

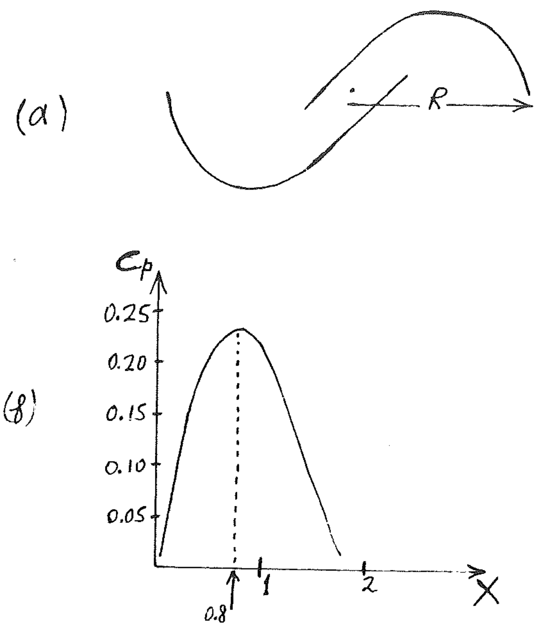

Fig. 8: (a) The best configuration of Savonius and
(b) its characteristic performance curve

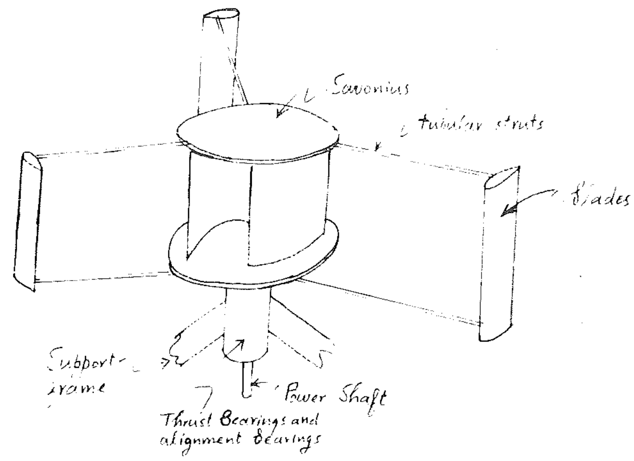

Fig. 9: Giromill with Savonius starter

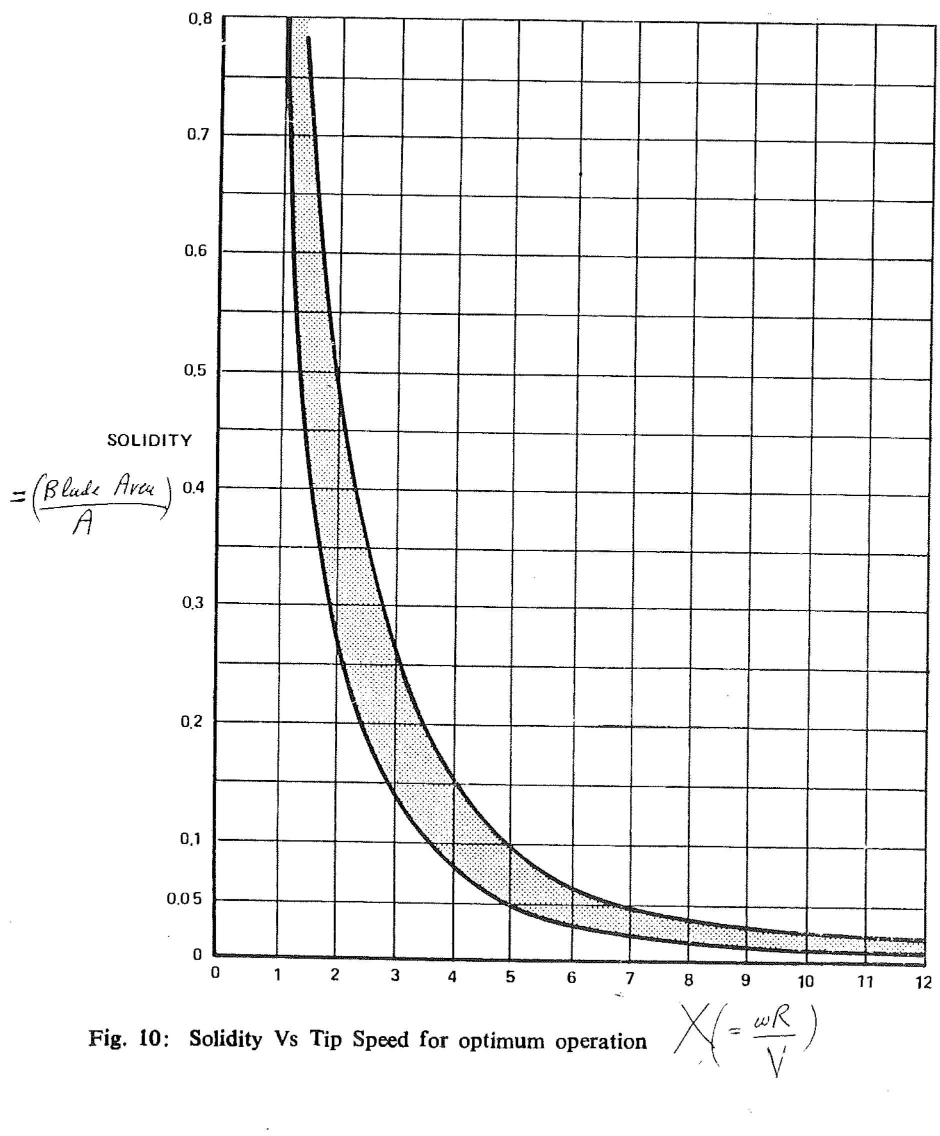

Fig. 10: Solidity Vs Tip Speed for optimum operation

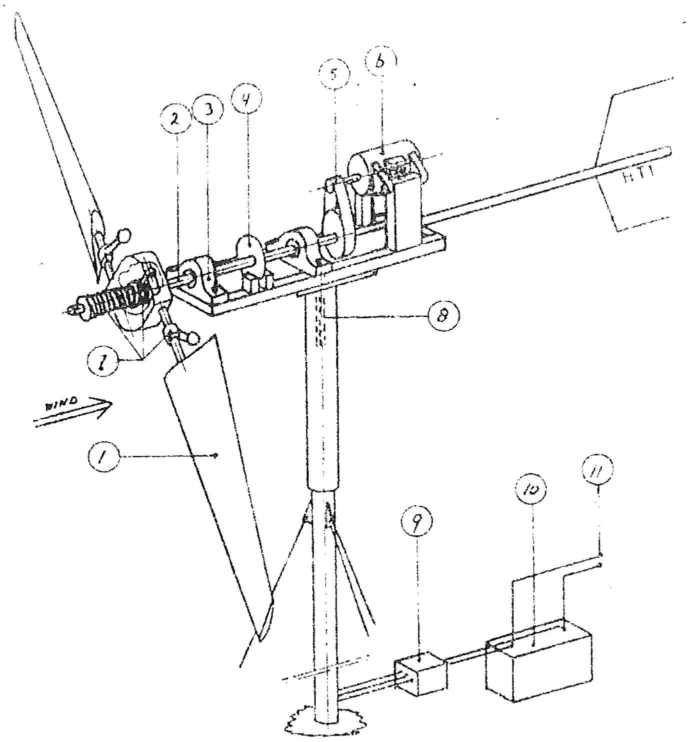

Fig 11: The components of a typical wind–electricity conversion system:

1. windrotor
2. rotor shaft
3. shaft bearings
4. brake
5. transmission
6. generator
7. protective device against high wind speeds and over speed of the rotor
8. wiring (eventually sliprings) to conduct the generated electricity to the foot of the tower
9. generator control device (field current, voltage control)
10. storage battery (in case of DC systems)
11. load connection

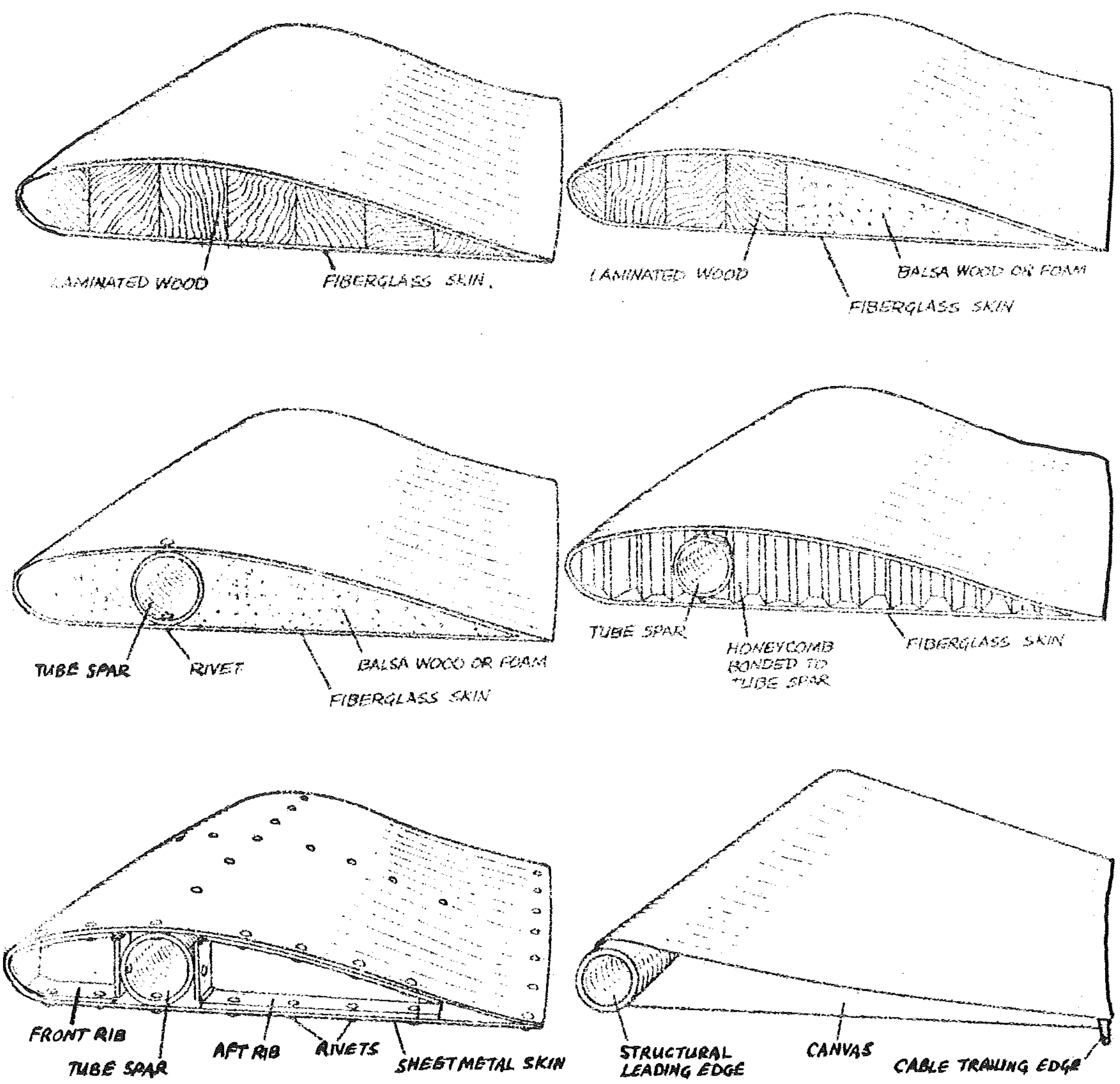

Fig. 12: Types of Construction for blades

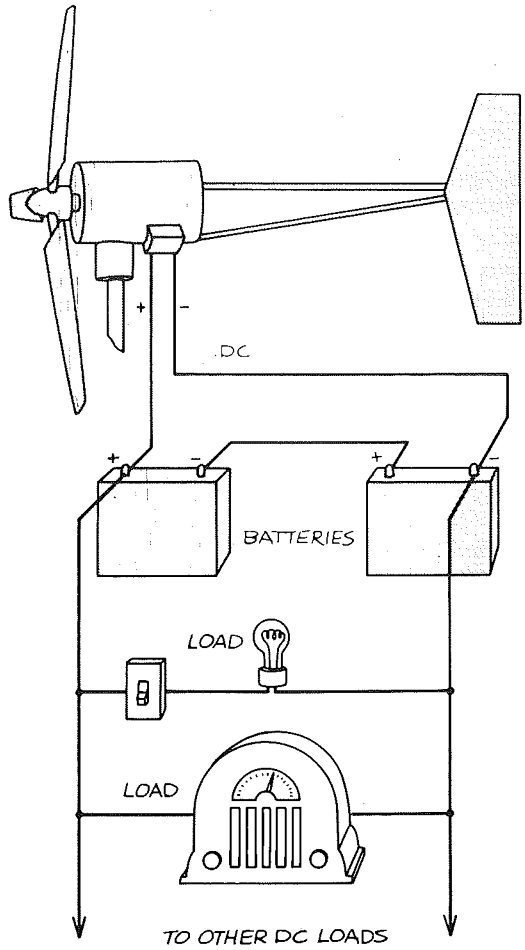

+
-
DC
BATTERIES
LOAD
LOAD
TO OTHER DC LOADS

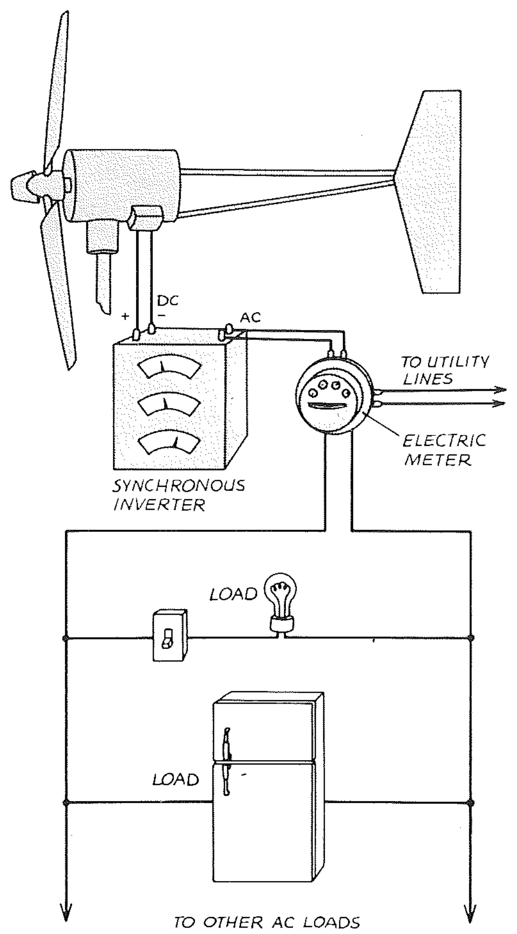

DC
+
-
AC
TO UTILITY LINES
ELECTRIC METER
SYNCHRONOUS INVERTER
LOAD
LOAD
TO OTHER AC LOADS

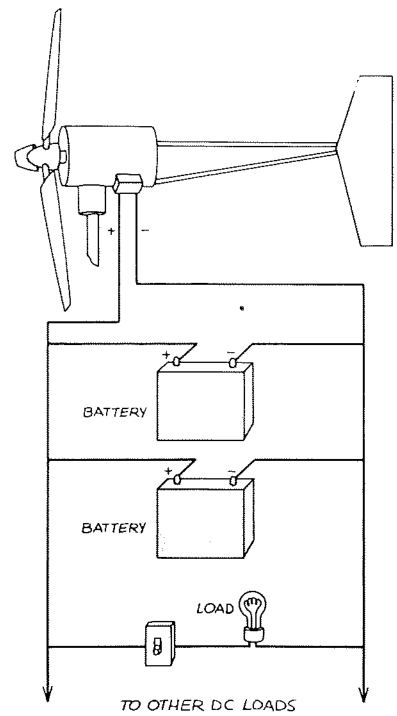

BATTERY
BATTERY
LOAD
TO OTHER DC LOADS

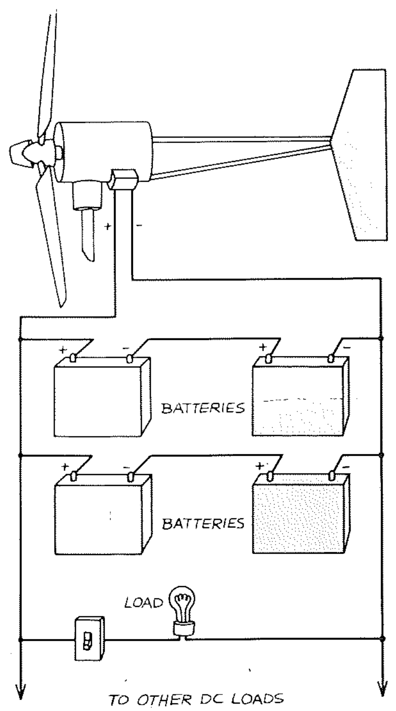

BATTERIES
BATTERIES
LOAD
TO OTHER DC LOADS

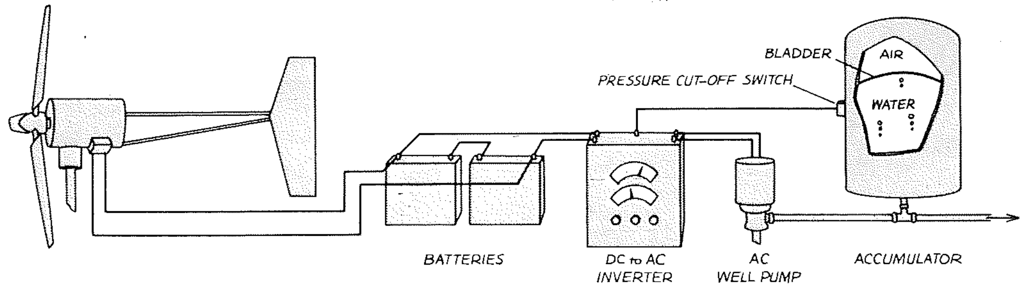

BLADDER
AIR
PRESSURE CUT-OFF SWITCH
WATER
BATTERIES
DC TO AC INVERTER
AC WELL PUMP
ACCUMULATOR

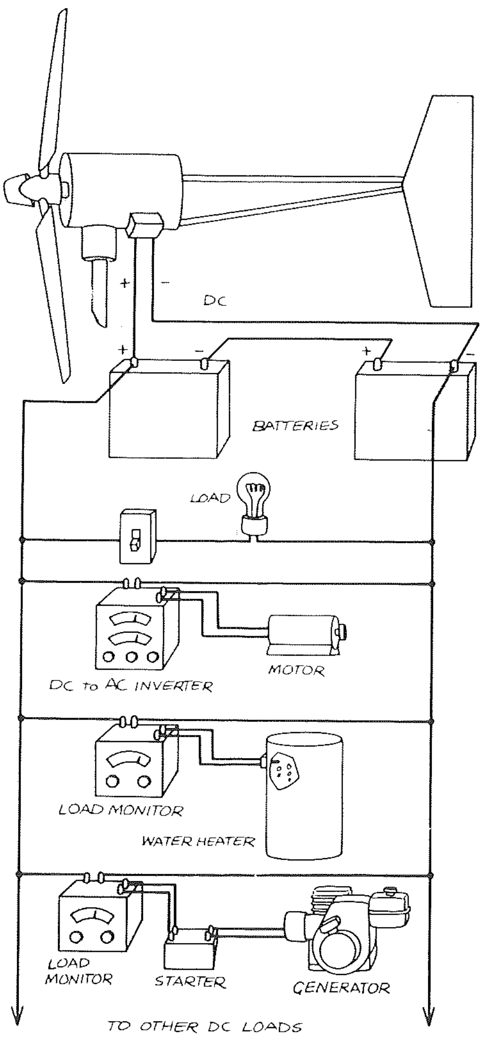

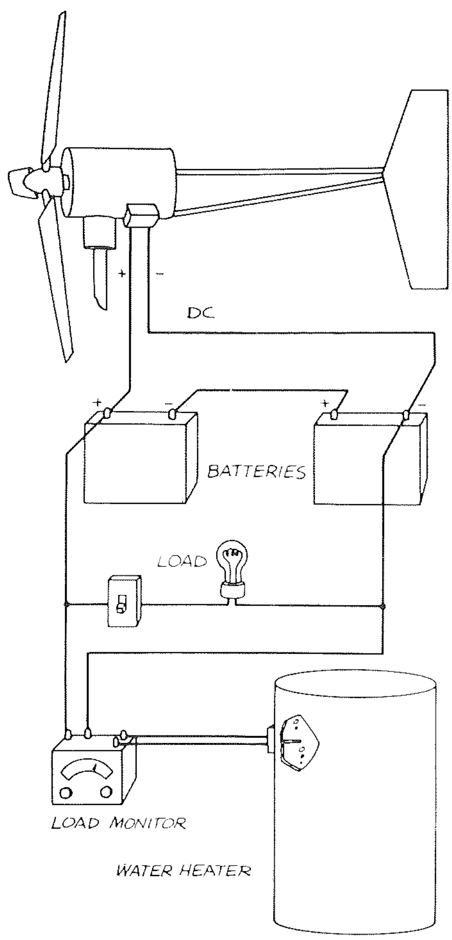

Series battery wiring with a load dumper. When the load monitor senses an overcharged battery, it diverts current to an electric water heater.

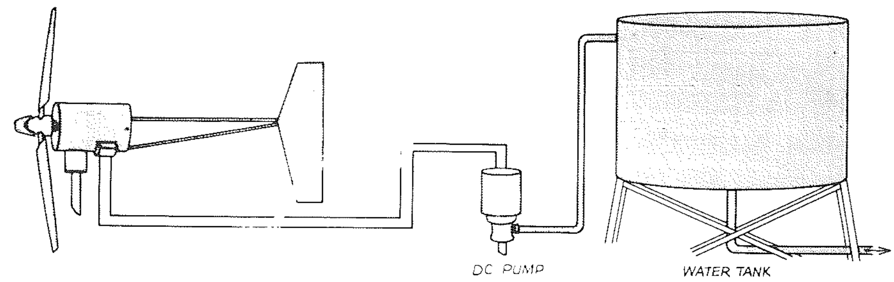

A simple wind-powered electric pumping system. The only storage is a large water tank.

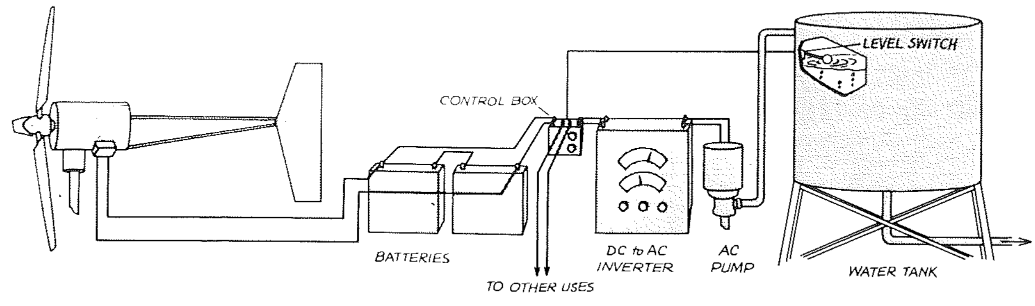

A complete wind-electric water-pumping system. The well pump is just one of several loads powered by this windcharger.

Fig. 13

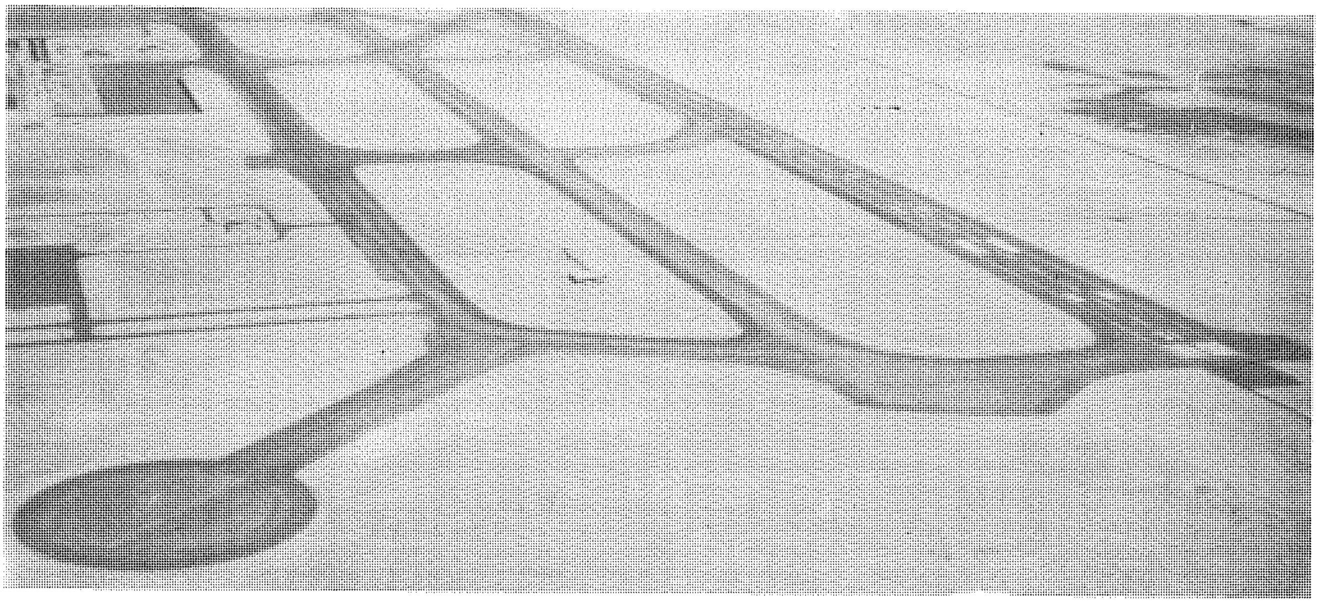

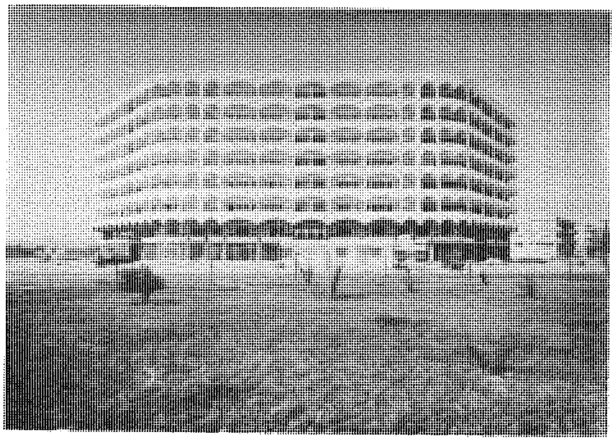

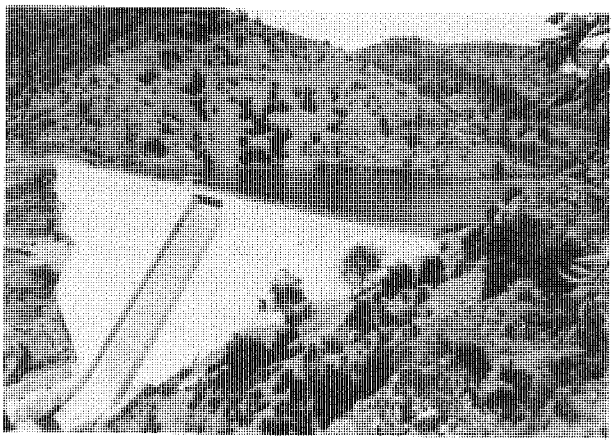

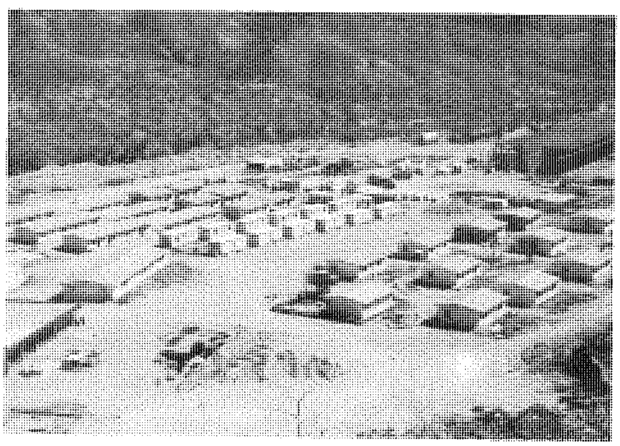

Solar Refrigeration System Zeolite-Water

by I.M. Michaelides, B. Sc. (Eng.) Dip. En. Sol. (FR), Lecturer, H.T.I.

Abstract.

The interest of solar refrigeration lies in the fact that the demand for cooling coincides with the availability of solar radiation. Of the various systems proposed the absorption and adsorption ones present some advantages over the vapour compression systems powered from electricity produced by photovoltaic or thermal conversion.

The zeolite–water adsorption system of the intermittent operation uses water as refrigerant and zeolite–13x as adsorbent; it is simple in construction, does not comprise any moving parts and operates with temperatures attainable with flat–plate solar collectors. The system can be developed and used in both the domestic (household refrigerator) and the industrial (preservation of fruits) sectors.

Introduction

The utilisation of solar energy for the production of refrigeration intended for either food preservation or air conditioning presents two main advantages:

(i) the demand for refrigeration (cooling) is generally maximum when the solar intensity is maximum;

(ii) the production of refrigeration for the preservation of food and medicines for the welfare of the humanity is of major importance in the hot rather than cold regions. Refrigeration and air conditioning, which under other circumstances could be considered as a luxury, tend to become a necessity for the developing countries with hot climates.

What is of primary importance in this case is that the technology must be s i m p l e and relatively n o e x p e n s i v e which implies the maximum use of local materials.

According to the system to be employed and the degree of cooling required, the temperature of the energy source can be of the order of 60, 90 or 120° C. The production of such temperatures is not in fact a problem if the heat source is a conventional one; however, for a solar system the situation is different: while a temperature of 60° C can be obtained easily with a flat plate solar collector, higher temperatures will bring about a considerable reduction in the collector efficiency in the case of flat plate collectors.

High temperatures can be produced by means of concentrating collectors the construction and operation of which are not simple and effectively their cost is high.

Of the various methods which can be employed to produce refrigeration from solar energy the vapour compression and the absorption systems are of particular interest. The first one utilises the cycle of a thermal machine using steam to operate a turbine which in turn transmits the work produced to a compressor being part of a conventional refrigeration system. This method assumes high temperatures and thus concentrating collectors, tracking systems etc, which mean high cost. On the contrary, the absorption refrigeration system does not require very high temperatures and can operate with temperatures attainable with flat–plate collectors; this is quite feasible in the developing countries and thus more interesting.

Absorption/Adsorption solar systems

Among the various absorption/adsorption refrigeration systems proposed for operation with solar energy the following could operate with flat plate solar collectors:

(i) Acqua–ammonia system (generator temperatures of the order of 80° C).

(ii) Lithium bromide–water system, employing water as the refrigerant (generator temperatures of the order of 90° C).

(iii) Zeolite–water, employing water as the refrigerant (70–80° C).

The zeolite–water system seems to be the simplest one in construction and operation and is quite promising. A brief description of the system will follow.

The zeolite-water couple

The zeolite is a microporous composite (aluminum–cilicate) which has great affinity to water vapour. In a solar adsorption system it plays, alternatively, the role of a "chemical pump" during the evaporation process and the role of a "chemical compressor" during the condensation process. It presents some advantages over other known adsorbents such as activated aluminum, activated carbon and silica gel, the most important being that it presents fort capacity of adsorption at ambient temperatures and low pressures (corresponding to the equilibrium pressure in the evaporator) and low capacity of adsorption at higher temperatures and higher pressures (corresponding to the equilibrium pressure in the condenser). At a pressure equal to one tenth of the saturation pressure of the refrigerant vapour at the adsorption temperature, the adsorption capacity of the zeolite is about 90% of its capacity at saturation conditions. However, the desorption temperature is relatively higher than that of the silica gel.

The refrigerant to be used with zeolite should have a high latent heat of evaporation and a small molecule easily adsorbable. The selection is between water, ammonia and methanol. Of the above fluids water is plentiful and readily available and does not present any technical problems in its use with zeolite.

Description of the system

The zeolite is placed in a closed metal container (preferably copper) under vacuum; the upper cover is externally painted black–matt to act as absorbing plate and the container is used as solar collector. When exposed to the sun, (day cycle: desorption) the collector absorbs the incident solar radiation and the temperature of the container could rise up to 100°C. At about 35–40°C the separation between the solid zeolite and the vapour adsorbed begins, and the pressure increases (desorption phase). The liberated vapour leaves the collector and flows to condenser through valve V1 (V2, V3 closed) fig. 1. When the pressure in the container and condenser reaches the water vapour saturation pressure, condensation begins; the heat of condensation is rejected to the atmosphere and the liquid (water) is accumulated in the liquid receiver.

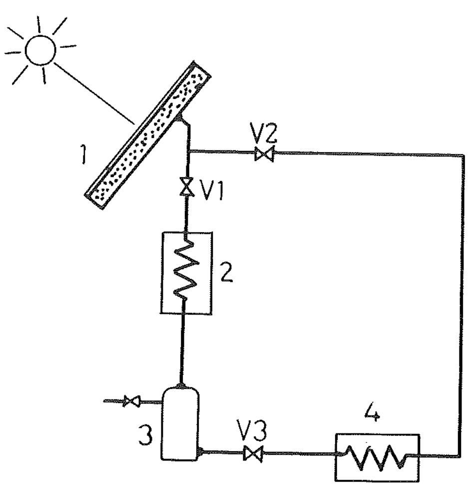

1. Zeolite container/ solar collector
2. Condenser
3. Liquid receiver
4. Evaporator

Fig. 1. Schematic diagram of a zeolite–water adsorption intermittent refrigeration svstem.

During the night (night cycle: adsorption) the zeolite is naturally cooled down to atmospheric temperatures and the necessary condition for the adsorption process is established. The liquid (water) coming from the liquid receiver is introduced into the evaporator where, due to the existance of low pressure, it evaporates by absorbing heat from the surrounding and thus produces refrigeration. Like in a conventional absorption machine, employing water as refrigerant, the pressure in the evaporator is of the order of 6 to 8 mbar and the refrigerant (water) tends to boil at 3 to 4°C.

At the same time, the evaporated refrigerant is adsorbed by the dry zeolite and the heat produced in the collector during the adsorption is rejected to the atmosphere by natural convection (in fact, this heat could be used to heat water for sanitary purposes). At the end of the night cycle the zeolite should have adsorbed the maximum possible quantity of water vapour.

In the morning, the cycle begins again with the sunrise.

Application

The solar zeolite–water refrigeration system can be employed in both the domestic and the industrial sectors to preserve food and other commodities.

A typical refrigerator for household application could incorporate a solar collector having an absorbing surface of 1.5m^2 and containing about 35 kg of zeolite. Under reasonable conditions of sunshine such a refrigerator could produce more than 10 kg of ice which would keep the refrigerator chamber, charged with 15–20 kg of food and other commodities, at a temperature of 3 to 7°C.

The same system could be used in a large scale for food preservation in cold stores (hospitals, hotels etc). It is anticipated that the refrigeration requirements of a cold store having a volume of 15m^3 and properly insulated to reduce heat gains, could be met by a zeolite–water system having a collector area of about 25m^2 containing about 550 kg of zeolite.

The above estimations are based on experimental results obtained in Montpellier (France) by CNRS (1981) and are valid for collectors having a selective coating.

Comments

The intermittent zeolite–water refrigeration system presents many similarities with the conventional cycle, like:

(i) operation at low evaporating pressures (6—8 mbar)

(ii, need for accumulation of liquid refrigerant

The theoretical maximum efficiency of the cooling cycle is practically equal to the ratio of the heat of evaporation of water and the heat produced during the adsorption of water vapour by the zeolite and is around 55%.

The inconveniencies of the system are mainly the following:

(i) need for creating and maintaining low pressures in the system (operation under vacuum)

(ii) need for large quantities of adsorbent; 1000 kg of zeolite are needed to produce one ton refrigeration. This means that the system should comprise bulky collectors.

The advantages of the system are met in its simplicity, its long-lifeness and its flexibility to work at low temperature levels in the hot source; it is also important that the heat produced during the adsorption process can be utilised effectively in heating water for domestic sanitary purposes.

Over and above the advantages outlined, the essential originality of the adaptation of the zeolite-water cycle in solar energy lies in the fact that the "chemical compressor" (zeolite) is integrated in the collector and the machine can operate without any moving parts.

BIBLIOGRAPHY

1. TROMBE F., FOEX M.—"The production of cold by means of solar radiation", Journal of solar Energy, Vol. 1 (1957).
2. CHINNAPA J.—"Performance of an intermittent refrigerator operated by a flat-plate collector", Solar Energy, Vol. 6 No. 4 (1962).
3. ASHRAE—Handbook of Fundamentals (1977).
4. CAHIERS AFEDES—"La Production de froid par l'energie solaire", No. 5 (1978).
5. CNRS—Froid Solaire zeolite—eau (1981).

Spur gears, their manufacture and accurancy testing

by C. K. Tavrou, Lecturer, H.T.I.

Introduction

Gears are a means of transmitting power or motion either by rotation, as in the case of transmission of power from one shaft to another, or linear motion as in the case of transmitting motion from a gear to a rack. A large variety of gear types is available for transmitting motion between parallel shafts or at any other angle required, for any angular velocity ratio, or direction of rotation. Gears are a major mechanical element in the engineering world, and they have been used in sizes varying from as small as having several of them in a lady's watch, to as large as rotating a whole radar installation.

Spur gears are one of the many types of gears and they are the most commonly used for transmission of power or motion in the same plane.

The spur gear

The characteristics of a spur gear are shown in fig. 1 where the face of the gear tooth has an involute profile which is based on the principle of construction

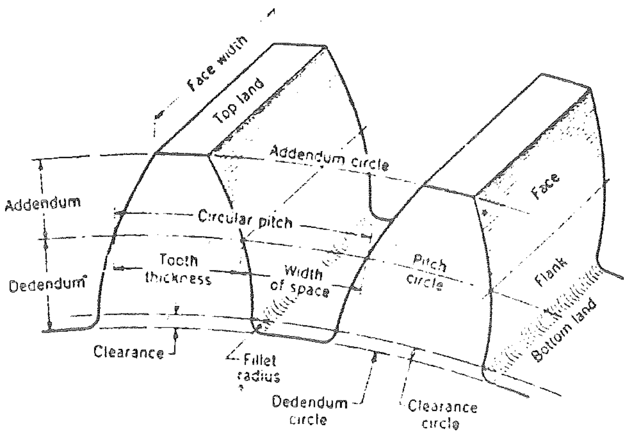

Fig. 1. Characteristics of a spur gear

shown in fig. 2. The formulas shown in Table 1 give the relationship of the various gear elements for both the Module and Diametral Pitch systems used for gear manufacture.

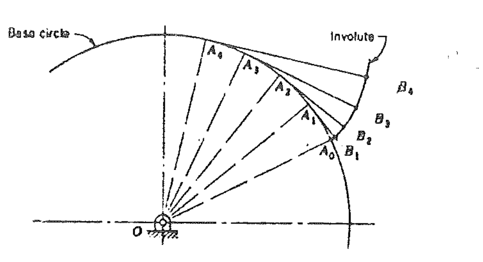

Fig. 2 Principle of constructing an involute curve

TABLE 1 : DATA FOR SPUR GEARS

ELEMENT	SYMBOL	MODULE "m"	DIAMETRAL PITCH
Addendum	A	$A=m$ or $\frac{PD}{Z}$	$A=\frac{1}{DP}$
Dedendum	D	$D=1.157 \cdot m$	$D=\frac{1.157}{D.P}$
Circular Pitch	CP	$CP=\pi.m$ or $\frac{\pi.P.D}{Z}$	$CP=\frac{\pi}{D.P}$
Diametral Pitch	DP	$DP=\frac{25.4}{m}$	$DP=\frac{Z}{P.D}$ or $\frac{\pi}{C.P}$
Number of teeth	Z	$Z=\frac{PD}{m}$	$Z=PD \cdot DP$
Pitch Diameter	PD	$PD=m \cdot Z$	$PD=\frac{Z}{DP}$
Total Depth of Tooth Space	Dt	$Dt=2.157\ m$	$Dt=\frac{2.157}{DP}$
Tooth Thickness	T	$T=\frac{CP}{2}$	$T=\frac{1.5708}{DP}$
Working Depth	WD	$WD=2m$	$WD=\frac{2}{DP}$
Clearance	C	$C=0.8\ m$	$C=\frac{0.157}{D.P}$
Cutside Diameter	OD	$OD=m(Z+2)$	$OD=\frac{Z+2}{DP}$
Centre Distance	Cd	$Cd=m(\frac{Z_1+Z_2}{2})$	$Cd=\frac{Z_1+Z_2}{2DP}$

Manufacture of spur gears

Having established the design elements of a spur gear, the next step is to manufacture it and this is where the difficulty lies. The proper function of a gear depends on the accuracy of its manufacture and the difficult part is to produce the curved part of the gear tooth in the shape of an involute curve. A number of different manufacturing methods are used for gear production, but the intention here is to introduce the most commonly used methods of spur gears either for one–of, or small batch production.

The gear milling method

The Universal Milling machine, is the most commonly used machine for manufacturing 'one–of' gears. The principle of operation here is that a cutter, which has the shape of the gear tooth space, removes material from the blank to produce an equispaced number of tooth spaces round the blank and consequently give an equivalent number of teeth on the gear blank. This can be achieved by both slab and end milling. The principle of gear milling is shown in fig. 3.

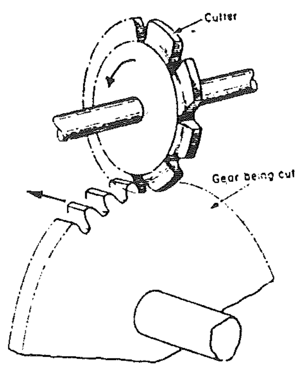

Fig. 3. Principle of gear milling

To achive an equispaced required number of teeth on the periphery of the gear blank, a dividing head has to be used. A dividing head is shown in fig 4.

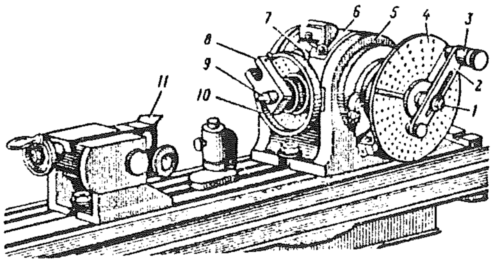

Index-plate universal dividing head
1—shaft; 2—index crank; 3—index-crank pin; 4—index plate; 5—housing; 6—swivel block of housing; 7—lock; 8—driving dog; 9—spindle; 10—plate for direct indexing; 11—tailstock.

Fig. 4. Dividing head

From the basic principle of constructing an involute curve, it can be shown that for each gear with a different Base Circle diameter, a different shape gear milling cutter is necessary in order to achieve the correct involute profile of the tooth. Now, if it is assumed that gears with 20 to 100 teeth with the same module are to be cut in steps of one tooth, then an equivalent number of cutters is necessary i.e. 80 different cutters. Thus, if in a workshop it is desired to cover the above range for 10 different modules, then a number of 800 different cutters should be available, which is obviously impracticable and very expensive. In practice, a compromise is made where a cutter is used for a range of teeth numbers to be cut i.e. The same cutter is used to cut gears with 20 to 25 teeth, another cutter is used for the range 26 to 35 teeth, so that with about 8 cutters the hole range of 20 to 100 teeth gears can be cut. Even though this is a good solution, it is made in sacrifice of the involute shape accuracy.

Gear Hobbing

This is a machiming method designed for spur gear cutting, but it can also be used for similar cutting operations i.e. spline cutting, sprocket cutting etc. The principle behind this method is completely different to that used for gear milling. The tooth profile is no longer produced by a cutter of the same shape as the tooth space. To explain the principle we must refer to fig. 2 and considering a circle with infinite diameter, the Base Circle will be a straight line. In such a case the invohite shape becomes a straight line too. An example of this case is the rack, where the flanks of the tooth are straight lines. When a gear is in mesh with a rack, the same rolling action occurs as when two gears are running in mesh. As mentioned earlier, the cutting tool in gear hobbing does not have the shape of the gear tooth space but it has the shape of a worm and if one imagines the cross section of the worm, the profile will be the same as in the case of a rack. The diffrence of the hobbing cutting tool (hob) and a worm is that the hob has the necessary rake and clearance angles to achieve cutting when brought in mesh with the gear blank. Figs 5 and 6 show a hobbing cutting tool and the action taking place during cutting.

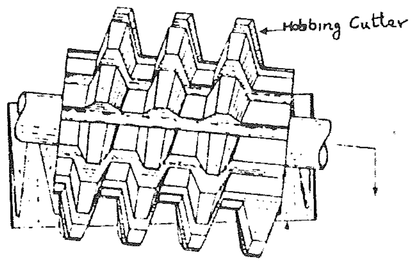

Fig. 5. Hobbing cutter

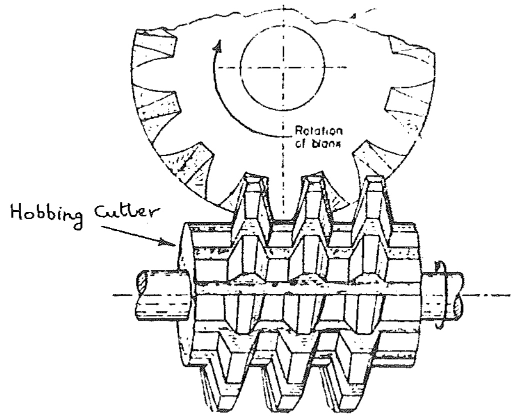

Fig. 6. Hobbing action

The hobbing machine has been designed to support the gear blank and the hobbing cutter, provide the cutting motions i.e. feed motion, rotational motion etc. and the proper relationship of rotation between the cutter and the blank so that they run in mesh. Fig. 7 shows the principle for achieving the rotational relationship between the cutter and the blank. This is done through the index change gears. It has to be noted that for the same module size, only one hobbing cutter is necessary irrespective of the number of teeth required on the gear blank, the same way a rack will mesh with gears of the same module irrespective of the number of teeth on the gear. Another difference from the gear milling method is that the gear being cut will have a true involute shape.

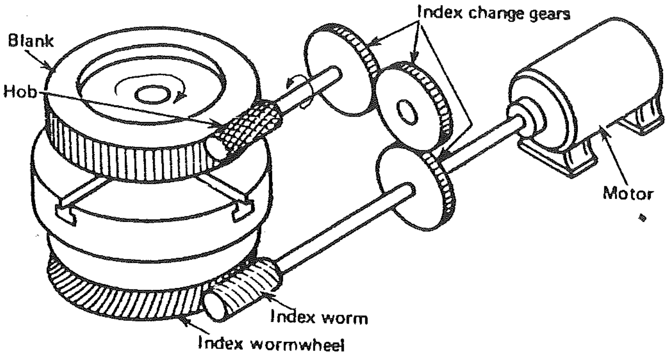

Fig. 7. Gear hobbing principle

Gear shaping.

In this case the cutter has the shape of a gear with the necessary rake and clearance angles to achieve the cutting action, fig. 8.

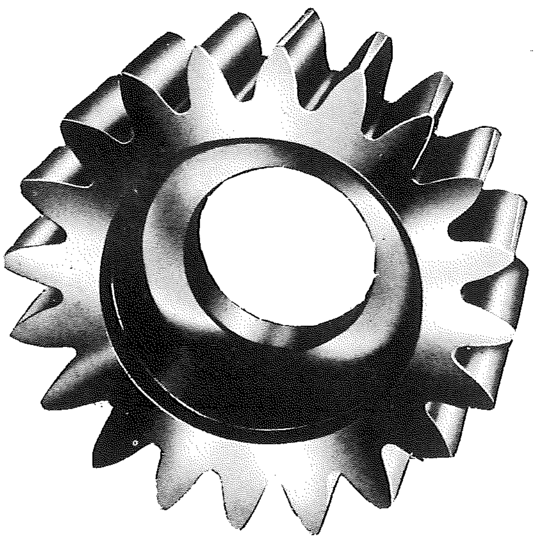

Fig. 8. Gear shaping cutter.

The cutter is reciprocating when brought in contact with the gear blank and at the same time rotating in mesh with the gear blank. At the end

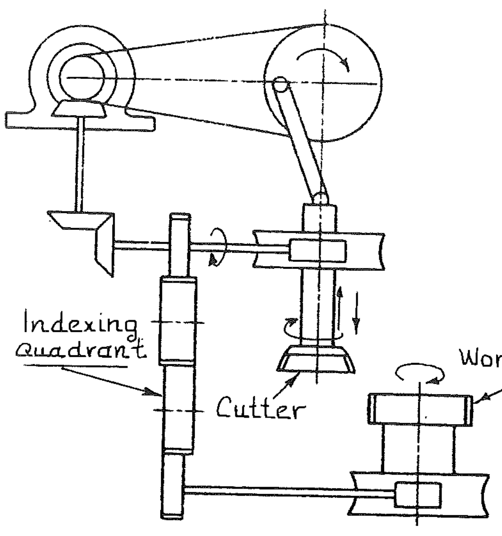

Fig. 9. Motions of gear shaping.

of this operation the gear blank is cut. The rotational relationship between the cutter and the blank is achieved through the indexing Quadrant. All the motions of the gear shaping method are shown in fig. 9. With this type of gear cutting, as in the case of gear hobbing, one cutter can be used for cutting gears with any number of teeth, and the profile of the gear tooth is also a true involute. One of the main advantages of this method over the other two is that internal gears can also be cut.

Accuracy tests on a gear

As in every other machining process, the final product has to be tested for its accuracy against the design requirements. Due to the nature of a gear, other than testing its external and root diameters, special methods or measuring instruments are required for gear testing. The elements to be tested on a spur gear are its tooth thickness, tooth profile, pitch, eccentricity and depth of cut. The method and instruments for testing the tooth thickness and pitch accuracy will only be covered in this article due to its limited space as well as because these two are the most important tests (in the opinion of the writer) and can be performed easily without the need of expensive instruments.

(i) Tooth thickness test

Due to the fact that gear tooth thickness is varying all along its height, the thickness has to be measured at a specific point and comparing the measured value with a calculate value for the same point on the gear, its accuracy can be established.

To calculate the thickness of the tooth, a formula shall be derived with the aid of fig. 10. The thickness 'W' of the tooth has to be determined at a specific height 'h'.

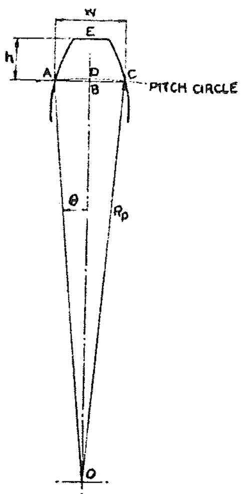

Fig. 10

$$W = 2AB$$

considering triangle ABO

$$AO = R_p = \frac{D}{2} = \frac{NM}{2}$$

$$\Theta = \frac{360^0}{4N} = \frac{90^0}{N}$$

$$\sin\Theta = \frac{AB}{AO}$$

$$AB = AO \sin\Theta = \frac{NM}{2} \sin\left(\frac{90^0}{N}\right)$$

$$W = NM \sin\left(\frac{90}{N}\right)$$

$$h = OE - OB$$

$$\text{and } OE = Rp + \text{Addendum} = \frac{NM}{2} + M$$

$$OB = OA \cos\Theta = \frac{NM}{2} \cos\left(\frac{90}{N}\right)$$

$$\therefore h = \frac{NM}{2} + M - \frac{NM}{2} \cos\left(\frac{90}{N}\right)$$

$$h = \frac{NM}{2} \left[1 + \frac{2}{N} - \cos\left(\frac{90}{N}\right) \right]$$

(D —Pitch Circle Diameter)

(N —no of teeth on the gear)

(M —module)

(Rp—Pitch Circle Radius)

The instrument to test the tooth thickness at a predetermined height is shown in fig. 11 which in fact is a double scale vernier caliper.

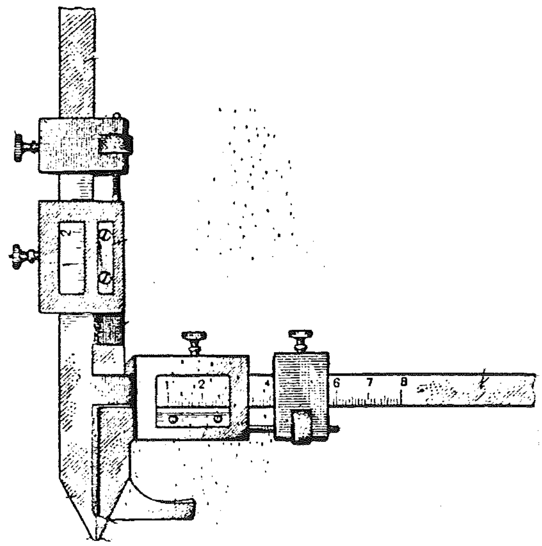

Fig. 11 Gear tooth veririer caliper

(ii) Pitch-to-pitch test

A special instrument shown in fig. 12 is adjusted so that its indicator reads zero when positioned approximately at the pitch circle, and then moved on each tooth of the gear indicating any difference between the adjacent distances. A graph may be drawn from the results which will indicate the cumulative pitch error of the gear.

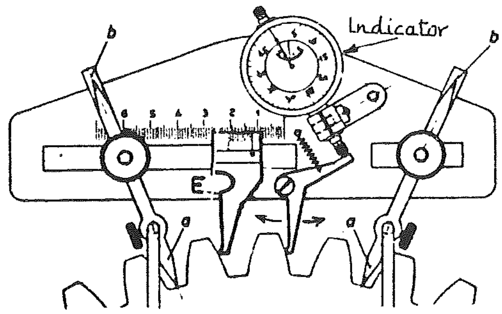

Fig. 12. Pitch to pitch comparator

Selection of overcurrent protective devices in electrical installation design

by E. Michael B. Sc. (Hons), Instructor H.T.I.

Abstract

This article deals with the procedures concerning the selection of overcurrent protective devices as laid down by the new 15th edition of the IEE wiring Regulations.

In particular the selection of the suitable devices for overload and short-circuit protection are dealt in detail. The principles of the "Energy let-through" approach are used in conjunction with the adiabatic line of the conductor for the estimation of the reliable time limits of the protective device.

Introduction

Among the fundamental requirements for the safe use of the electrical installation is the need for overcurrent protective devices (fuses and circuit breakers). The aim of these devices is to prevent any damage of the electric circuits or the electrical equipment, resulting from overheating due to excess currents through these circuits.

For the efficient functioning of the protective devices Regulation 13.3 of the IEE Wiring Regulations requires that they must:–

a) Operate automatically in case of faults and overloads.

b) Be of adequate breaking and or making capacity.

c) Are suitably located and are constructed so as to prevent danger from overheating, arcing or the scattering of hot particles when they come into operation and to permit ready restoration of the supply without danger.

Types of Overcurrents.

The conditions of overcurrents in an electrical installation are classified as "Overload Currents" and "Short Circuit Currents".

Overload currents are defined as overcurrents occurring in a circuit which is electrically sound. They range from a few percent above the rated current to four or five times this current. The protective device must interrupt the circuit to avoid the heating effects of the excess current in the conductors which will melt or deteriorate their insulation or even destroy the overloaded equipment.

Short circuit currents are defined as overcurrents resulting from a fault of negligible impedance between live conductors having a difference in potential under normal operating conditions. This current is very often of the order of 1000 times the nominal current of the protective device. Under such conditions the speed of operation and the ability of the protective device to withstand the enormous energy released are of prime importance. In addition the arcing problems during operation and the electromagnetic stress due to the high currents must be seriously considered. For this reason switchgear and circuit breakers are rated according to the fault current, they can withstand during operation, in orders of kilo-Amperes.

Protection against Overload Currents.

Overload protection is afforted by the following devices:–

a) Semi-enclosed (vewirable) Fuses (BS 3036) and cartridge fuses for use in plugs (BS 1362).

b) High Breaking Capacity (HBC) fuses (BS 88 and BS 1361)

c) Circuit Breakers, both miniature and moulded-case types (BS 3871).

For effective overload protection a protective device must be used to protect any circuit where change of equipment capacity or conductor size is existing. The protective device nominal current (In) should be greater than the design or load current (I_B) so that smooth operation is ensured. Similarly the current carrying capacities of any conductor (I_Z) should be greater than (In).

Thus

$$I_Z \geq I_n \geq I_B$$

1. Protective device effective operation

The current causing effective operation of the protective device (I2) is defined as that current which when flowing through the device will cause its operation within the "conventional time" which is 1 hour. Thus for a BS 88 fuse I2=1.6 In, for a B5 3871 Circuit breaker I2=1.5 In and for semienclosed fuses I2=2 In.

Following Regulation 433-2 which requires in part 3 that the current causing effective operation of the protective device should not be greater than 1.45 Iz, but in spite of that for the first two types of devices this Regulation is satisfied. However for a semienclosed fuse is not acceptable and the conductor current rating must be multiplied by 0.725.

The protective devices are specified by their nominal current or current setting (In) which tney allow indefinitely to the circuit they protect.

If then an excess current is drawn from the supply they will interrupt the circuit at a time which is getting rapidly smaller as the excess current increases. The following figure 1 shows the typical Time/current characteristic for a 30A semienclosed fuse and a 30A miniature circuit breaker. More graphs are included in Appendix 8 of the IEE Wiving Regulations.

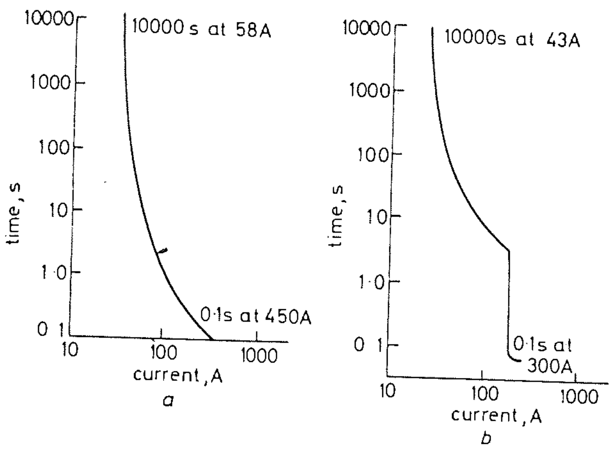

Fig. 1 *Time/current characteristics*
a 30A semi-enclosed fuse
b 30A miniature circuit breaker type 3

The Time/current characteristics are drawn on a logarithmic scale. The different shape for the miniature circuit breaker is due to the completely different principles of operation. The circuit breakers are mechanically operating devices and they face problems of the inertia of their moving parts. Also they require a minimum time for operation irrespective of the value of the fault current.

2. *Position of the Overload Protective Devices.*

The devices shall be connected at every point where a reduction of the current carrying capacity of a conductor is existing. However if there are no branch connections on this conductor the device for overload protection may be installed at any position of this conductor.

3. *Omission of devices for overload protection*

Under certain conditions Regulation 473–3 disregards overload protection as indicated below:–

a) For conductors which are not likely to be overloaded.

b) For circuits where unexpected opening could cause danger such as lifting magnets or exciter circuits.

c) Secondary circuits of current transformers.

d) For conductors situated on the load side of the point where a reduction occurs with effective overload protection on the supply side of that point.

Short Circuit Protection

In determining suitable protective devices for short circuit currents we must first estimate the "Prospective Short Circuit Current" (I_P). This is the current which is likely to flow in that part of the electrical installation when a short circuit occurs after the protective device on the load side. This current is affected by the circuit impedance (z) which is composed of the distribution transformer impedance and the impedances of the distribution lines including any suitchgear. The circuit impedance may be given by the Electricity Authority or known from experience or even estimated from the volt–drop when a given load is connected on the line. Thus if when a load of 50 A is switched on, the voltage drops from 415V to 410V then

$$Z = \frac{415\text{-}410}{50} = \frac{5}{50} = 0.1\Omega$$

So prospective short circuit current at that circuit is $Ip = \frac{415}{0.1} = 4150$ A

Following Regulation 434–3 the breaking capacity of the protective device at that point of the installation shall not be less than Ip. A lower capacity is permitted only it a second device in the supply side with the suitable breaking capacity is existing. However in such case the "Energy Let–through" by the second device must not exceed the capabilities of the conductors and the equipment of the first circuit as examined in the next section. Similar calculations have to be carried out for overload protective devices, which are combining also short circuit protection, whose operating time is not reliable for the whole range of short circuit currents.

1. *Energy Let-through*

It is defined as the total energy which is let to pass through the protective device into the faulty circuit. It is proportional to I^2t where 'I' is the effective short circuit current and 't' is the time at which the device will operate. This time is of great importance and it is the deciding factor for the heat which will be generated in the faulty conductors under a certain short circuit current. If this time is long enough so that the conductor will have its temperature rise over its temperature limits then the insulation will be destroyed by the time the protective device will operate.

For conductors above 10mm2 and short circuit currents with duration upto 5 seconds the time which will rise the conductor temperature from its highest permissible temperature to the limit temperature is given by:–

$$t = \frac{K^2 S^2}{I^2}$$ where:– S=cross–sectional area in mm2

I=effective short circuit current in Auperes.

K—115 for copper conductors PVC insulated, 76 for aluminium conductors PVC insulated.

The above equation is known as the adiabatic equation and indicates the maximum time for which a conductor can sustain a corresponding short circuit current. Drawing this line on the Time/current characteristic of the protective device we can find the minimum and the maximum fault currents which a certain cable can sustain when protected by a certain device.

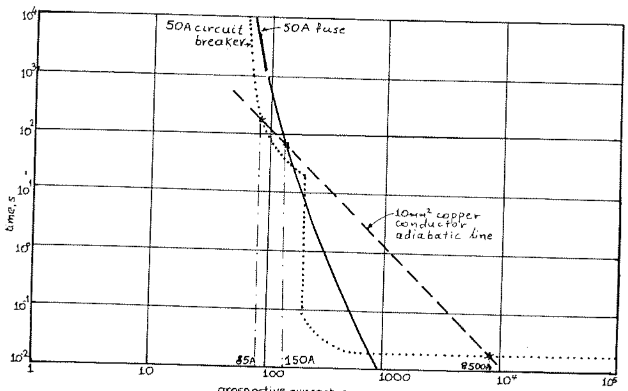

Figure 2. Time/current characteristics and conductor adiabatic line when K=115

Figure 2 shows the Time/current characteristics for a 50A fuse to BS 88, that of a 50A circuit breaker together with the adiabatic line of a 10mm2 PVC insulated copper conductor (K=115). From this graph it is noted that the minimum fault current at which the conductor will be properly protected is that of 150A in which case the fuse (BS 88) will operate at 60 seconds. If the current is slightly lower then the time of operation will increase dramatically and the energy let–through will be over the adiabatic line of the conductor, resulting in overheating and burning of the insulation.

For the case where the protective device is the circuit breaker the minimum current for safe operation is 85A with the time of operation of 200 seconds. However due to the Time/current characteristics of these devices there is also a maximum fault current of about 8500A with an operating time of 0.02 seconds. This is also the smallest time of operation for this group of circuit breakers.

2. *Position of the short-Circuit Protective Devices*

Such devices shall be placed at the point where a reduction occurs in the value of current–carrying capacity of the conductors of the installation. This condition may be relaxed if the device is installed within three meters from the circuit origin and is erected in such a manner as to reduce the risk of short circuit to a minimum.

3. *Combined Overload and short Circuit Protection*

In practical applications the overload and short circuit protection are usually afforded by the same device for simplicity and economy. However the requirements for both protections must be met and the positioning of such devices must be the same as for short circuit protection.

Conclusions

The new edition (15th) of the IEE wiving Regulations deals more precisely with the problems of overcurrent protection as compared to the last edition. In particular short circuit protection is thoroughly examined and the development of the adiabatic equation for a conductor, together with the Time/current curves for most of the protective devices, give an excellent tool to the designer of the electrical installations. The consept of the "Energy Let–through" also explains most of the broblems of breaking capacities and can also be used to design a system more reliable on discriminative operation.

References.

1) IEE Wiving Regulations, 15th edition, IEE

2) B.D. Jenkins, "Commentary on the 15th edition of the IEE Wiving Regulations", Peter Peregrinus Ltd

3) J.F. Whitfield, "A Guide to the 15th edition of the IEE Wiving Regulations, Peter Peregrinus Ltd.

Improved design and fabrication of flat plate solar collectors

by Th. Symeou, B. Sc., Lecturer H.T.I.

Heat storage containers, fluid transport and transportation systems, heat exchangers, controls etc play an important role in the efficient and reliable operation of all solar energy systems. But the most important component—which can be called as the heart of a solar system—is the s o l a r c o l l e c t o r.

This article aims in giving information on how the thermal performance of a flat-plate solar collector could be increased further more, how the life-time of a collector could be prolonged, how a solar collector could become more reliable.

1. Absorber plate:

The absorber plate absorbs the incoming solar radiation, converting it into heat at the absorbing surface and transfers this heat to a fluid (usually water or air) flowing through the collector. This heat transfer is done either by c o n d u c t i o n through the material of the absorber plate or by c o n v e c t i o n when fluid flows in pipes which are not in contact with the absorber plate (Figure 1).

From the above it can be concluded that:

i) materials of high thermal conductivities or low thermal resistance (i.e. copper, aluminium, steel etc) are preferable

ii) the convection heat transfer coefficient is lower than the thermal conductivity of almost all the metals and therefore the rate of heat transferred to the fluid by conduction is much better than that by convection. At the same time the absorber plate can be kept at lower temperature and consequently the efficiency of the collector increases.

Unfortunately, in many flat-plate solar collectors water flows in metal tubes which are not carefully welded (or bonded with heat transfer cement) in their full length onto the surface of the absorber plate but they are fastened to the plate with only a few strips or brackets. In such a case there is no good thermal contact between the tubes and the absorber plates and the efficiency of the collector decreases.

On the other hand "double sheet" or "roll-bond" plates are very good in fabricating flat-plate solar collectors.

Because heat is easily conducted through the metal fins of the absorber plate, the tubes do not need to be spaced closer than a few inches. Optimum spacing depends on the thickness and conductivity of the absorber material.

In general factors that determine the choice of absorber material are its thermal conductivity, and ease of handling, its availability and cost and the energy required to produce it. Therefore, although plastics have a low thermal conductivity, they can not be excluded among the possible materials in fabricating solar collectors.

2. Water flow rate

The temperature of the absorber plate, which is an important parameter in the performance of a flat-plate collector, depends largely on the working fluid in the channels, its flowrate, and its temperature. A high flowrate decreases the temperature difference between the plate and the ambient air, resulting in a lower heatloss rate and a higher efficiency. (However, more pumping power is then required to circulate the fluid.) A satisfactory flowrate for a flat plate collector is about 0.18 lb/min of water per ft2 of collector (0.88 kg/min m2). The above flow can be achieved by using circulating pumps. Systems working on the thermosyphon principle have a much lower flow rate and consequently their efficiency is lower.

3. Surface coating

Absorber plates are usually given a surface coating—which may be black paint—that increases the fraction of available solar radiation absorbed by the plate (its absorptance α). Black paints, for which $\alpha=0.92$ to 0.98, are usually applied by spraying and are then heat-treated to evaporate solvents and improve adherence. These surfaces must be able to withstand repeated and prolonged exposure to high temperatures without appreciable deterioration or outgassing.

But a surface that has a high absorptance (α) and is a good absorber of solar radiation usually has a high infrared emittance (ε) as well and is a good radiator of heat. A flat-black paint that absorbs 95% of the incoming solar energy will also reradiate much of the energy as heat, the exact amount depending on the temperature of the absorber plate and the glazing.

Ideally, one would like a surface to be selective, absorbing all the solar wavelengths and emitting none of the heat wavelengths, so that more heat could be transferred to the working fluid; for such a surface, α=1.0 and ε=0. Selective absorbers can be manufactured that approach this ideal, and several are available commercially. Others are still in the research stage (Table 1).

Selective absorbers often consist of a very thin black metallic oxide on a bright metal base. The oxide coating is thick enough to act as a good absorber.

To date, the most successful and stable selective absorber is made by electroplating a layer of nickel onto the absorber plate and then electrodepositing an extremely thin layer of chromium oxide onto the nickel. This combination is more resistant to water damage than the commonly used nickel–oxide coating.

Selective coatings are also made by chemical methods or thermal treatment of copper or steel plates. The manufacturing processes by which selective coatings are applied tend to make selective absorbers expensive. Eventually, innovations in methods and materials may bring the cost down.

Figure 2 shows typical efficiency curves for three flat–plate collectors. It can be seen that collector C with selective coating has a better performance over collector A of matt black paint.

4. **Cover plate:**

With a transparent cover placed above the absorber plate, heat loss is decreased in two ways: first, the infrared radiation emitted by the plate is stopped by the glazing, with a portion re–radiated back toward the plate; second, the glazing also traps a layer of still air next to the plate, which reduces the convective heat loss. (Fig. 3).

Although a number of materials are being used for collector covers–including glass, fiberglass–reinforced plastics, plexiglass, and thin plastic sheets —these materials vary considerably in their ability to transmit sunlight and trap heat, as well as in their durability. Glass is still one of the best choices for collector covers. Its solar transmittance is reasonably high—0.85 to 0.91—depending on iron content (if high in iron, glass looks green on the edge and should be avoided because it absorbs light); and it is opaque to infrared radiation. Typically, the heat–loss rate of a collector can be reduced to 5 to 10 W/m2C (1 to 2 Btu/hft2F) by the use of one cover glass, and to half this value with two cover glasses. Glass also is stable at high temperatures and is fairly resistant to scratches and weather. Its disadvantages are that it must be handled carefully and in small pieces, and that it is comparatively expensive and heavy.

Plastics are cheaper than glass and come in large lightweight sheets. Their solar transmittance is usually high if the sheets are thin.(Table 2) However, all thin plastics are partially transparent to infrared radiation from the absorber and therefore let some of the heat escape. They also soften and weaken at high temperatures, and degrade quickly in sunlight unless treated with ultraviolet inhibitors. Thick plastics (40 mil) absorb almost all the infrared radiation, and are often less sensitive to ultraviolet.

The thermal performance of a collector is influenced by the number of cover plates it has. A collector with only one glazing transmits more energy than a double–glazed collector; but if it is very much warmer than the surrounding air, it also loses more energy. It is generally felt that triple–glazing absorbs and reflects too much energy and is too expensive for any but the most severe climates.

For heating wind–sheltered swimming pools in the summertime when the temperature difference between the pool water and the air is modest, unglazed collectors (which are relatively inexpensive) are considered. Temperature gradients in the glass (or other cover material) near to its edges should be minimised because of the risk of thermal stress cracking; examples of good and bad practice are shown in Figure 4.

5. **Thermal insulation material**

Thermal insulation material for use in a solar collector must have a long life, withstand high temperatures and have a high thermal resistance (not below 1 m2K/W. Thermal insulating materials commonly employed in buildings generally are suitable for solar energy installations.

Problems with water type flat-plate collectors

The prevention of freeze damage, corrosion, and leaks has been the major worry of professionals working with flat–plate collectors of this type. Occasionally, heat damage has also been a problem.

(a) **Freezing.** Water is by far the most economical liquid to use in flat–plate collectors; but since freezing temperatures occur even in mild climates, some sort of precaution must be taken in most places to protect the collector and piping from bursting during a freeze.

One way to protect the collector is to add antifreeze to the heattransfer fluid. The ethylene glycol used in automobile radiators is a satisfactory antifreeze additive for water collectors; a 30 to 40% solution will prevent freezing. However, the substance is poisonous and must be kept out of the domestic water supply. This separation can be accomplised by having two separate flow loops: one passing through the collectors and containing a relatively small amount of water—may be 10 gal (38 1)—to which antifreeze is added; the other loop includes the water supply and the storage tank and may thus contain 100 gal (380 1). A heat exchanger transfers the heat from the collector loop to the storage loop. Because antifreeze is needed only in the collector loop, the quantity required will be relatively small.

Other methods to protect the collector from freezing is by draining the collectors every night or just on cold nights or by heating the collectors either with electric heating elements or by circulating warm water from storage through the collectors. These operations should be made automatic.

(b) **Leaks.** With water continually circulating through the solar-system pipes, from one part of the building to another, there is always some chance of having plumbing leaks. This problem is not unique to solar systems, however; and as usual, the solution is top-quality work-manship and careful maintenance.

(c) **Condensation.** Condensation within the collector assembly is likely to prove more of a problem in some humid areas. There are very good reasons why condensation should not be allowed to form in solar collectors in any substantial quantity. All types of insulation material that are subject to water vapour absorption lose a substantial part of their insulating ability when damp, and insulation materials of this type are usually employed in solar collectors because they are substantially cheaper than the genuinely water repellent alternatives.

Condensation dripping off the underside of a cover glass on to the collector plate may produce degradation of the plate surface and will certainly decrease the thermal performance of the unit. The most usual design error is to seal the cover glass to the outer casing completely, whilst allowing a very small amount of air infiltration where the pipes pass into the unit, and also through joins in the outer casing.

Either the whole collector unit should be truly hermetically sealed (with a guarantee that it will remain so) or adequate provision for ventilation should be provided. The former option is not easily realised in practice and it would probably be expensive to manufacture a collector that could maintain the necessary degree of integrity over its design life (say 20 years). The latter option may therefore be preferred and adequate ventilation, should be provided at the bottom edge of the collector.

But provision of excess air leakage at both top top and bottom of collector units (again a feature of a few designs) whilst preventing condensation may lead to a chimney effect with hot air being driven out of the collector, to the detriment of its thermal performance.

In conclusion, the only satisfactory design solution is probably to allow adequate ventilation at the base of all units, or to provide a small amount of leakage at both the bottom and the top, sufficient for the purpose but not so as to seriously degrade the thermal performance.

(d) **Corrosion.** Any pipe or water channel that carries tap water must be made of copper, galvanized steel, or plastic. Aluminium and untreated steel will corrode within a few months in a solar-collector situation. In a closed system where the same water is used over and over again, steel and aluminium can be protected by adding chromate-based chemicals called corrosion inhibitors. Again, a heat-exchanger must be used to keep the domestic water completely separate from the chemically-treated water. When inhibitors are used, the acidity (pH) of the water must be checked and corrected every few months; for aluminium, the pH should always be between 6 and 7. Commercial antifreeze solutions also contain corrosion inhibitors, but the various brands differ; one should check to see what materials are protected by a specific brand.

(e) **Heat damage:** Some concern must be given to making sure the liquid keeps moving through the collector all the time the collector is exposed to the sun. If the flow stops during a period of high insolation, many absorber plates can reach temperatures of over 300F (149C) with disastrous results: glass breaks; selective surfaces deteriorate; and plastics, sealants, and paints decompose and outgas.

TABLE 1 Selective absorber coatings

Type	Price	Status	Absorptance α	Emittance ε
Interference	High	Research	0.95	0.08
Black chrome	Medium	Commercial	0.95	0.12
Black nickel	Low	Commercial	0.90	0.05
Copper oxide	Low	Commercial	0.90	0.12
Lead oxide	Medium	Commercial	0.95	0.30
Aluminum conversion	Medium	Pilot	0.93	0.35
Dendrites	High	Research	0.89	0.30

TABLE 2 Solar transmittance (τ) for various cover-plate materials; exact value depends on cover thickness and the direction of the solar beam.

Material	Transmittance (τ)
Crystal glass	0.91
Window glass	0.85
Polymethyl methacrylate (acrylic)	0.89
Acrylite	
Lucite	
Plexiglas	
Polycarbonate	0.84
Lexan	
Merlon	
Polyethylene terephthalate (polyester)	0.84
Mylar	
Polyvinyl fluoride	0.93
Tedlar	
Polymide	0.80
Kapton	
Polyethylene	0.86
Fluorinated ethylene propylene (fluorocarbon)	0.96
FEP Teflon	
Fiberglass-reinforced polyester	0.87
Kalwall	
Fiberglass-reinforced, acrylic-fortified polyester with polyvinyl fluoride weather surface	0.86
Tedlar-clad Filon	

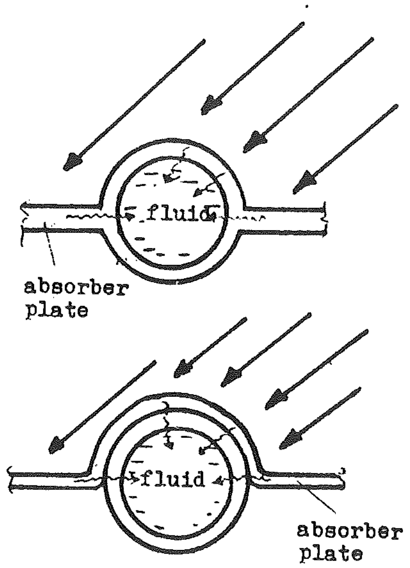

Heat transferred to the fluid
by conduction

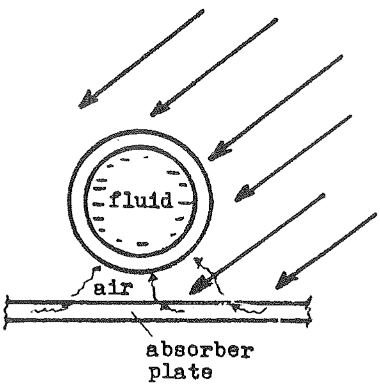

Heat transferred to the fluid
by convection

Fig. 1

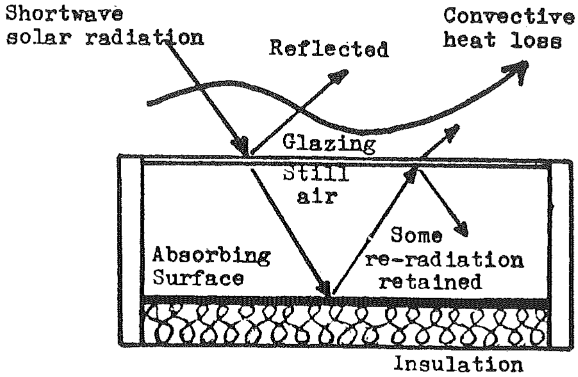

Fig. 3

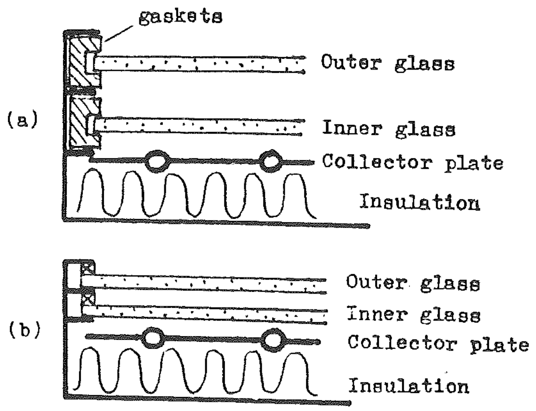

Figure 4
Avoidance of thermal stress in the cover glasses of flat plate collectors: (a) A good design, in which the edges of the glass are thermally insulated from the collector casing, (b) A poor design, in which there is good thermal contact between the edges of the glass and the collector casing

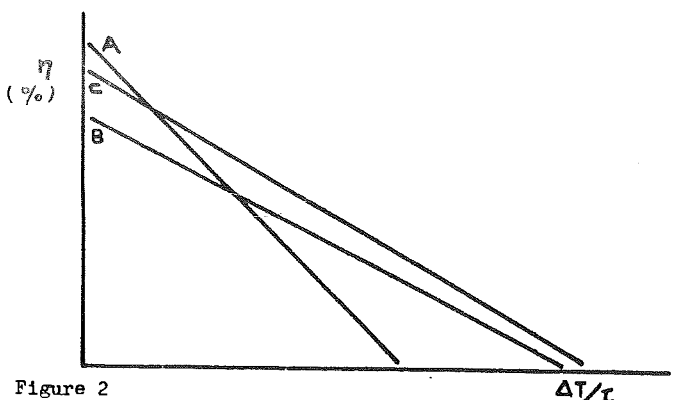

Figure 2
Linearised performance curves of three collectors A,B,C. Where: A=Single glazed, matt black absorber. B=Double glazed, matt black absorber, C=Single glazed, high absorption low emission selectively coated absorber

Selection of live conductors for Electrical installations

by Savvas Savvides T. Eng. (CEI) MITE Electrical Installations Instructor Higher Technical Institute.

Abstract

In Cyprus the Regulations followed for the electrical installations are the "IEE Wiring Regulations". Recently there was a major change in the Regulations with the issue of the 15th Edition, aiming towards the International standardization and harmonization. Those working with the 14th Edition may find much in the 15th Edition that is familiar in the detail of the Regulations; however, there is also much that is new, not least in the format; the structure and the terminology used.

The purpose of this article is to describe the method for the selection of the live conductors (phase and neutral conductors) as covered by the 15th Edition of the IEE Wiring Regulations.

SELECTION OF LIVE.........INSTALLATION

General Requirements

According to the environmental conditions of the installation (mechanical damage, corrosion, maximum operating temperatures etc) is the type of cable that must be used. Appendix 10 of the IEE Wiring Regulations is giving notes on the selection of types of cable and flexible cord for particular uses and external influences.

The size of the cable to be used on the other hand is depending on the current carrying capacity that the cable is required to have and the voltage drop limitations.

The current carrying capacity of conductors is affected by the following:

(i) the type of insulation

(ii) the conductor material

(iii) the conductor size

(iv) the method of installation

(v) the supply voltage (1-phase, 3-phase)

(vi) the grouping of conductors together

(vii) the ambient temperature

(viii) the installation of cable in thermal insulation

(ix) the type of protective device.

The current carrying capacities of conductors together with correction factors required are given in Appendix 9 of the IEE Wiring Regulations.

Co-Ordination of Conductors and Overload Protectors

The design current of a circuit (I_B) must be equal or smaller from the nominal current rating of the protective device (I_n), and the protective device nominal current rating must be equal or smaller from the conductor current carrying capacity (I_Z).

$$I_Z \geq I_n \geq I_B$$

Determination of Conductor Size

In Appendix 9 of the IEE Wiring Regulations the absolute maximum current carrying capacity of conductors is given, above which the temperature of the cable will lead to deterioration and degration of the insulation.

All values given are related to miniature circuit breakers and fuses other than BS 3036 semi-enclosed fuses i.e. what was previously called "close protection". All values given are applicable for 30°C ambient temperature.

In order to change the tabulated values of current carrying capacities to the real conditions of our installation correction factors shall be applied as follows:

C1—correction factor for grouping

C2—Correction factor for ambient temperature

C3—correction factor for thermal insulation

C4—correction factor for type of protective device

Having now in mind the co-ordination of conductors and overload protectors, the current carrying capacity of conductor, must not be less than:

$$I_z \geq I_n \times \frac{1}{C_1} \times \frac{1}{C_2} \times \frac{1}{C_3} \times \frac{1}{C_4} \text{ in Amperes}$$

In addition to the current carrying capacity of the conductor consideration shall be given to the limitations in the voltage drop stated by the Regulations. Regulation 522-8 states that the permissible voltage drop from the origin of the installation to any point in that installation shall not exceed 2.5% of the nominal voltage. Voltage drop in mV per ampere per meter for each cable size is given in the tables of Appendix 9 of the IEE Wiring Regulations. After the cable is selected and sized a check shall be carried out to make sure that the voltage drop is within the limits stated above.

Explanation of Correction Factors

Grouping

Where spacing between adjacent cables does not exceed twice their overall diameter grouping factor is applied. The correction factor to be applied may be obtained from table 9B of the IEE Wiring Regulations. The information given in the table is limited, and it is likely that in practical applications, the assumption must be made that all cables are loaded equally. In addition, it may be necessary to give early consideration to circuit arragements to ensure (as far as practicable) that all grouped cables are of the same size.

Ambient temperature

This is the maximum ambient temperature through which the run of cable passes and does not include the heat generated by the cable itself. The correction factors for ambient temperature may be obtained from Appendix 9 of the IEE Wiring Regulations. If a comparatively short part of the run is through an area of high ambient temperature consideration might be given to a change of cable type for that part or to an increase in the cross-sectional area.

Thermal Insulation

If a significant length of the cable installed is in contact with or surrounded by thermal insulation a correction factor must be applied in accordance with Regulation 522–6. For a cable installed in a thermally insulating wall or above a thermally insulated ceiling, the cable being in contact with a thermally conductive surface on one side, the rating factor to be applied may in the absence of more precise information, be taken as 0.75 times the current carrying capacity for that cable clipped direct to a surface and open. For a cable likely to be totally surrounded by thermally insulating material, the applicable correction factor may be as low as 0.5.

Type of protective device

Regulation 433–2 gives the relationship between the load, the protective devices and the conductors. To achieve good protection of the conductors by the protective devices it is stated that the current causing effective operation of the protective device (I_2) shall not exceed 1.45 times the lowest of the current carrying capacities (Iz) of any of the conductors in the circuit

$$I_2 \leq 1.45\ I_Z$$

For semi–enclosed fuses to BS 3036

$$\text{fusing factor} = 2 = \frac{\text{current to give effective operation } (I_2)}{\text{nominal current of protective device } (I_n)}$$

$$\therefore \quad I_2 = 2I_n \leq 1.45\ I_Z$$

$$\therefore \quad I_n \leq \frac{1.45}{2}\ I_Z$$

$$\therefore \quad I_n \leq 0.725\ I_Z.$$

Therefore if a protective device to BS 3036 (semi–enclosed fuse) is to be used a correction factor of 0.725 must be applied, for obtaining the conductor current carrying capacity.

For all other types of protective devices no correction factor is required as the fusing factor is considered to be of the order of 1.45

Cable Sizing Examples

Note: For the solution of the following examples tables of Appendix 9 of the IEE Wiring Regutions were used. All tables used are appearing at the end of this article.

Example 1:

Two heating loads 6 KW, 240V are to be supplied with PVC insulated cables installed in the same conduit. The ambient temperature is 45° C. The protective device to be used is a semi–enclosed fuse to BS3036. Find the minimum cross sectional area of the cable to be used. The length of the circuit is 50 meters.

$$I_B = \frac{6000}{240} = 25A \text{ for each circuit}$$

$$I_Z \geq I_n \geq I_B$$

$$\therefore \quad I_n = 30\ A.$$

$$I_Z \geq I_n \times \frac{1}{C_1} \times \frac{1}{C_2} \times \frac{1}{C_3} \times \frac{1}{C_4}$$

C1—grouping correction factor

C2—ambient temperature correction factor

C3—thermal insulation correction factor

C4—protective device correction factor

Grouping factor is obtained from table 9B

The number of loaded conductors is 4 so C1=0.80

Ambient temperature correction factor is obtained from table which is giving ambient temperature correction factors when BS 3036 fuses are used. C2=0.91

Thermal insulation correction factor C3 no information is given so this is taken as one.

Protective device correction factor is 0.725 as fuse to BS 3036 is used

$$\therefore \; I_Z \geq 30 \times \frac{1}{0.80} \times \frac{1}{0.91} \times \frac{1}{0.725}$$

$$I_Z \geq 56.84 \text{ Amps}$$

From table 9DI installation method A single phase we read at column 2 the current carrying capacity of cable required.

$16mm^2$ is having a rating of 74Amps which is the next bigger to 56.84 Amps.

So this is suitable for this load under the condiconditions specified.

We have to check finally for the voltage drop.

From table 9DI column 3 for 16mm2 cable voltage drop in mv per ampere per meter is 2.7

$$\therefore \; \text{Total voltage drop} = \frac{2.7 \times 50 \times 25}{1000} = 3.38 \text{ volts}$$

This is less than 2.5% of 240V (6V) so the cable is suitable for use and from the voltage drop point of view.

Example 2:

Four circuits 3 KW 240V each are supplied with twin PVC insulated cables fixed together on the wall. The ambient temperature is 25° C and the protective devices used are miniature circuit breakers. The cables for a significant part of their length come in contact with thermal insulation. The length of the circuits is 25m long. Find the minimum size of cable to be used.

$$I_B = \frac{3000}{240} = 12.5 \text{ Amps}$$

$$I_Z \geq I_n \geq I_B$$

$$\therefore \; I_n = 15 \text{ Amps}$$

$$I_Z \geq I_n \times \frac{1}{C1} \times \frac{1}{C2} \times \frac{1}{C3} \times \frac{1}{C4}$$

Grouping correction factor obtained from table 9B The number of multicore cables used is 4 so C1=0.65

Ambient temperature correction factor is obtained from table 9D2
C2=1.06

The thermal insulation correction factor is 0.75 as the cables are coming in contact with thermal insulation.

The protective device correction factor is one as protective device other than fuse to BS 3036 is used.

$$I_Z \geq 15 \times \frac{1}{0.65} \times \frac{1}{1.06} \times \frac{1}{0.75}$$

$$I_Z \geq 29.02 \text{ Ambs}$$

From table 9D2 installation method E column 6 cable of $4mm^2$ is having a current carrying capacity of 36 Amps and 11 mv/A/m voltage drop.

Check for voltage drop

$$\text{total voltage drop} = \frac{11 \times 12.5 \times 25}{1000} = 3.437 \text{ volts}$$

This voltage drop is less than 6 volts (2.5% of 240V) so we can use $4mm^2$ cable for these circuits.

Example 3:

Two heating loads of 18 KW at 415V 4-wire supply are to be fed with PVC insulated cables installed in the same conduit. The ambient temperature is 40° C and the loads are to be protected by semi-enclosed fuses to BS 3036. The length of the circuit is 20 meters. Find the minimum cable size to be used.

$$I_B = \frac{18000 \text{ watts}}{\sqrt{3} \times 415 \text{ volts}} = 25 \text{ Amperes}$$

$$I_Z \geq I_n \geq I_B$$

$$I_n = 30\text{A}$$

$$I_Z \geq I_n \times \frac{1}{C1} \times \frac{1}{C2} \times \frac{1}{C3} \times \frac{1}{C4}$$

C1—Grouping factor

The total number of loaded conductors is 6 if we consider that the load is balanced.

Therefore from table 9B a correction factor of 0.69 must be applied.

C2—Ambient temperature.

The ambient temperature is 40° C and the protection is a fuse to BS 3036. Therefore the correction factor is obtained from the table in Appendix 9 and this is 0.94.

C3—thermal insulation

No information is given about thermal insulation and it is considered that thermal insulation does not affect this installation at all i.e. C3=1

C4—Protective device.

The protective device used is a semi–enclosed fuse to BS 3036 so a correction factor of 0.725 is considered.

$$\therefore I_Z \geq 30 \times \frac{1}{0.69} \times \frac{1}{0.94} \times \frac{1}{0.725} \geq 63.8 \text{ Amps}$$

From table 9D1 column 2, 16mm² have a current carrying capacity of 74Amps, so the cable to be used is 16mm².

Finally a check must be carried out for the voltage drop.

From table 9DI column 5 a voltage drop of 2.3 mv/A/m is given for the 16 mm² cable.

$$\text{Therefore total voltage drop} = \frac{2.3 \times 25 \times 20}{1000} = 1.15\text{V.}$$

2.5% of 415V is 10.37 volts therefore the 1.15 volts voltage drop is well within the permissible limits.

Considering the correction factors which limit the current carrying capacity of the cable we can easily see that by just replacing the protective devices with circuit breakers and by installing two separate conduits one for each circuit the cable size reduces considerably as follows:

The only correction factor now is the correction factor for the ambient temperature. From table 9DI for 40° C ambient temperature the correction factor is 0.87.

$$\therefore I_Z \geq 30 \times \frac{1}{0.87} \geq 34.4 \text{ Amps}$$

From table 9DI column 4, 6mm² is having a current carrying capacity of 37Amps and a voltage drop of 6.2 mv/A/m.

$$\text{The voltage drop is now} = \frac{6.2 \times 25 \times 20}{1000} = 3.1 \text{ volts}$$

So 6mm² cable is now suitable for the circuits.

Examble 4:

Two single phase 4 KW loads A and B are supplied from a miniature circuit breaker distribution board. The circuits are run in twin and cpc cable and pass through a boiler room where they are together protected from mechanical damage by enclosure in a common steel conduit. The ambient temperature in the boiler room is 45° C.

After leaving the boiler room the circuits separate and cable B is clipped to timberwork and semi–enclosed in thermal insulation. The length of each circuit is 25 meters.

Find the minimum cable size for each circuit.

$$I_B = \frac{4000 \text{ watts}}{240 \text{ volts}} = 16.66 \text{ Amps}$$

$$I_Z \geq I_n \geq I_B$$

$$\therefore I_n = 20\text{A.}$$

The minimum current carrying capacity (Iz) shall be calculated for each cable separately.

Cable A:

Correction factors to be applied:

C1—grouping correction factor is obtained from table 9B and this is 0.8 for two cables together.

C2—ambient temperature correction factor is obtained from table 9D2 and this is 0.79 for 45°C

$$\therefore I_Z \geq I_n \times \frac{1}{C1} \times \frac{1}{C2}$$

$$\therefore I_Z \geq 20 \times \frac{1}{0.8} \times \frac{1}{0.79} \geq 31.64 \text{ Amps}$$

From table 9D2 column 2 the 4mm² cable have a current carrying capacity of 32 Amps, and 11mv/A/m voltage drop.

$$\text{Total voltage drop} = \frac{11 \times 16.66 \times 25}{1000} = 4.565 \text{ Volts}$$

This is within the permissible limits of 2.5% of the nominal voltage so this cable is suitable for the circuit A.

Cable B:

Cable B may be separated into two sections. The first section which is having grouping and ambient temperature correction factors and second section which is having thermal insulation correction factor only.

In the first section of the cable the correction factors are exactly the same as for cable A so the minimum current carrying capacity of cable required is 31.64 Amps and the cable size is 4mm².

In the second section of the cable the correction factor for thermal insulation in accordance with Regulation 522–6 is 0.75

$$\therefore I_Z \geq I_n \times \frac{1}{C3}$$

$$\therefore I_Z \geq 20 \times \frac{1}{0.75} \geq 26.6 \text{ Amps}$$

From table 9D2 of the IEE Wiring Regulations, column 6, the 2.5 mm² cable have a current carrying capacity of 28 Amps.

Therefore in order to cover the current carrying capacity needs of the cable for both sections 6mm² cable is used throughout the circuit B.

References:

Regulations for Electrical Installations, 15th Edition 1981, Institution of Electrical Engineers.

TABLE 9A

Typical methods of installation of cables and conductors

'Enclosed'

Type	Description	Examples
A	Single-core and multicore cables, enclosed in conduit.	
B	Single-core and multicore cables enclosed in cable trunking.	
C	Single-core and multicore cables enclosed in underground conduit, ducts, and cable ducting.	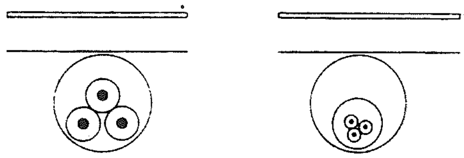
D	Two or more single-core cables contained in separate bores of a multicore conduit and intended to be solidly embedded in concrete or plaster or generally incorporated in the building structure (may be used as a prefabricated wiring system).	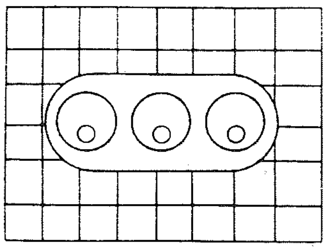

'Open and clipped direct'

Type	Description	Examples
E	Sheathed single-core and multicore cables clipped direct to or lying on a non-metallic surface.	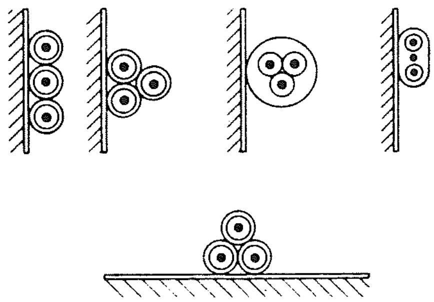
F	Sheathed single-core and multicore cables on a cable tray, bunched and unenclosed.	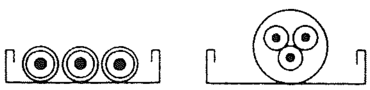
G	Sheathed cables embedded direct in plaster other than special thermally insulating plasters.	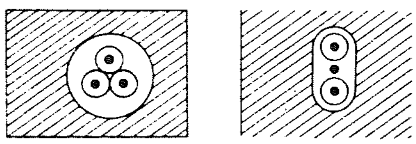
H	Sheathed single-core and multicore cables suspended from or incorporating a catenary wire.	

TABLE 9B

Correction factors for groups of more than three single-core cables or more than one multicore cable

Type of cable and installation condition	Number of loaded conductors											
	4	6	8	10	12	16	20	24	28	32	36	40
Single-core cables: Factor to be applied to the values for two single-core cables	0.80	0.69	0.62	0.59	0.55	0.51	0.48	0.43	0.41	0.39	0.38	0.36
	Number of cables											
	2	3	4	5	6	8	10	12	14	16	18	20
Multicore cables: Factor to be applied to the values for one cable	0.80	0.70	0.65	0.60	0.57	0.52	0.48	0.45	0.43	0.41	0.39	0.38

NOTES: 1. These factors are applicable to groups of cables all of one size, equally loaded, including groups bunched in more than one plane.

2. Where spacing between adjacent cables exceeds twice their overall diameter, no reduction factor need be applied.

AMBIENT TEMPERATURE CORRECTION FACTOR

(ii) *Where the protective device is a semi-enclosed fuse to BS 3036*

– DIVIDE the nominal current of the protective device by the appropriate ambient temperature correction factor given in the following table.

Ambient temperature °C	25	30	35	40	45	50	55	60	65	70	75	80
PVC-insulated	1.02	1.0	0.97	0.94	0.91	0.88	0.77	0.63	0.44	–	–	–
85°C rubber-insulated	1.02	1.0	0.97	0.94	0.92	0.89	0.85	0.77	0.68	0.59	0.47	0.33

COPPER CONDUCTORS

TABLE 9D1

Current-carrying capacities and associated voltage drops for single-core p.v.c.-insulated cables, non-armoured, with or without sheath (copper conductors)

BS 6004
BS 6346

Conductor operating temperature: 70°C

Conductor cross-sectional area	Installation methods A to C† of Table 9A ('Enclosed')				Installation methods E to H of Table 9A ('Clipped direct')				Installation method J of Table 9A ('Defined conditions')					
	2 cables, single-phase a.c., or d.c.		3 or 4 cables, three-phase a.c.		2 cables, single-phase a.c., or d.c.		3 or 4 cables, three-phase a.c.		Flat or vertical (2 cables, single-phase a.c., or d.c., or 3 or 4 cables three-phase)				Trefoil (3 cables three-phase)	
	Current carrying capacity	Volt drop per ampere per metre	Current carrying capacity	Volt drop per ampere per metre	Current carrying capacity	Volt drop per ampere per metre	Current carrying capacity	Volt drop per ampere per metre	Current carrying capacity	Volt drop per ampere per metre: Single-phase	d.c.	Three-phase	Current carrying capacity	Volt drop per ampere per metre
1	2	3	4	5	6	7	8	9	10	11	12	13	14	15
mm²	A	mV	A	mV	A	mV	A	mV	A	mV	mV	mV	A	mV
1.0	14	42	12	37	17	42	16	37	–	–	–	–	–	–
1.5	17	28	14	24	21	28	20	24	–	–	–	–	–	–
2.5	24	17	21	15	30	17	26	15	–	–	–	–	–	–
4	32	11	29	9.2	40	11	36	9.2	–	–	–	–	–	–
6	41	7.1	37	6.2	50	7.1	45	6.2	–	–	–	–	–	–
10	55	4.2	51	3.7	68	4.2	61	3.7	–	–	–	–	–	–
16	74	2.7	66	2.3	90	2.7	81	2.3	–	–	–	–	–	–
25	97	1.7	87	1.5	118	1.7	106	1.5	–	–	–	–	–	–
35	119	1.3	106	1.1	145	1.3	130	1.1	–	–	–	–	–	–
		a.c. d.c.				a.c. d.c.								
50	145	0.97 0.91	125	0.84	175	0.93 0.91	160	0.82	195	0.95	0.91	0.85	170	0.80
70	185	0.71 0.63	160	0.62	220	0.65 0.63	200	0.59	240	0.68	0.63	0.62	210	0.59
95	230	0.56 0.45	195	0.48	270	0.48 0.45	240	0.45	300	0.52	0.45	0.49	260	0.42
120	260	0.48 0.36	220	0.42	310	0.40 0.36	280	0.38	350	0.44	0.36	0.43	300	0.34
150	–	– –	–	–	355	0.34 0.29	320	0.34	410	0.39	0.29	0.39	350	0.29
185	–	– –	–	–	405	0.29 0.24	365	0.30	470	0.35	0.24	0.36	400	0.25
240	–	– –	–	–	480	0.24 0.18	430	0.27	560	0.36	0.18	0.38	480	0.22
300	–	– –	–	–	560	0.22 0.14	500	0.25	660	0.33	0.14	0.35	570	0.19
400	–	– –	–	–	680	0.20 0.12	610	0.24	800	0.30	0.12	0.33	680	0.17
500	–	– –	–	–	800	0.18 0.086	710	0.23	910	0.28	0.086	0.31	770	0.16
630	–	– –	–	–	910	0.17 0.068	820	0.22	1040	0.26	0.068	0.30	880	0.15

†For installation method C, the tabulated values are applicable only to the range up to and including 35mm². For larger sizes in this installation method, see ERA Report 69–30. For cables in ducts in the floor of a building, the ERA ratings must be adjusted by the appropriate factor for ambient temperature. For installation method D, the current-carrying capacities for twin and multicore sheathed cables in methods A to C, up to 35mm², are applicable (see Table 9D2).

NOTES: 1 – **WHERE THE CONDUCTOR IS TO BE PROTECTED BY A SEMI-ENCLOSED FUSE TO BS 3036, SEE ITEM 4(ii) OF THE PREFACE TO THIS APPENDIX.**

2 – The current-carrying capacities in columns 6 and 8 are applicable to flexible cables to BS 6004 Table 1(b) when the cables are used in fixed installations.

CORRECTION FACTORS

FOR AMBIENT TEMPERATURE

Ambient temperature	25°C	35°C	40°C	45°C	50°C	55°C	60°C	65°C
Correction factor	1.06	0.94	0.87	0.79	0.71	0.61	0.50	0.35

FOR GROUPING

See Table 9B except that the factors for 32, 36 and 40 conductors do not apply to three-phase.

COPPER CONDUCTORS

TABLE 9D2

Current-carrying capacities and associated voltage drops for twin and multicore p.v.c.-insulated cables, non-armoured (copper conductors)

BS 6004
BS 6346

Conductor operating temperature: 70°C

Conductor cross-sectional area	Installation methods A to C† of Table 9A ('Enclosed')				Installation methods E to H of Table 9A ('Clipped direct')				Installation method K of Table 9A ('Defined conditions')			
	One twin cable, with or without protective conductor, single-phase a.c., or d.c.		One three-core cable, with or without protective conductor, or one four-core cable, three-phase		One twin cable, with or without protective conductor, single-phase a.c., or d.c.		One three-core cable, with or without protective conductor, or one four-core cable, three-phase		One twin cable, with or without protective conductor, single-phase a.c., or d.c.		One three-core cable, with or without protective conductor or one four-core cable, three-phase	
	Current carrying capacity	Volt drop per ampere per metre	Current carrying capacity	Volt drop per ampere per metre	Current carrying capacity	Volt drop per ampere per metre	Current carrying capacity	Volt drop per ampere per metre	Current carrying capacity	Volt drop per ampere per metre	Current carrying capacity	Volt drop per ampere per metre
1	2	3	4	5	6	7	8	9	10	11	12	13
mm²	A	mV	A	mV	A	mV	A	mV	A	mV	A	mV
1.0	14	42	12	37	16	42	13	37	–	–	–	–
1.5	18	28	16	24	20	28	17	24	–	–	–	–
2.5	24	17	21	15	28	17	24	15	–	–	–	–
4	32	11	29	9.2	36	11	32	9.2	–	–	–	–
6	40	7.1	36	6.2	46	7.1	40	6.2	–	–	–	–
10	53	4.2	49	3.7	64	4.2	54	3.7	–	–	–	–
16	70	2.7	62	2.3	85	2.7	71	2.3	–	–	–	–
25	79	1.8	70	1.6	108	1.8	90	1.6	114	1.8	95	1.6
35	98	1.3	86	1.1	132	1.3	115	1.1	139	1.3	122	1.1
50	–	–	–	–	163	0.92	140	0.81	172	0.92	148	0.81
						a.c. d.c.				a.c. d.c.		
70	–	–	–	–	207	0.65 0.64	176	0.57	218	0.65 0.64	186	0.57
95	–	–	–	–	251	0.48 0.46	215	0.42	265	0.48 0.46	227	0.42
120	–	–	–	–	290	0.40 0.36	251	0.34	306	0.40 0.36	265	0.34
150	–	–	–	–	330	0.32 0.25	287	0.29	348	0.32 0.25	302	0.29
185	–	–	–	–	380	0.29 0.23	330	0.24	400	0.29 0.23	348	0.24
240	–	–	–	–	450	0.25 0.18	392	0.20	474	0.25 0.18	413	0.20
300	–	–	–	–	520	0.23 0.14	450	0.18	548	0.23 0.14	474	0.18
400	–	–	–	–	600	0.22 0.11	520	0.17	632	0.22 0.11	548	0.17

FLAT CABLES ONLY (columns 10–13, sizes 1.0 to 16 mm²)

†For installation method C, the tabulated values are applicable only to the range up to and including 35 mm². For larger sizes in this installation method, see ERA Report 69–30. For cables in ducts in the floor of a building, the ERA ratings must be adjusted by the appopriate factor for ambient temperature.

NOTES: 1 – **WHERE THE CONDUCTOR IS TO BE PROTECTED BY A SEMI–ENCLOSED FUSE TO BS 3036, SEE ITEM 4(ii) OF THE PREFACE TO THIS APPENDIX.**

2 – The current carrying capacities in columns 6 and 8 are applicable to flexible cables to BS 6004 Table 1(b) where the cables are used in fixed installations.

CORRECTION FACTORS

FOR AMBIENT TEMPERATURE

Ambient temperature	25°C	35°C	40°C	45°C	50°C	55°C	60°C	65°C
Correction factor	1.06	0.94	0.87	0.79	0.71	0.61	0.50	0.35

FOR GROUPING
See Table 9B.

The "Competitors" of Metals

by G. Katodrytis, B. Sc. (Eng.), Lecturer, H.T.I.

Abstract

There is no doubt that the prices of metals are continuously increasing mainly due to the Energy Crisis and the shortage of raw materials. The increasing needs of modern civilisation increases the consumption of metals and also seek for the use of new materials.

This article intends to introduce the plastics as the new engineering materials which many engineers are still reluctant to use although they solve in many cases economical and other proplems which can not be avoided by the use of metals. The advantages and disadvantages of these materials are outlined and their future is discussed.

1. Introduction

With the growing cost and shortage of many of the world's raw materials, particularly metals, the use of non-metallic materials as engineering materials has become an economic solution.

Man's evolutionary development has also demonstrated that as he becomes more skilled his use of materials becomes increasingly more sophisticated. Historically, man has been characterised as living in the Stone Age, then progressing through a period when wood was predominant and more recently as living in the Metals Age. It is now may be said that modern civilization is entering in the Plastics Age.

Many engineers are accustomed to think first in terms of metals when considering a new design Quite wrongly, they view non-metals and particularly plastics as substitutes for metals rather than as engineering materials in their own right.

2. The Future of Metals:

The Steel World Crisis which appeared in 1974 and continues today has forced the West Europe industrial countries to renew the old production plants in order to achieve high efficiency, low production cost and better quality of their products.

Tonnage or bulk steels, as used in structural and heavy engineering, and for general purposes, are likely to be made almost entirely by the oxygen process. Special steels, as used for tools, highly stressed components and many special engineering applications, will be made in developed electric furnaces. Both these processes are more efficient than the older ones they are superseding and this, if it does not bring the prices down—which nobody is daring to forecast—should at least help to prevent too rapid a rise. Both processes, and the finishing operations which go with them are capable of large outputs. The oxygen process for tonnage steels, particularly, is a high-tonnage producer. Thus both are less flexible than the older methods; consequently longer production runs of fewer specifications, sizes and shapes are what the steel makers now aim to produce—Indeed some of the plant now coming into commission is so expensive that only by long production runs can there be any real hope of paying for it.

The World steel production which was 110 tons in 1938 becomes 276 tons in 1958, reaches 535 tons in 1968 and 714 tons in 1978. It is expected that this rise in steel production will continue at about the same rate for the next two decades. The production of stainless steels in even greater due to the increasing human needs in modern society. Due to the above and the shortage of raw materials, it has been noticed that most of the world's steel production has been transferred to the countries of the Third World which possesse the raw materials and at the same time the developed industrial countries offer consultancy services to these countries making use of their experienced personnel in this field.

Although efforts have been made to control the rise in the cost of metals by reduction in the amount of total energy required by processing, by reduction in man-hours per ton and by improvement in the yield of metal-smelting processes, the increasing supply and demand of metals especially in the case of ferrous metals, as it can be seen above, won't stabilize the prices of metals. Miner's strikes, which used to occur frequently lately due to the increasing reluctance of people to face the hazards to health and safety and put up with dirt and isolation, also cause steep rise in the prices of metals.

When the price of a metal rises in one part of the world due to the reasons mentioned above or any other reason, one feels that somewhere a frustrated user of that metal starts planning to stop or limit its use in the future.

3. Ceramics, Plastics and Composites as today's engineering materials:

C e r a m i c s were known until recently as the pottery materials. Ceramics technology has undergone rapid expansion during the last decade and todays technical ceramics are now being accepted by designers as practical engineering materials. One of the reasons of this rapid expansion is the rise of prices in other materials due to heavier demand as mentioned before. The vast resources of ceramics offer a cheaper alternative that will certainly not become exhausted during this century. The high temperature properties of ceramics, allied to their hardness and abrasion resistance constitute the main reason for the switch over to ceramics in certain engineering applications. Ceramics are not only used as alternatives to metals in various cases but also have solved a lot of engineering problems that metals couldn't do. For example Silikon-Nitride has solved high temperature problems due to its low thermal expansion, good thermal conductivity and high strength, especially in gas turbine design.

Plastics are polymer—based materials which are divided to three groups, the Thermoplastics, the Thermosettings and the Elastomers. The Thermoplastic types are resins that soften repeatedly when heated and harden when cooled; the Thermosetting types are plastics that undergo chemical change during processing to become permanently insoluble and infusible; and the Elastomers are materials that can be stretched repeatedly to at least twice their original length and which will return with force to their approximate original length when an immediate stress is released. Components made of plastics are widely used nowdays in place of metals and other materials, partly due to the increasing needs of modern society, and due to their properties and characteristics. Plastics have made and will continue to make an impact in so many aspects of our lives because of the following characteristics: light weight, electrical insulation, pleasant to the touch, color, ability to be metallised, transparency, corrosion resistance, chemical resistance, hygienic and non-allergic, can be mass-produced, provide design freedom and adaptability.

As engineering materials, plastics are widely used nowdays in place of metals and in many situations they solve design and service problems that metals failed to do. Unless reinforced will fibrous glass or other strengthening materials, plastics are not used for applications involving a high degree of sustain loading and therefore their use is restricted mainly for components in light engineering. Many types of plastics have mechanical properties that make them ideal for applications which used to need much more costly materials. In many cases they cut down machining and assembly costs, because a single moulding can often be used in place of several components in a complex structure. The saving in weight is important too and this makes plastics suitable for many aircraft components. For example, acetal copolymers are being used in place of metals for many kinds of mechanical and electrical parts in aircrafts and fibre—reinforced polyimides with boron and carbon fibres have been suggested as of value for aircraft structures. Many new plastic materials are superior to metals as far as toughness at low temperatures is concerned, and due to this property scratches, sharp corners and the effects of stress concentration are no longer critical design problems. For example Zytel Super Tough Nylon made by Du Pont is a new thermoplastic material which is supertough on impact and repeated impact and stays also tough at low temperatures. It resists chemicals and corrosion and it processes quickly and economically. It is also half the weight of an equal volume of Aluminium and it needs no costly finishing operations.

The Engineering Composites tailor-made to replace mainly the costly metals, solve in a way the problem of shortage of many of the world's raw materials. Special high strength alloys can be produced for high-strength and/or high-temperature applications but frequently high density and high cost limit their use. Similarly, many plastics excibit good lubricity, good chemical resistance, low density and ease of processing, but suffer from low mechanical strength, low hardness, low service temperature maxima and excessive creep under quite moderate load. One way to solve these difficulties with the desized characteristics is to form composites.

Composites generally consist of a matrix material with filaments, fibres or particulate material to give enhanced properties that are often better than those of the matrix or reinforcement materials alone. The matrix can consist of ceramics, metals or plastics, but plastics, are by far the most common matrix materials. The reinforcement can be of metal rods or filaments, whiskers of silikon carbides or nitride, sapphire, carbon fibres and various forms of glass, asbestos and other fibres. Composites find wide applications in aircraft components, gear wheels for low-load bearing applications, dry bearings, slideways, cams, compression blades, piston rings and a host of other applications.

The widespread use of plastics as engineering materials is also made obvious by the recent awards of the design Council Awards in U.K. Amongst the other awards in the category of engineering products for the year 1981 was the award given for the design team of Comp Air Construction & Mining Ltd. for the Ziter 20 pneumatic road breaker. The new machine has a tough polyurethane exterior which incorporates a long exhaust passage to reduce noise. It is also easier to handle because it weighs only 20 kg. The weight has been reduced by replacing heavy forgings with polyurethane components which can be easily formed or machined, and the number of components has been reduced by 50 per cent, thus simplyfing maintenance and reducing spares holdings. Another revolutionary (in more senses than one) design won an award in the engineering components category for the tank of the Variatronic front loading washing machine, manufactured by Phillips Domestic Appliances. The award winning component is made of glass-reinforced polypropylene structural foam and is probably the largest single shot moulding so far produced in the material. The alternative design, in production in Europe, comprises 16 pressed steel parts, welded together and vitreous enamelled. To set up a "production line at the Halifax factory in U.K. would have meant very high tooling costs of about £750,000. The tools for the new-design component cost one tenth of this amount and the productivity per man is about five times that with the original component.

With the development of plastics, the Adhesives followed a consequent development which nowdays replace all kinds of fasteners due to their high–bond strength. The new adhesives are superior from the traditional household adhesives in that they are versatile, they replace traditional fastening techniques like bolting, riveting, brazing, soldering and welding. They are also used for minor crack repairs, especially in internal combustion engines. Lately, a member of the Mechanical Engineering Dept, has solved his problem with the cracked aluminium alloy cylinder cover of his car using the appropriate adhesive.

From a production point of view, the adhesives, can reduce appreciably manufacturing costs because very few engineering products can be made as one–piece structures and most requiring some form of fastening or joining procedure. So using adhesives in place of traditional fasteners, a great deal of money and time are saved and in many cases stronger joints are produced. Other advantages of adhesive–bonding are the damping out of sound and vibration due to the absence of metal–to–metal contact, bi–metallic corrosion is avoided, and as far as welding is concerned, post–weld finishing, residual stresses and change of structure next to weld are avoided since no heat is evolved during the curing of modern engineering adhesives.

However, the use of adhesives involves certain disadvantages because the surfaces to be joined must be chemically clean and this involves pre–treatment and care in handling and storage. The rapid curing of certain adhesives and especially the cyanoacrylates which are the latest ones, has been misused recently from certain people to make nasty jokes.

4. **The Future Trends:**

Various conflicting opinions have been expressed about the future of plastics in the past. Many people referred to an "All Plastics World" in the future to be reached within this decade. This is made obvious by the figure shown below, which shows the world consumption of raw materials by volume.

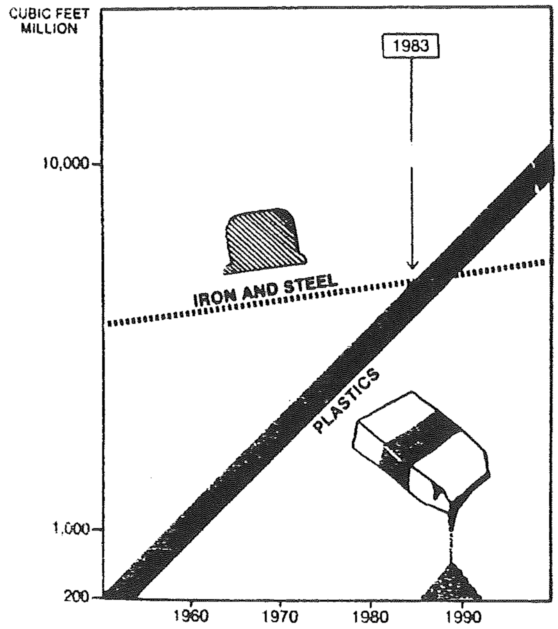

The figure shows that by the beginning of this decade the volume of plastics will exceed that of metals and the Plastics Age will arrive. Although the predictions of this figure, which are based of course on certain statistical data are backdated, they are not far from todays reality. Perhaps today, the plastics consumption may not have exceeded the steels production but the fact is that the plastics consumption is still increasing and this may happen in the future if one considers the increasing rise in cost of metals.

Some people have expressed a weak opinion about the future of plastics and their competitiveness over metals, based on two main reasons. The first reason, is that today's at least plastic materials can not reach the strength of many metallic alloys and superalloys although in certain other properties plastics are superior. The second reason, is that the recycling of plastic's scrap presents a problem. Injection moulded articles can be shredded and recycled provided the materials are not mixed up and the compression moulded plastics are difficult to recycle. Scrap thermoplastic can be re–used, although it normally has somewhat inferior properties to the virgin thermoplastic due to some degradation during the initial processing cycle.

It is difficult really to predict what will happen in the future because we are living in the century of revolutionary developments. So nothing must be declined nor strongly predicted because no–one knows what the future developments or discoveries are going to be. It is left of course to the reader to induce his own opinion about what the future of these materials will be.

The Quality Manager and Quality Costs

by S. Vassiliou C. Eng., M. I. Mech. E.,
Quality Control Officer
Ministry of Commerce and Industry

Abstract

A quality cost analysis can assist management to improve quality and at the same time to reduce costs.

Introduction

The operation of every business is based on cost. There are costs for marketing, designing, manufacturing, testing, along with other costs that are necessary to produce and to ship to the market place, products which would meet customer requirements.

This article is devoted mainly to the costs related to assurance of product quality because all industry is presently plagued with continuing pressure by customers for better and better quality products. And this pressure comes at a period when quality costs are very high.

It is however possible to maintain customer satisfaction while reducing quality costs.

To develop such a situation the Quality Control Manager should become adept in analysing the whole business cycle from the stantpoint of quality effort and quality costs. To do this analysis there is a need to establish quality objectives and quality programmes, that will assure the success of any planned quality control activity. Along with the establishment of these objectives and programmes it is necessary to measure the progress of the quality control effort in the attainment of its objectives and the extent to which quality control makes a contribution to the business as a whole.

Quality Level and its cost

As a first approach to measurement the Quality Manager must have available the following information:

(a) What is the company's level of quality.

(b) How is this level controlled and

(c) How much does it take in quality costs to support this control.

This information however can be, at times, very difficult to obtain without proper methods and maintenance of adequate records.

A good method that has been found useful is this connection is the Quality Cost Analysis Method. This method segregates quality costs into four distinc categories:

1. Prevention costs. This element of cost includes money spent for the purpose of preventing defects from occuring in the first place. Included here are such costs as quality engineering, quality personnel training, maintenance of testing equipment and writing of quality control instructions.

2. Appraisal costs. This element of cost includes the expenses for maintaining company quality levels by means of evaluations of product quality. This involves such costs as inspection, test, quality audit and laboratory acceptance examinations.

3. Internal Failure Costs. This element of cost includes costs arizing within the manufacturing organization of failure to achieve the required quality (before the transfer of ownership to the customer). This includes such losses as sorting, scrap, rework, reinspection, etc.

4. External Failure Costs. The costs arising outside the manufacturing organization of failure to achieve the required quality (after the transfer of ownership to the customer) i.e. analysis of complaints, after sales obligations, warrantly, replacement etc

These costs can tell how much money should be spent for each cost element in order to achieve optimum quality at minium cost To do this, however, it is necessary to have comparison bases to enable these quality costs to be compared with other business operations.

To set up such a quality cost work sheet it is necessary to be sure that the cost accounting methods in a particular business have identified and grouped quality costs in a form suitable for the development of adequate control.

Once a system is developed regarding the method to be used in determing a business's quality costs, and the bases used for comparison purposes, subsequent changes in the original basis obviously invalitates all past data.

To be assured that the quality costs used for analysis purposes are dependable the Quality Control Manager must look for the following specific things:

(a) See that the quality costs are accurate according to the definitions of the elements under the four areas, Prevention, Appraisal and Internal and External failure costs.

(b) Be sure that the measuring basis i.e. sales or labour costs fits the ups and downs of the particular business.

(c) Ensure that the quality costs are issued periodically, preferably on a monthly or a quarterly basis.

This is one of the Quality Control Manager's responsibilities to ensure that the right amount of money is being spent is this area in order to achieve the quality level required and also to assure a correct balance between Prevention and Appraisal costs that lead to maintaining quality levels and reducing failure costs.

Ratios for Quality Cost Categories

The optimum cost can be found through analysis of the interrelationships between the various cost categories. The basic model for this concept is shown in Figure 1. This model shows the principal quality costs which enter the achievement of fitness for use. They consist of:

1. The cost of appraisal and prevention which have been group together for convenience. When this costs are zero the product is 100% defective. To improve conformance, prevention and appraisal costs are increased until perfection is approached. Here the prevention costs rise asymptotically, becoming infinite at 100% conformance.

2. The failure costs due to the existence of defects. At the right-hand boundary the product is 100% good. Hence there are no defects and zero failure costs. As nonconformance sets in, failure costs rise until, at 100% nonconformance where the product is 100% defective. At this point none of the products are good and the failure costs per good unit become infinite, i.e. the denominator of the fraction is zero.

The curve of total quality costs (prevention—abraisal plus failure costs) is seen to have a minimum which has a practical meaning and application.

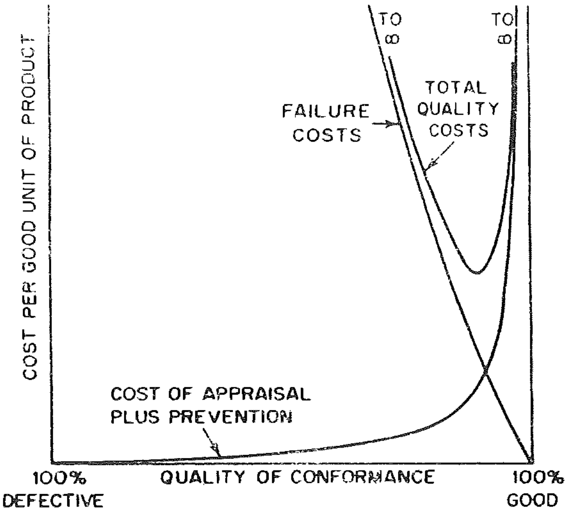

Fig. 1: Model for optimum quality costs.

The application of the model is seen in Figure 2 where an enlarged view of the bottom part of the total quality cost curve is devided into three zones. These zones can usually be identified from the prevailing ratios of the quality costs in the principal categories as follows:

Quality Improvement Zone. This is the left-hand portion of the curve. The usual distingushing features are that failure costs constitute over 70% of the total quality costs, while prevention costs are under 10% of the total. In such cases improvent projects can be undertaken profitably.

Perfectionism Zone. This is the right-hand zone of Figure 2 and is usually characterised by the fact that appraisal costs exceed failure costs. Now the improvent projects consist of discovering and removing the undue cost of perfectionism.

Indifference Zone. This is the central zone if Figure 2. In this zone the optimum has been reached and hence every effort should be directed towards controling (maintaining) this optimum level. This zone is generally characterized by the fact that about half the quality costs are failure costs, while prevention costs are about 10% of all quality costs.

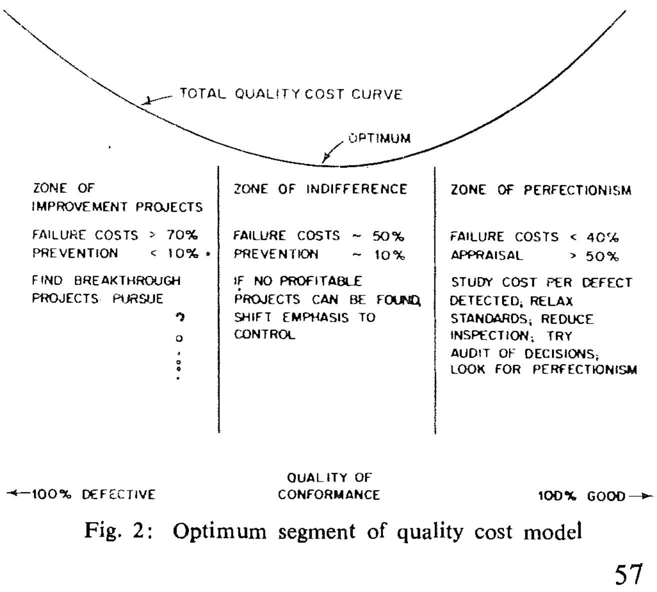

Fig. 2: Optimum segment of quality cost model

(a) See that the quality costs are accurate according to the definitions of the elements under the four areas, Prevention, Appraisal and Internal and External failure costs.

(b) Be sure that the measuring basis i.e. sales or labour costs fits the ups and downs of the particular business.

(c) Ensure that the quality costs are issued periodically, preferably on a monthly or a quarterly basis.

This is one of the Quality Control Manager's responsibilities to ensure that the right amount of money is being spent is this area in order to achieve the quality level required and also to assure a correct balance between Prevention and Appraisal costs that lead to maintaining quality levels and reducing failure costs.

Ratios for Quality Cost Categories

The optimum cost can be found through analysis of the interrelationships between the various cost categories. The basic model for this concept is shown in Figure 1. This model shows the principal quality costs which enter the achievement of fitness for use. They consist of:

1. The cost of appraisal and prevention which have been group together for convenience. When this costs are zero the product is 100% defective. To improve conformance, prevention and appraisal costs are increased until perfection is approached. Here the prevention costs rise asymptotically, becoming infinite at 100% conformance.

2. The failure costs due to the existence of defects. At the right-hand boundary the product is 100% good. Hence there are no defects and zero failure costs. As nonconformance sets in, failure costs rise until, at 100% non-conformance where the product is 100% defective. At this point none of the products are good and the failure costs per good unit become infinite, i.e. the denominator of the fraction is zero.

The curve of total quality costs (prevention—abraisal plus failure costs) is seen to have a minimum which has a practical meaning and application.

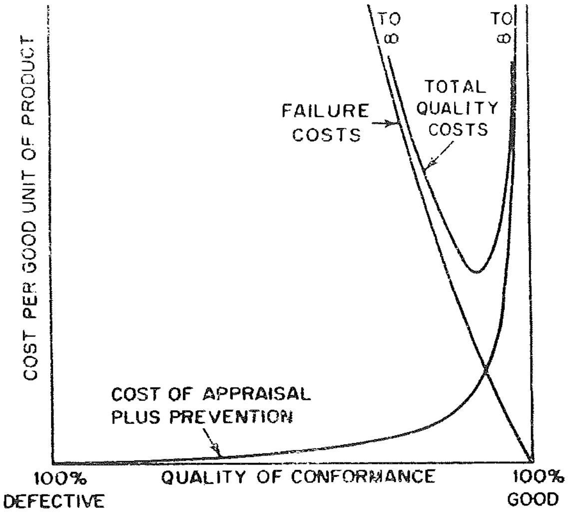

Fig. 1: Model for optimum quality costs.

The application of the model is seen in Figure 2 where an enlarged view of the bottom part of the total quality cost curve is devided into three zones. These zones can usually be identified from the prevailing ratios of the quality costs in the principal categories as follows:

Quality Improvement Zone. This is the left-hand portion of the curve. The usual distingushing features are that failure costs constitute over 70% of the total quality costs, while prevention costs are under 10% of the total. In such cases improvent projects can be undertaken profitably.

Perfectionism Zone. This is the right-hand zone of Figure 2 and is usually characterised by the fact that appraisal costs exceed failure costs. Now the improvent projects consist of discovering and removing the undue cost of perfectionism.

Indifference Zone. This is the central zone if Figure 2. In this zone the optimum has been reached and hence every effort should be directed towards controling (maintaining) this optimum level. This zone is generally characterized by the fact that about half the quality costs are failure costs, while prevention costs are about 10% of all quality costs.

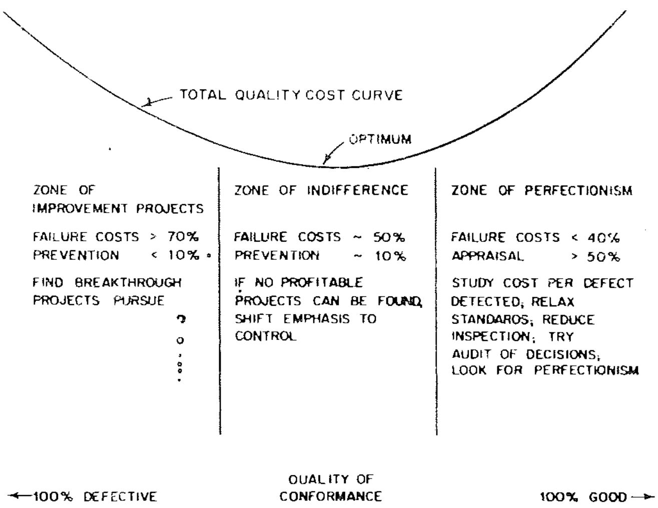

Fig. 2: Optimum segment of quality cost model

Practical Applications

To illustrate the importance of quality costs in assisting management to achieve optimum quality at miniumum quality cost consider the following practical application.

Figure 3 has been compiled from data obtained from a study that has been carried out in Holland. It demonstrates the appreciable savings that can be made within an organization by the introduction of an efficient quality cost system.

Irrespective of whether a quality cost system is in operation all manufacturers are likely to have a certain amount of appraisal and prevention costs although it is obvious that these are not effective in the situation illustrated as they are totally out of balance with the external and internal failure costs. When a situation like this with 20% external failure costs occurs it is perhaps easier to get investment in the prevention and appraisal functions by the establishment of a quality engineering unit. However, before this can be achieved it is usually necessary for quality personnel to reduce all the technicalities to financial terms for the benefit of management. Such investment is likely to be maintained until such time that the failure costs balance the appraisal and prevention cost or 'a' equals 'b'.

The study also gave the following quality costs for different industries as a percentage of turnover before and after optimization.

Industry	Before	After
Automotive	6–9%	4–6%
Food	7–12%	3–6%
Chemical Products	7–12%	4–7%
Manmade Fibres	8–16%	5–8%
Ceramics	15%	10%

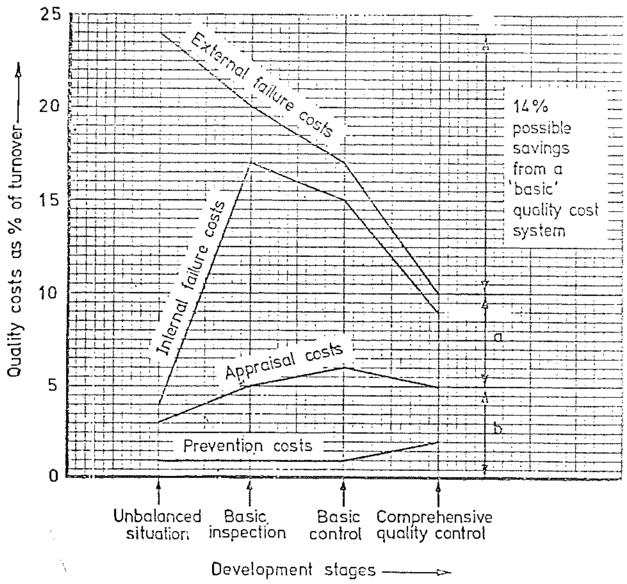

Fig. 3: Development of a 'basic' quality cost system

All of the quality cost data and information are vitally important for the management of quality control. There are four major results obtained from accurate quality costs.

(a) Quality costs provide an accurate tool for measurement of overall business quality performance.

(b) Quality costs are an analysis tool, used to indicate where quality money is being spent.

(c) They provide information as to when, where and how to plan for quality improvements.

These assist the quality manager in making his plans for achieving optimum quality at minimum quality cost.

References

BS6143:1981 —The determination and use of quality related costs.

A.S.Q.C. —Quality Costs–What and How

Siemens —Statistical Technology of Quality Control

J. M. Juran—Quality Planning and Analysis

J. M. Juran—Quality Control Handbook.

ENTROPY: Some Philosophical Projections

by Constantinos Neocleous, B. E. (Mechanical), Lecturer H.T.I.

Symbols

S *Entropy*
T *Temperature (absolute)*
Q *Heat (positive when transfered into a system)*
P *Pressure*
F *Force*
A *Area*
Ω *Thermodynamic Probability*
K *Boltzman constant*

Subscripts:

R *Reversible*
I *Irreversible*

Entropy, the word given to a property of a substance is derived from the greek εν τρωπει Conceptually entropy is hard to understand so that one could say "Its Greek to me!" What is entropy and what is its significance in the quest for a deeper understanding of the universe we live? This short article will present some aspects of entropy, aiming at helping those who seek to have a general understanding of it, and to create a platform for further discussion.

Definition of entropy

In classical thermodynamics entropy is defined by

$$ds \equiv \left(\frac{\delta Q}{T}\right)_R \quad (1)$$

When a system of pure substance undergoes a reversible transformation from state 1 to state 2, the total change of entropy is given by

$$S_2 - S_1 = \int_1^2 \left(\frac{\delta Q}{T}\right)_R \quad (2)$$

If the process is irreversible,

$$ds > \left(\frac{\delta Q}{T}\right)_I \quad (3)$$

The third law of thermodynamics states that the entropy of all perfect crystals is zero at the absolute temperature and thus equation 2 may be used in determining the absolute entropy of substances.

Equation 2 is difficult to apply, and the quantity defined by this hard to "feel". This may be evident by considering the thermodynamic pressure which is defined by

$$P = \frac{F}{A} \quad (4)$$

This equation indicates that the pressure is defined by a simple ratio of two easily measurable quantities, the force and the area. Furthermore, pressure can easily be felt and measured. With entropy, however, things are not so simple. In the definition of entropy a special situation is required, the reversible process, which is difficult to obtain. The calculation of entropy is not a simple arithmetic division as with pressure, but rather a complex integration. Thus, the apparent difficulty in understanding entropy is partly due to the difficulty of sensing and measuring it.

In statistical thermodynamics entropy is given by

$$S = k \ln \Omega \quad (5)$$

Where Ω is the thermodynamic probability which is defined as the number of microstates corresponding to a given macrostate. A macrostate of a system is defined by the thermodynamic properties of pressure, temperature, specific volume, internal energy e.t.c. while a microstate is defined by the totality of the individual properties (position, velocity, e.t.c.) of each particle of the system. Also, the mathematical probability (defined as the ratio of the number of cases favouring a given occurence to the total number of equally possible cases and thus having a value from zero to one) is different from the thermodynamic probability as defined above, which has a very large value. The mathematical probability of a state is, thus, equal to the ratio of thermodynamic probability of the state to the total number of possible microstates having the same energy.

As the number of microstates in a given macrostate increase, the system becomes more disordered and thus the entropy of a system may be thought of as a measure of its disorder.

This result gives a new insight into the second law of thermodynamics, which in classical thermodynamics is stated as "It is impossible to have a process whose sole result is the flow of heat from a heat reservoir and the performance of an equivalent amount of work". Even though it is highly improbable to have the molecules of a gas, which have a random distribution of position and velocity, to get together in a cooperative manner in order to acquire simultaneously a common velocity, this may occur.

Thus the second law is merely a statement of the improbability of the spontaneous passage of a system from a highly probable state (random or disordered) to one of lower probability (ordered).

Principle of the Increase of Entropy

It may be shown that when a system undergoes a process, the total net entropy change of the system and its surroundings is equal to zero if the process is reversible and greater than zero if the process is irreversible.

This shows that entropy is not conserved except in reversible processes. All spontaneous processes (e.g. mixing of tea with ice) are irreversible, and thus there is an increase in the entropy of the system and surroundings during such processes. Where did this entropy come from? And what is even more astonishing is that once entropy is created, it cannot be destroyed.

The first law states: "Energy can neither be created nor destroyed".

The second law states: "Entropy cannot be destroyed, but it can be created".

Some Philosophical Repercussions

In the following discussion, the assumption is made that the physical laws applicable on earth are also applicable in the entire universe.

It has been stated that spontaneous processes are irreversible, and during an irreversible interaction between a system and its surroundings there is a net entropy increase. Since entropy is associated with disorder, then one may suggest that during actual processes the total disorder increases. It is more probable that during an interaction between a system and its surroundings the result will be an increase in the total disorder. For example, there is only one way a house is being built but there are many ways it can be destroyed and transformed into rumbles. There are many ways that a given amount of gas in a container may be distributed in order to have a certain macrostate, while there is very little chance to so happen that all the molecules are concentrated in half the container, while the other half is void.

If then the universe is assumed to be a closed system, one can say that the universe tends to a disordered (dead) state, since from the principle of increase of entropy there is a continual increase in the entropy of the universe. If this is the case, we are faced with a non–conservational law (unlike the law of conservation of mass–energy) in which entropy is continuously being created (out of what?). Some scientists suggested that biological evolution is itself an antientropic process (contrary to all probabilities for unevolution) since it transforms disordered, scattered atoms and molecules into well organised, ordered living matter. If such is the case, what then about the billions of years ago when there was no biological living matter (at least on earth). Was there any living ordered matter elsewhere in the universe? Is there any oscillatory process in the universe, such as some parts of the universe are antientropic and some parts entropic? What about the interfacing regions between the two or more parts? Humans, it seems, are not unique in the world but only a small "role playing" fragment in the universe. Buckminster Fuller suggested that the human brain is the supreme antientropic source, since it organizes, through thought, the world.

I think that, intelligence as such, human or extraterrestrial could be antientropic. The universal ever existing intelligence.

If no–where in the universe antientropic processes exist and the entropy (disorder) of the universe continuously increase, the question arises on when, where and how this entropy increase start and where does it lead. Was the world originally stable, ordered, perfect and suddenly it started a one way process to disorder, to thermal death? What made this happen, why, when and how? Is this process to continue at infinitum, or the entropy will reach a maximum? When it reaches a maximum will the universe start a reverse process, towards order and back to disorder, and so on in an oscillatory manner? Is the Big Bang theory fitting to all this? What is the role of man to this dynamic universe? It seems to me that all these questions will remain unanswered for many years, if they are ever at all answered.

It is hoped that I have given some insights into the concepts of entropy and that the frame–work has been established for further discussions and suggestions.

References

1. G. J. Van Wylen and R. E. Sonntag "Fundamentals of Classical Thermodynamics", John Wiley and Sons, Inc.
2. D. B. Spalding and E. H. Cole "Engineering Thermodynamics" Edward Arnold Ltd.
3. F. H. Sears and G. L. Salinger "Thermodynamics, Kinetic Theory, and Statistical Thermodynamics" Adison–Wesley Publishing Company.
4. V. A. Kirillin, V. V. Sychev, A. E. Sheindlin "Engineering Thermodynamics" Mir Publishers.

The fate of the universe

by A.Z. Achillides, M.Sc., Lecturer, H.T.I.

The astronomers are now confident that the Universe has evolved from a single "singularity" something over 15 thousand millions year ago. The remaining puzzle of cosmology concerns the ultimate fate of the Universe. Will the universe expand for ever into infinity or is it destined ultimately to collapse back into a "fireball" reminiscent of the "Big-Bang" of creation?

According to the book of Genesis the Universe began in a single flashing act of creation. The Divine intellect willed all into being "ex nihilo". It is not surprising that scientists have generally stayed clear of the question of ultimate uthorship of the final "Uncaused cause". In years past in fact they held to the Aristotelian idea of a universe that was "ungenerated" and "indestructible" with an infinite past and an infinite future. This was known as the "steady state" theory of creation.

In recent decades however the steady state model of the universe has yielded in the scientific mind to an even more difficult idea full of cosmic violence. Most astronomers now accept the theory that the universe had an instant of creation, that it came to be in a vast "fireball" explosion 15 thousands of millions of years ago. The "shrapnel" created by that explosion is still flying outwards from the focus of the blast. One of whose hundreds of billions of stars is our own Sun with its tiny orbiting grains of planets one of which is our home planet, the Earth.

The ideas above were put forward by a Belgian priest the late Abbe Lemaitre who claimed that the Universe was born as a primeval atom–perhaps as little as 200 million miles in diameter—that exploded setting matter flying apart. "Naturally too much importance must not be attached to this description of the primeval atom" Lemaithe wrote.

"It will have to be modified perhaps when our knowledge of atomic nuclei is more perfect". The important thing was that the universe began violently in "fireworks" as Lemaitre put it.

Astronomers arrived at the Big-Bang" theory through its admirably painstaking and ideologically disenterested process of hypothesis and verification and sometimes happy accident. In 1913 Astronomer Y.M. Slipher of the Lowell observatory in Arizona discovered Galaxies that were receding from the earth at extraordinary high speeds up to 3.2 million km.p.h.

In 1929 the American Astronomer Edwin Hubble developed Slipher's findings to formulate the law bearing his name "the farther away the greater the speed of the Galaxy" which it presupposes a primordial explosion. In the meantime A. Einstein without benefit of observation developed his general theory of relativity and included in it the idea of the expanding Universe. But the steady state theory still held many Astronomers like the eminent Sir A. Eddington who was in favour of a Universe of steady stars cold space and galaxies perfect as "flowers". The idea that everything has once been crammed into a "Hellish" ball offended him. "Since I cannot avoid introducing this question of a beginning" he wrote "it has seemed to me that the most satisfactory theory would be one which made the beginning not too unaesthetically abrupt!!".

In 1948 an elegant steady state theory has been proposed by T. Gold, H. Bond, and F. Hoyle all from Cambridge. The theory proposed was based on the famous "Cosmological principle" of the mathematician and astronomer Milne stating that "any model of the Universe must allow every one in the Universe the same general view". Bond and Gold took Milne's principle a step further. Since relativity requires that we regard the Galaxies as inhabiting a continuum of time as well as space they asked why confine the cosmological principle to space alone? Why not demand that the Universe present the same aspect to observers not just in all places but at all times? Their answer was to postulate what they called the "perfect cosmological principle" stating that "Our overall outlook on the Cosmos out to be shared by observers in all quarters of the Universe and at all times in its History". "Evolving" Universe theories violate the perfect Cosmological principle because they imagine the universe was once very different, before the galaxies formed, and imply that in the future whether Universe expands for ever or eventualy collapses, things will be much different than at present. Only the steady state theory where new Galaxies constantly formed to fill unfolding space between the old satisfies the principle its authors devised.

One of the implications of the Big-Bang theory was that if such an explosion has taken place in the remote past a residual radiation should be left in the Universe which may be detected as a "background" radiation coming from all parts of the sky. When first proposed by G. Gamow this idea was met with reservations and later completely ignoned. But in 1965 two scientists at Bell Telephone Laboratories Arno Penzias and Robert Wilson using a sofisticated antenna picked up, without knowing the cause, the "noise" made by the remnants" of the Great explosion in a publication signed by Penzias and Wilson and titled" A measurement of excess antenna tempenature at 4080 Gigahertz began: "Measurements of the effective zenith noise temperature of the 20-foot horn reflector antenna have yielded a value about 3.5 Kelvin highen than expected. This excess "temperature" is within the limits of our observations, Isotropic unpolarised and free from seasonal variations. A possible explanation for the excess "noise termperature" observed is that it may be the remnants of the "explosion" that gave birth to the Universe Further observations at Princeton and at Cambridge verified the results of Penzias and Wilson and they further confirm that this "back ground" radiation follows a "black body" radiation distribution. The detection of the back ground radiation on the Earth does not imply that it exists everywhere in the Universe. Other measurements from the remote parts of the Universe were needed to verity that the background radiation was really the "echo" of the Big–Bang. So the astronomers started the painstake task to detect this "echo".

Fortunately the Cyanogen molecule consisting of one Nitrogen and one Carbon atom was among the first interstellar molecules to be detected. It is excitable by radiation at 2.6 millimetre wavelength that happens to lie close to the peak of the blackbody curve predicted by Big–Bang theory. By measuring the degree of excitation of interstellar Cyanogen. Radioastronomers therefore could vintually "dip a thermometer in space"! This was soon done. Cyanogen excitation levels were measured in diverse regions of space and in every case the levels were indicated a true "Cosmic temperature" of between two and three kelvin degrees. It was the most powerful confirmation of the most violent genesis of the Universe. But the story of creation does not end here. The big puzzle of Cosmology is the ultimate fate of the Universe. Only two choices are available if the standard models of relativistic Cosmology are as reliable as current observations suggest. The expanding Universe may have been born in an outburst so violent that the expansion can never be halted in which case it is "open" in the sense that it expands for ever and must be infinite in size. Or if may be "closed" in the sense that it is finite in size and contains enough matter for gravity to halt the expansion eventually and then cause the Universe to collapse back into a "singular state" or at least another Cosmic "fireball."

At present observations favour the open models; but over the past few years there has been a marked tendency for new observations and the application of new techniques to the problem, suggest that the Universe contains more mass and therefore sits closer to the dividing line between being open the cloused, that was previously thought.

The Big–Bang theory has subversive possibilities. For example a religious enthusiasm rose for the apparent convergence of Science and Theology because as K. Jastrow director of NASA'S Goddard Institute for space studies put it "The Big–Bang theory suggests that the Bible was right after all and that people of his own kind by this description now found themselves confounded". But Isaac Asimov the prodigious populizer of Science reacts hotly to the Jastrows views. "Science and religious proceed by different methods" he says. "Science works by persuasive reason. Outside of Science the method is intuitional which is not very persuasive. In science it is possible to say we were wrong based on data. Science is provisional; it progress from one hypothesis to another, always testing, rejecting the ideas that do not work, that are contradicted by new evidence. Faith said St. Augustine is to believe on the word of God what we do not see". Faith defies proof; Science demands it If new information should require modification of the "Big Bang" theory' that modification could be accomplished without the entire temple of knowledge collapsing".

Some scientists—matter of factly—dismiss the problem of creation. As Harven Tanambaum an X–ray astronomer put it like this. "That first instant of Creation is not relevant as long as we do not have the laws to begin to understand it. It is a question for Philosophers and Religionists not for Scientists. Geoffrey Burbidge director of Kitt Peak National observatory adds "Principles and concepts cannot be measured. A question like who imposed the order is metaphysical. Still virtually every one both Scientists and laymen, is taken by the sheer unthinkable opacity of the creation and what preceded it".

The theory of the Big–Bang is surely not the last idea of creation that will be conceived; it does suggest that there remain immense territories of mystery that both the Scientists and the Theologians should approach with becoming awe.

Adolescence

by S. Messiou, Welfare Officer HTI

Adolescence may be defined in general terms as the period of transition from childhood to maturity. The word adelescence is commonly used with more than one connotation. In its simplest sense, it is applied to those within the age–group which is developing from childhood to adult status. The term as so used is somewhat elastic but it refers roughly to young people of chronological ages between twelve and twenty, or, more accurately, to those who are physiologically old enough to have experience puberty but not yet sufficiently mature to have developed the physical stability of adult life.

The period of adolescence consists of various phases differring fundamentally from one another. It may be subdivided into:

(a) **Puberty**, from twelve to fourteen, characterised by the "gang spirit" and rapid development of the physiological sex functions;

(b) **The Transition Period**, about the age of fifteen, in which the youth is passing to the heterosexual phase; and finally

(c) **Later Adolescence**, from sixteen to eighteen or twenty, characterised by heterosexuality and idealism.

The period of adolescence presents the indindual with the problem of reformulating his concepts of himself as being different in many significant respects from the childhood image.

Adolescence terminates physically with the establishment of the mature body structure and the mature functioning of the reproductive system. It terminates phychologically with the establishment of relatively consistent patterns for dealing with the internal conflicts and the demands of reality experienced by the physically mature individual.

Adotescence is a stage of emotional growth. it cannot be avoided if adulthood is to be attained. It is a period in which many conflicts dormant since childhood return to be solved. It is a period also of new problems, problems created by the physical changes that have occurred in the individual.

During the early part of adolescence the pressures from physical, psychological, and social changes are of such intensity that the adaptive capacity of the individual is strained to the point of relative inadequacy. During the period of rapid physical development the lack of physical stability adds to the strain. When physical maturation is ralatively complete the strain lessens. Physical functioning of the body becomes more uniform. Once the physical structure is somewhat stabilised the individual has an opportunity to become familiar with it and this familiarity results in progressive mastery. Similarly, familiarity with the social demands and the phychological pressures clarifies the issues and facilitates their mastery. Until this stabilisation and clarification have been achieved, the individual has no real foundation upon which to build an adult personality structure. When the foundation is laid, he can deal in a more orderly fashion with those psychological problems that relate to his early experiences, to his early defences, and to his drive towards integrated maturation.

The period of adolescence is usually the most difficult from the point of view of personal relationships in the home, both for the adolescent and the other members of the family. The first manifestation of adolescent change consists in a growing demand for independence and this extends to every field. The adolescent resents being controlled and guided, and begins to want to think for himself and to act as an independent person. He begins to despise what he regards as childish things and his one desire is to appear grown–up. This shows itself in a refusal to accept the family pattern as the only desirable one and leads to continual arguments about every trivial detail of daily life. From about thirteen onwards the adolescent wants to choose his own friends and to choose his own clothes.

The younger adolescents are prone to feel that everybody is trying to fustrate their efforts to achieve independence. Their emotions are inclined to be unstable because of the physical and psychological changes through which they are passing, they feel everything very intensely and take themselves immensely seriously. They are eager to grasp at every new experience and to try to seize life with both hands.

The development of a sense of self–awareness is the most important characteristic of adolescence from the psychological point of view. Until a child does reach the stage of self–awareness it cannot be regarded as fully awakened or as having developed anything but a rudimentary degree of maturity. The development of the capacity to abstract thinking is a characteristic of adolescence. This brings with it the power of comparing and contrasting relationships and of making assessments and judgments. The child for the first time becomes interested in itself as a person and also in the people around it. This new attitude of mind is extremely disturbing to many children. It alters their relationships with their families, especially their parents and also with their friends; and makes them feel extremely unsure of themselves. At this stage, adolescents seem to be extremely sensitive to criticism from others. They probably feel that many of the criticisms are unjust and that people do not really understand them. The adolescent wishes to be valued and accepted for his own sake. Adolescents who believe that everyone thinks that nothing they do is right may become, at least for a time, entirely discouraged and feel that it is quite useless to make any effort at all.

One of the characteristics of adolescence is the desire to have an intimate friend. The friendships of the pre-adolescent period are usually much more superficial and a matter of companionship in activities rather than involving any close personal ties. From about twelve onwards, however, children of both sexes begin to want someone with whom the can have much deeper and more personal relationship, with whom they can share their troubles and ideas, their joys and sorrows, their hopes and fears, and the more intemate and personal interests which they begin to develop at this period of their lives. Many adolescents who are good mixers like to have a group of friends of a more superficial type, and they greatly enjoy belonging to some kind of organisation where they feel they are accepted for their own sake.

In later adolescence many boys and girls begin to find it necessary to evolve for themselves some kind of phylosophy of living. This may be more or less uncouscious, but in a large number of cases they are no longer prepared to accept blindly the beliefs of their parents and the adults around them.

Many adolescents "live through" adolescence without any couscious planning or assistance from others. Some have the advantage of living in an environment that is inherently helpful; others have more consciously planned assistance. Regardless of whether the adolescent is struggling through his problems alone or is aided in his adjustment by means of group activities, close personal relationships, environmental manipulation through guidance to the parents and the school, or whether he is receiving supportive or insight therapy, one generalisation has validity: adolescence is a stage of emotional growth. It cannot be avoided if adulthood is to be attained. It may be prolonged because the individual is unable to find a solution to his couflcts. On the other hand, adolescence cannot be too greatly foreshortened without serious adverse effects. The normal adolescent needs time to grow up. He needs support, encouragement, and guidance, and above all, adequate time before he is forced to crystalise his final personality pattern.

References:

1) The Adolescent and his world—I.M. Josselyn

2) Problems of Youth: Transition to Adulthood in a changing World M. Sherif and C.W. Sherif

3) Journey through Adolescence—D. Odlum

4) Adolescence—C.M. Fleming

HTI: A regional role in Hospital Engineering

by Dr. A. Mallouppas, Ph. D, C. Eng., Head, Regional Training Centre, HTI.

Summary

In 1978 *the Government of Cyprus signed a four year agreement with the World Health Organisation, which set up in the HTI a Regional Training Centre in the field of Hospital and Medical Equipment. This agreement has been extended for another five years* (82–87) *with a more comprehensive and enhanced role for the RTC. In this article the regional activities of the next five years are reviewed and possible new fields of interest are identified and assessed.*

Introduction

The first agreement foresaw a limited programme of training Hospital Technicians in the Repair and Maintenance of Hospital and Medical Equipment beginning with the Polyvalent (General) Technician Courses and different types of specialised technichian courses. After two years, however, the original work schedule of one course per year was surpassed with the signing of the First Addendum to the Project where more than one course per year was held simultaneously. Based on the work and results of the period 78–81 a new five year agreement, covering the period 1982–1987, was signed in March 1982. As a result of the new agreement the Regional Training Centre, RTC, was restructured into a separate entity within the HTI framework with its own full–time staff, facilities and administrative set–up. Also the activities envisaged for the RTC are far more extensive than before with an enhanced regional role.

In the present article the Regional nature of the activities foreseen in the new agreement will be examined and future areas of expansion identified. The three main areas of regional activity foreseen for the RTC are:

(i) Consultancy on behalf of WHO in the field of Hospital Technical Management.

(ii) Coordination with other training centres and related institutions.

(iii) Feedback and evaluation of trainees and assessment of their work.

Future regional activities, not foreseen specifically in the project, but may probably be incorporated during the second agreement period into the RTC activities are:

(i) Adoption of training on Maintenance and Repair as Policy for the whole of WHO, leading to an Inter –Regional Status for the RTC.

(ii) Development work in the field of Medical Equipment and instruments

(iii) The setting up of a Hospital or Bio–Medical Engineer Course of at least Assistant Engineer Status.

Consultancy

The expertise being built up at the RTC in the field of Hospital Technology and Technical management can be used by WHO to advise other countries in the Region concerning their Hospital Technical Services. This has already begun with RTC staff undertaking on–the–spot surveys in North and Sourth Yemen and shortly to Sudan and Somalia. These were concerned with evaluating the situation concerning Repair andMaintenance facilities in particular and Technical Management in general. Eventually most of the countries in the Region will be surveyed and from the country reports a Regional Report will be compiled. This will enable WHO and the RTC to plan their policy on training and other related activities for the future.

Based on feedback and experience from the surveys and on the personal contacts that will be established then other collaborative relationships can develop between the countries and the RTC through and within the framework of WHO.

Technical advise on particular problems can be given such as formulating specifications for specialised equipment, Technical Assistance even provision of consumables and spare parts that are easily available in the Cyprus market.

Coordination

Other national training centres exist in the region dealing with the training of hospital technicians. The RTC has been nominated to act as coordinator between the various centres so that information and assistance can be made available to everyone. It is hoped that in the future close ties will be established and exchange of information and teachers can take place.

Through the HTI the RTC is able to develop links to industry and several European firms have been invited by the HTI and have participated in the training activities. Particularly useful are the contacts built–up which should improve communications between the various parties.

Feedback and Evaluation

One of the most important factors to the training programmes of the RTC is the post graduation follow

–up of the students in their home working environments. This will give the RTC the feedback that is necessary in order to judge the performance of the students on–the–job and assess the effectiveness of the training programmes offerred. Based on the information found in the countries the training will be modified accordingly. Also the Governments involved can be advised through WHO to create the work environment and set–up required for the technicians trained to develop their skills.

Future Activities

WHO Policy on Maintenance

WHO is split up into five regions, each one with its own regional autonomy but also following common WHO policies agreed upon by the Assembly of all member states. Once an issue is adopted as WHO policy by the Assembly then it is implemented by all Regions. Adoption of Maintenance and Repair as WHO Policy will mean that the RTC, which belongs to the Easten Mediteranean Region of WHO, can become an Inter–Regional Training Centre. This will be possible since funds will be made available to all regions for such a purpose. In such an eventually then the RTC's training activities may be extended considerably.

Development Work

The need arises many times to modify existing equipment to suit particular circumstances or to construct new ones either because they are not readily available or because they are expensive. Development work in constructing or modifying medical or test equipment is normal practice in many developed countries and this is one field in which the RTC has already made some attempts (construction of an E.C.G. (Electro Cardiograph) simulator, continuity meter etc) but has also the capability of developing medium technology medical and para–medical equipment.

The benefits from such development work can be made available to country workshops or hospitals through WHO. At the moment due to the recent restructuring of the RTC such work is not given high priority but is a field which the RTC intends to enter in the near future. The type of development work to be undertaken will also be determined from regional needs hence the results of the on–going country survey will be an important deciding factor.

Hospital Engineer

In most of the countries of the Region the lacl of qualified professional personnel is hindering the progress of Hospital Technical Services. Most countries rely on expatriate help and particularly WHO Technical Officers. However the aim is to train local staff who will replace the expatriates so that each country will fully take over their own Hospital Technical Services.

Recent Surveys to the counties have shown that a training programme leading upto the level of Hospital Engineer is necessary in order to achieve the above goal.

The level can be that of an Assistant Engineer or University graduate or both. It is hoped that the regional Surveys being carried out at the moment will help WHO, the RTC and the Regional Governments to decide what is needed.

In the first Project document a Hospital Engineer course was foreseen, however this was soon realised to have been too optimistic and in the Second Project Agreement it was not planned for Specifically. The Specialised courses and present HTI courses will form the basis of such a course. The future of the course will be decided at a later stage. Once such a course is undertaken by the RTC, then it will have achieved its aim of training all the different levels of technical personnel required for a Hospital Service.

Cyprus Example Sparks Interest in Solar Heating

by Asif Khan

This is an extract from 'Commonwealth Features' published in March 1982 by Asif Khan (Information Division, Commonwealth Secretariat) on the occasion of the Regional Workshop on Solar Water Heating which took place in Nicosia on 9–12 February 1982. The Workshop was part of the Commonwealth Science Council (CSC) African Energy Programme a project of which is coordinated by the Higher Technical Institute. Lecturers from HTI presented technical papers and participated actively in the workshop. HTI was also represented in the Organizing Committee of this Workshop.

Visitors to Cyprus are often struck by a distinct feature of almost every roof top in this Commonwealth island in the Mediterranean—a small structure comprising two tanks and a panel.

The structures are evidence of the advances made by Cyprus in using energy from the sun. They absorb and store solar energy for domestic and industrial heating.

These solar water heaters began to spring up all over Cyprus soon after independence in 1960 —long before the rest of the world was struck by the energy crisis.

Today, the island is a world leader in solar energy technology. The private sector has brought the country to the solar age, a desirable development in view of the high cost of oil.

Last month (February), Cyprus was appropriately the venue for the Commonwealth Science Council's first–ever workshop on solar water heating. The CSC is the main inter–governmental organisation for promoting scientific co–operation between member countries.

Although the CSC has organised a large number of meetings and workshops in the 36 years of its existence, this was the first time that the successful national experience of a member country in a particular field had provided the subject for discussion.

The main object was to give Commonwealth countries in the African region an opportunity to study Cyprus's progress in this field, and to see what they could learn from its experience.

The workshop was part of the CSC's African Energy Programme, which was launched in 1979 following a meeting of Commonwealth scientists in Arusha, Tanzania.

The development of new and renewable sources of energy is the major aim of the Programme. The CSC is also running a similar Programme for the Caribbean.

Cyprus is keen to share its knowledge and experience with other Commonwealth developing countries, says Dr Azam Khan, a deputy secretary of the CSC which organised the workshop in conjunction with the Government of Cyprus.

Ghana, Kenya, Mauritius, Malawi, Seychelles, Sierra Leone, Swaziland, Tanzania, Uganda, Zambia and Zimbabwe sent representatives to the workshop.

The workshop, partly supported by the Commonwealth Fund for Technical Co–operation, the developmental arm of the Commonwealth Secretariat, was not confined to discussion; much emphasis was placed on practical aspects of the new technology.

The CSC wanted to hold the workshop in winter to show "beyond any doubt that the system does work on sunny days in cold weather and saves electricity", said Dr Khan, 41, previously director of scientific information in the Atomic Energy Commission of Bangladesh.

Dr Khan pointed out that all the participating countries had a hotter climate—and more sunshine— than Cyprus. "What is possible here should be possible in those countries".

Tourist hotels which have to provide both hot and cold water in bathrooms were identified as ideal candidates for going solar.

However, the transfer and adoption of technology of this kind does not depend on the availability of sunshine alone, and the workshop therefore looked at other factors like technical know–how and economic viability.

Solar water heating is cheaper to run than conventional methods. But the high initial cost due to the use of imported material in fabricating the equipment is impeding its widespread use, believes the CSC.

The workshop was left in no doubt that climate of participating countries was ideal for the system, both for domestic and industrial use.

Participants at the workshop urged governments to encourage consumers and manufacturers by giving them incentives in the shape of low–interest loans and tax exemptions on imported raw material. These are already provided in some member countries.

The workshop also recommended regional co-operation for joint manufacture, development of standards and testing facilities, information exhange, and training.

The Indian Ocean island of Seychelles is to look into the possibility of joint manufacture of solar water heaters with the rest of the countries at the workshop.

The Commonwealth Secretariat, of which the CSC secretariat forms a part, will assist with research and training, standardisation and information exchange.

This is a far cry from the pre-1973 days before the world energy crisis when solar water heaters were only a curiosity.- Commonwealth Feature.

Compiled by I. Michaelides, Lecturer H.T.I.

Test and Calibration facilities in Cyprus

by C.K. Tavrou, Lecturer H.T.I.

The Calibration laboratory of the Cyprus Standards and Control of Quality department has been housed at the Higher Technical Institute.

The laboratory is in fully operational order with high accuracy equipment for testing and calibration services to industry.

The equipment available enables the trained personnel to test and calibrate both electrical and mechanical instruments.

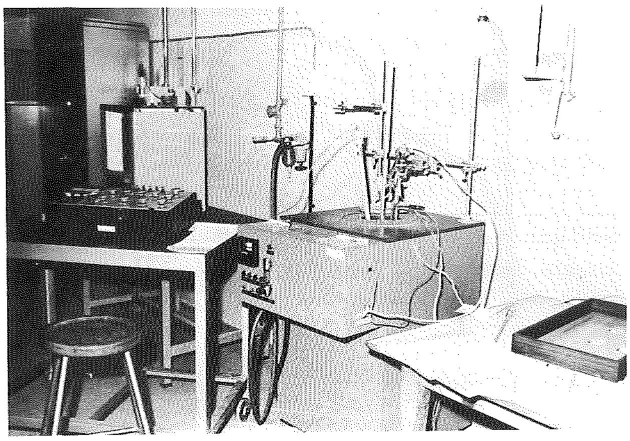

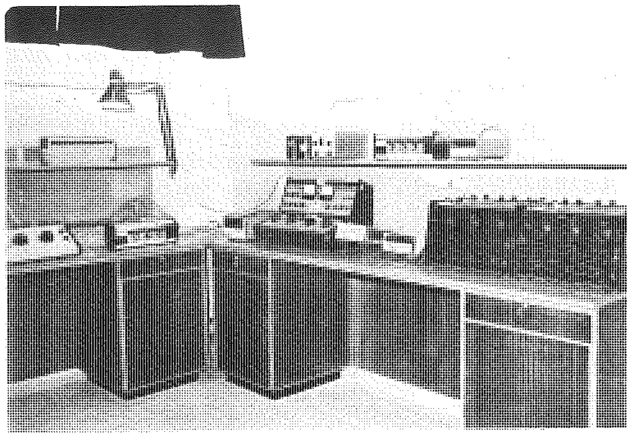

Some of the parameters that can be tested are as listed below.

Electrical	**Mechanical**
Capacitance	Pressure
Current	Temperature
Frequency	Viscocity
Inductance	Force
Resistance	Length
Voltage	Profile.

For every test or calibration, a certificate is issued with the results and a nominal fee is charged according to the time taken for the test.

A number of companies have already taken the oportunity to calibrate their instruments to ensure the good quality of their products. Others may not yet know of our laboratory, and with this brief note we invite anyone interested to contact us either by letter addressed to the Director, Higher Technical institute, P.O. Box 2423, Nicosia and marked Calibration laboratory, or by telephone for enquiries at 403053.

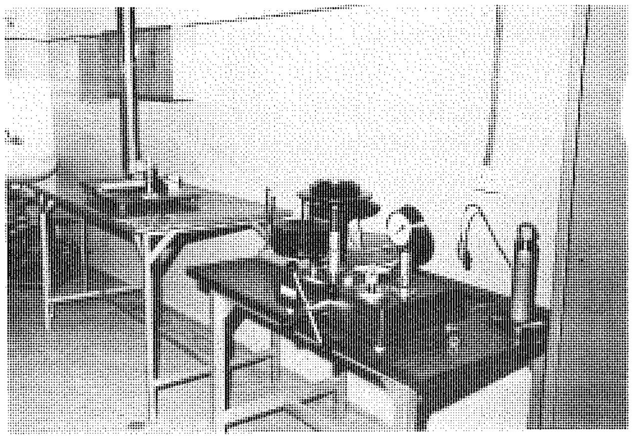

H.T.I. CALENDAR OF EVENTS

Academic Year 1981-82

by Ms. D. Charalambidou, H.T.I. Lecturer.

September

* The 1981–82 academic year was launched on September 7th Four hundred and forty–two students were enrolled including twenty–seven overseas students on regular courses.

* The Electrical Part–time Course continues with seventeen students on its fifth (final) year running.

* The Polyvalent course for Medical technicians has ten students from various Middle East countries. The X–ray Course admitted five overseas students and two Cypriots. Both courses are sponsored by the World Health Organisation (W.H.O.).

* The W.H.O. and the Cyprus Government agreed to set up the Regional Training Centre (RTC) as a new entity of H.T.I.

* The H.T.I. Director in his circular dated 18th September called for volunteers to organise extra–curricular activities which will enhance the academic and social life of the Institute and improve the H.T.I. premises.

October

* The Third–year Marine Officers return after a four–month training on board.

* The Astronomy Club organises its first lecture. Mr. A. Achillides talks on "Space Travels" at the H.T.I. lecture Theatre. The talk is accompanied by a short film, "Columbia: the space–bus"

* Mr Christos Kokkinos is elected President of the Student Union.

November

*Professor Neal of Aston University gives a lecture in the H.T.I. Lecture Theatre on "Heat lumps'›

* UNESCO DAY was celebrated on November 6th. Early in the morning students and staff set off for the Tekke of Hala Sultan where an officer from the Department of Antiquities spoke on the religious and historic significance of this famour Moslem shrine.

Then the whole party headed for the little church of Angeloktistis at Kiti. There the priest outlined the historical background of the church and elaborated on the archaeological value of the frescoes and ikons

Then the party made its way to the beach where at "Spyros Beach" they feasted till late afternoon when they reluctantly had to make their way back to Nicosia

* On the twenty–fifth of November a "get–together" party was organised for H.T.I. overseas students in the students' Canteen where drinks and snacks were served.

* Mr S. Savides returns from his study visits to London and Glasgow sponsored by W.H.O. where he attended seminars on Hospital Electrical Installation and I.E.E. Wiring Regulations.

December

* Dr A. Mallouppas returns from a Survey Visit as WHO Short Term Consultant to North and South Yemen. The visit was concerned with evaluating Hospital Technical Services in these countries.

* The H.T.I. Badminton Club is set up for the first time. Twenty–six staff and twenty students join it. A "Competitive Ladder" and "Challenge" matches were arranged.

* This month is marked by the Christmas festivities: A joined staff–student party was held in the Students' Canteen on Tuesday 22nd December. Drinks and snacks were served.

* The Association of H.T.I. Graduates held their annual Christmas Dinner at the Philoxenia Hotel on December 26th.

January

A hectic time for both students and staff as the first semester exams approach.

February

Exams are over Tension slackens again and the routine of lectures and seminars is resumed

* Daala Praviiva and Sidhayoganandah give a lecture on "Voga Philosophy and Practice" on February 7th. The lecture was accompanied by slides.

* Mr A. Hall from Luton College of Higher Education arrived in Cyprus to replace Mr G. Oxinos,

H.T.I. lecturer, who left for Luton following an agreement for staff exchange between H.T.I. and L.C.H.E. Mr Hall left at the beginning of April.

* Dr. Regenda from The Slovak Technical University of Bratislava arrived on February 24th within the cultural exchange agreement between Cyprus and Czechoslovakia.

* The H.T.I. Badminton Club played against the Falcon School Badminton Club. The Falcon School won by 5 to 2.

* Mr Kroezen, a W.H.O. Short Term Consultant, arrives to work with RTC and advise on future courses. Mr Kroezen is expected to stay till June.

March

* On March 23rd the Student Union honoured Ms Olga Demetriades for her fourteen year services rendered to the student community. The Ceremony took place in the Students' Canteen.

* On March 3rd the Film Club screened "STRAW DOGS" at the H.T.I. Lecture Theatre starring Dustin Hoffman.

April

* An organised group from the staff went to the Nicosia Municipal Theatre to see Shakespeare's "Taming of the Shrew" by the London Cambridge Theatre.

* On April 7th a "Guided Tour of Nicosia" was organised for the H.T.I. overseas students. The students were guided round the Archaeological Museum, the Byzantine Museum, the Museum of Popular Arts and Crafts and the Cathedral of St. John with its famous frescoes and ikons. The outing ended at the Garden Cafe' where the students were offered some light refreshnents.

* On April 12th an exhibition of Power Transmission Elements by Renold LTD was opened at H.T.I. During the exhibition various films on power transmission elements were shown.

* On April 14th the Film Club Showed "LOVE AND DEATH" at the H.T.I. Lecture Theatre Starring Woody Allen

* Mr I. Michaelides, lecturer, attended the "Expert Group Meeting on Solar Cooling for Food Preservation" held in London, 19–21 April, on an invitation from the Commonwealth Science Council (CSC)

* On April 27th the First Aid Certificates were awarded to the successful participants of the First Aid Course organised by the H.T.I. First Aid Committee.

May

* Mr Theodoros Symeou, lecturer, has returned from his visit to Marseilles to attend the "Fourth International Exhibition of Solar Energy and New Energy Sources" (SETSO) held in Marseilles from 11–15 May following an invitation by the French Government.

* SPORTS DAY was on May 19th The finals and semi-finals of various sports activities which went on during the academic year 1981–82 were held on Sports Day.

These activities included: football, chess, Badminton, Volley-ball, Basketball, Darts, Softball, Seven-A-Side etc.

* On May 11th the Film Club screened the "French Connection" at the H.T.I. Lecture Theatre.

* Mr Spyros Spyrou, lecturer, returns from a WHO S.T.C. to Somalia and Sudan.

* H.T.I. students donated blood on May 21st responding to an urgent call for an emergency from the Nicosia General Hospital.

June

* The third of June was proclaimed "Environment Day" for H.T.I. following the UN decision to proclaim June 5th as "Day for the Environment" The Staff and Students have agreed to clean and beautify the grounds of the Institute by planting trees and flowers. Feasting will crown the activities at the end of the day.

* The final exams for the first and second years will start on June 11th.

* The annual Graduation Ceremony will be held on July 9th.

Printed by KAILAS PRESS, Tel. 41184, Nicosia.